PilT and PilU are homohexameric ATPases that coordinate to retract type IVa pili

Jennifer L. Chlebek[1], Hannah Q. Hughes[1], Aleksandra S. Ratkiewicz[2], Rasman Rayyan[2], Joseph Che-Yen Wang[3], Brittany E. Herrin[1], Triana N. Dalia[1], Nicolas Biais[2], and Ankur B. Dalia[1,*]

[1]Department of Biology, Indiana University, 1001 E. 3rd Street, Bloomington, IN 47405.

[2]Biology Department, CUNY Brooklyn College, 2900 Bedford Avenue, Brooklyn, NY 11210 and Graduate Center of CUNY, 365 5th Avenue, NY 10016.

[3]Electron Microscopy Center, Indiana University, Bloomington, IN 47405.

*Correspondence to: ankdalia@indiana.edu.

Short Title: PilU is a PilT-dependent type IVa pilus retraction ATPase

Abstract

Bacterial type IV pili are critical for diverse biological processes including horizontal gene transfer, surface sensing, biofilm formation, adherence, motility, and virulence. These dynamic appendages extend and retract from the cell surface. In many type IVa pilus systems, extension occurs through the action of an extension ATPase, often called PilB, while optimal retraction requires the action of a retraction ATPase, PilT. Many type IVa systems also encode a homolog of PilT called PilU. However, the function of this protein has remained unclear because *pilU* mutants exhibit inconsistent phenotypes among type IV pilus systems and because it is relatively understudied compared to PilT. Here, we study the type IVa competence pilus of *Vibrio cholerae* as a model system to define the role of PilU. We show that the ATPase activity of PilU is critical for pilus retraction in PilT Walker A and/or Walker B mutants. PilU does not, however, contribute to pilus retraction in Δ*pilT* strains. Thus, these data suggest that PilU is a *bona fide* retraction ATPase that supports pilus retraction in a PilT-dependent manner. We also found that a Δ*pilU* mutant exhibited a reduction in the force of retraction suggesting that PilU is important for generating maximal retraction forces. Additional *in vitro* and *in vivo* data show that PilT and PilU act as independent homo-hexamers that may form a complex to facilitate pilus retraction. Finally, we demonstrate that the role of PilU as a PilT-dependent retraction ATPase is conserved in *Acinetobacter baylyi*, suggesting that the role of PilU described here may be broadly applicable to diverse type IVa pilus systems.

Author Summary

Almost all bacterial species use thin surface appendages called pili to interact with their environments. These structures are critical for the virulence of many pathogens and represent one major way that bacteria share DNA with one another, which contributes to the spread of

43 antibiotic resistance. To carry out their function, pili dynamically extend and retract from the
44 bacterial surface. Here, we show that retraction of pili in some systems is determined by the
45 combined activity of two motor ATPase proteins.

46

47 Introduction

48 Type IV pili are ubiquitous surface appendages in Gram-negative bacteria that promote diverse
49 activities including attachment, virulence, biofilm formation, horizontal gene transfer, and
50 twitching motility [1-5]. These structures can dynamically extend and retract from the cell
51 surface, which is often critical for their function. A detailed mechanistic understanding of pilus
52 dynamic activity, however, remains lacking.

53 Type IV pili are composed almost exclusively of a single protein called the major pilin, which
54 forms a helical fiber that extends from the cell surface [6]. Extension and retraction of the pilus is
55 hypothesized to occur through the interaction of cytoplasmic hexameric ATPases with the inner
56 membrane platform of the pilus machine, whereby ATP hydrolysis likely facilitates turning of the
57 platform in order to incorporate or remove major pilin subunits from the pilus fiber [7]. All type IV
58 pilus systems encode a predicted ATPase, often called PilB, that facilitates pilus extension [8-
59 11]. Many type IVa pilus systems also contain a retraction ATPase, called PilT, which
60 depolymerizes the pilus fiber and recycles pilin subunits into the inner membrane. Many type
61 IVa pilus systems also encode another putative ATPase called PilU. PilU is a homolog of the
62 retraction ATPase PilT, however, the function of this protein has remained unclear because PilU
63 is relatively understudied compared to PilT and because of phenotypic inconsistency for *pilU*
64 mutants in different organisms. For example, a *pilU* mutant of *Pseudomonas aeruginosa*,
65 exhibits reduced twitching motility [12], but in other type IV pilus systems, including the *V.*
66 *cholerae* competence pilus, loss of *pilU* does not reveal any overt phenotypes.

67 The facultative bacterial pathogen *Vibrio cholerae* uses a type IV competence pilus for DNA
68 uptake during natural transformation. We have recently demonstrated that the type IV
69 competence pili of *V. cholerae* can be fluorescently labeled by using a technique [13-15] in
70 which an amino acid of the major pilin subunit PilA is replaced with a cysteine ($PilA^{S67C}$;
71 previously misannotated as $PilA^{S81C}$) [16], which allows for subsequent labeling with a
72 fluorescently-labeled thiol-reactive maleimide dye (AF488-mal). This labeling approach does not
73 impede dynamic pilus activity and allows for the direct observation and measurement of pilus
74 extension and retraction by time-lapse epifluorescence microscopy. Using this labeling
75 technique, we have recently demonstrated that the retraction of DNA-bound type IV
76 competence pili is required to initiate the process of DNA uptake during natural transformation
77 [16].

78 Here, we employ our pilus labeling approach and complementary molecular methods to address
79 the role that PilU plays in type IV competence pilus retraction, and we extend our findings to the
80 type IVa competence pilus of *Acinetobacter baylyi*. Our results indicate that PilT and PilU form
81 independent homo-hexamers and that the ATPase activity of PilU promotes type IV pilus
82 retraction in a PilT-dependent manner.

83

84 # Results

85

86 ## PilU promotes type IV competence pilus retraction in a PilT-dependent manner

87 In order to study the function and role of ATPases in the retraction of type IV competence pili in
88 *V. cholerae*, we utilize two main methods: (1) our labeling approach to directly measure pilus
89 retraction via epifluorescence time-lapse microscopy and (2) assessing natural transformation,
90 which is dependent on competence pilus retraction [16, 17]. Also, as for other pili [18-20],

91 competence pili can mediate cell to cell interactions [21], which causes hyperpiliated strains to
92 aggregate and pellet to the bottom of culture tubes. Consistent with prior work [17, 22-27],
93 mutant strains that lack the retraction ATPase PilT are poorly transformable, exhibit markedly
94 reduced rates of pilus retraction, aggregate, and are hyperpiliated (≥3 pili per cell) compared to
95 the parent strain (**Fig 1A, 1B, 1D** and **1E**). Also, the number of cells that exhibit dynamic pilus
96 activity is reduced in the Δ*pilT* strain as observed by time-lapse epifluorescence microscopy,
97 which is consistent with the hyperpiliated phenotype of this mutant (**Fig 1C**). Because the
98 frequency of retraction was reduced by ~2 logs in the Δ*pilT* strain (**Fig 1C**), we could not obtain
99 enough events to make rigorous statistical comparisons. Regardless, these data show that
100 retraction rates are markedly reduced, albeit not significantly, in the Δ*pilT* background.

101 The residual retraction in a Δ*pilT* strain is not due to PilU because a Δ*pilT* Δ*pilU* double mutant
102 strain displays the same phenotype as a Δ*pilT* strain (**Fig 1A-E**). By contrast, Δ*pilU* mutants are
103 highly transformable, do not aggregate, exhibit normal numbers of pili and are largely
104 indistinguishable from the parent strain (**Fig 1A** and **1C-E**) aside from a significant 1.3-fold
105 reduction in retraction rates compared to the parent strain (**Fig 1B**). This effect of PilU on
106 retraction rate is much smaller compared to the ~50-fold reduction in retraction rate observed in
107 the Δ*pilT* and Δ*pilT* Δ*pilU* mutants (**Fig 1B**). This suggests that PilT can still mediate retraction
108 in a Δ*pilU* strain (because retraction frequency and rates for Δ*pilU* are closer to the parent than
109 the Δ*pilT* Δ*pilU* strain), while PilU cannot mediate retraction in a Δ*pilT* strain (since the Δ*pilT*
110 strain resembles the Δ*pilT* Δ*pilU* strain). Thus, these data support a model where PilT plays the
111 dominant role in pilus retraction, which is consistent with prior reports [16, 17, 25].

112 PilT is a predicted ATPase and its ATPase activity has been shown to be important in the
113 function of other type IV pilus systems [11, 28]. Therefore, we hypothesized that the ATPase
114 activity of PilT would be required for retraction of the competence pilus. We found, however, that
115 strains harboring mutations in PilT that putatively ablate the ATPase activity of this protein—due

116 to a mutation in either an invariantly conserved lysine in the Walker A motif required for ATP
117 binding (*pilT*^{K136A}), a mutation in a conserved glutamic acid in the Walker B motif required for
118 ATP hydrolysis (*pilT*^{E204A}), or a double mutant containing both mutations (*pilT*$^{E204A/K136A}$)— all
119 transform similarly to the parent strain and retract competence pili at rates that are at most ~4-
120 fold lower than the parent (**Fig 1A-B**). This is in stark contrast to a Δ*pilT* strain where the
121 transformation frequency is reduced ~4-logs and retraction is >50-fold slower compared to the
122 parent strain (**Fig 1A-B**). These results were quite surprising and suggested that either (1) the
123 ATPase activity of the retraction machinery is not critical for promoting pilus retraction, (2) that
124 the mutations to the Walker motifs do not ablate PilT ATPase activity, or (3) that another
125 retraction ATPase may promote retraction in the absence of PilT ATPase activity.

126 We tested the third model and specifically assessed whether PilU could promote retraction in
127 predicted PilT ATPase-deficient mutants. Indeed, we found that *pilT*^{K136A}Δ*pilU*, *pilT*^{E204A}Δ*pilU*
128 and *pilT*$^{E204A/K136A}$Δ*pilU* strains all display reduced transformation, are hyperpiliated, aggregate,
129 exhibit markedly reduced retraction frequency, and reduced retraction rates similar to a Δ*pilT*
130 Δ*pilU* strain (**Fig 1A-E**). This is consistent with PilU promoting retraction in the *pilT*^{K136A}, *pilT*^{E204A}
131 and *pilT*$^{E204A/K136A}$ backgrounds. Importantly, the *pilT*^{K136A}Δ*pilU*, *pilT*^{E204A}Δ*pilU* and
132 *pilT*$^{E204A/K136A}$Δ*pilU* strains could be complemented via ectopic expression of *pilT* or *pilU* (**S1**
133 **Fig**). Since loss of *pilT* alone (i.e. Δ*pilT*) results in a phenotype comparable to a Δ*pilT* Δ*pilU*
134 mutant, this result indicates that PilU is not sufficient to drive pilus retraction in the absence of
135 PilT (**Fig 1A-E**). Consistent with this, ectopic expression of *pilU* does not rescue the
136 transformation deficit of a Δ*pilT* Δ*pilU* mutant (**S1 Fig**). Together, these data suggest that PilU
137 supports pilus retraction in a PilT-dependent manner.

138 Interestingly, whereas a *pilT*^{K136A} Walker A mutant displays normal piliation, the *pilT*^{E204A}Walker
139 B mutant is hyperpiliated (**Fig 1D-E**). The frequency of cells that exhibit pilus retraction in the
140 *pilT*^{E204A} mutant is much lower than the parent and comparable to the Δ*pilT* Δ*pilU* strain (**Fig**

141 **1C**), which may explain this hyperpiliated phenotype; however, when pilus retraction is
142 observed, the rate of retraction is closer to that of the parent than the Δ*pilT* Δ*pilU* mutant (**Fig**
143 **1B**). Considering the canonical functions of the Walker A and B motifs in ATP-binding and
144 hydrolysis, respectively, the $pilT^{E204A}$ Walker B mutant should be able to bind to ATP but not
145 hydrolyze it. Because the putative ATP-binding deficient $pilT^{K136A}$ Walker A mutant exhibited
146 parental levels of piliation (**Fig 1D-E**), we hypothesized that the hyperpiliation observed in
147 $pilT^{E204A}$ may be due to the ATP-binding state of this mutant. Consistent with this, we found that
148 the Walker A and B double mutant ($pilT^{E204A/K136A}$) exhibits parent levels of piliation in contrast to
149 the $pilT^{E204A}$ single mutant (**Fig 1D-E**). These results indicate that the phenotype of the putative
150 ATP-binding deficient Walker A mutation ($pilT^{K136A}$) is dominant over the putative ATP-hydrolysis
151 deficient $pilT^{E204A}$ Walker B mutation. Both of these mutations should result in loss of ATPase
152 activity. Therefore, to avoid phenotypic consequences of variable states of ATP binding that
153 may be associated with the $pilT^{E204A}$ mutant, we utilized the $pilT^{K136A}$ mutant as a putative
154 ATPase-defective allele of PilT moving forward.

155

156 **PilU is required for forceful retraction**

157 The data thus far suggest that PilU is capable of supporting pilus retraction in putative PilT
158 ATPase-deficient mutants, but that PilU is not necessary to mediate pilus retraction (since Δ*pilU*
159 mutants transform at frequencies that are similar to the parent). PilU, however, is present in
160 many type IVa pilus systems, so the question remains: Why is PilU so widely conserved if it is
161 not necessary for pilus retraction? Recent work in *Pseudomonas aeruginosa* indicates that PilU
162 may be required for forceful retraction [29]. Our data thus far indicate that the Δ*pilU* mutant only
163 causes a modest reduction in the retraction rate (**Fig 1A**), which does not have a phenotypic
164 consequence on pilus-dependent DNA uptake (**Fig 1C**); however, these measurements are
165 based on free pili that are not retracting under load. We hypothesized that PilU might be

166 required for forceful retraction, such as when pili are attached to a surface. To test this, we
167 assessed pilus retraction using a micropillar assay in which binding of pili to micropillars and
168 subsequent retraction results in measurable bending and displacement of the micropillars.
169 These data can then be used to calculate the rates and force of pilus retraction [30]. In
170 agreement with our cell biological approach (i.e. pilus labeling), the micropillar assay showed
171 that retraction rates were reduced in both Δ*pilU* and Δ*pilT* strains; with PilT having a larger effect
172 on this rate (2-fold reduction for Δ*pilU* vs 14-fold reduction for Δ*pilT*) (**Fig 1B** and **1F**).
173 Importantly, the micropillar assay is more sensitive at detecting rare pilus retraction, which
174 allowed us to collect enough events to show that Δ*pilT* mutants are statistically significantly
175 reduced for retraction rates compared to the parent strain, which is consistent with previous
176 work [16]. In contrast, the Δ*pilU* and Δ*pilT* strains exhibited a similar reduction in the retraction
177 force (~2-fold for both) compared to the parent strain (**Fig 1G**). As other groups have also
178 reported, data collected on pilus retraction forces tend to be highly variable [16, 29, 31], which
179 we also observed here (**Fig 1G-H**). Despite this variability, a histogram reveals that PilT and
180 PilU promote retraction forces >12 pN because retraction events exceeding this force are
181 relatively rare in the Δ*pilT* and Δ*pilU* strains (**Fig 1H**). Thus far, we have shown that Δ*pilU* and
182 Δ*pilT* mutants display distinct phenotypes for transformation frequency (**Fig 1A**), retraction rates
183 (**Fig 1B** and **1F**) and piliation state (**Fig 1D-E**). Interestingly, the micropillar data reveal that
184 Δ*pilU* and Δ*pilT* mutants have a similar effect on retraction force (**Fig 1G-H**). This suggests that
185 PilU and PilT are both necessary for generating maximal retraction forces in the *V. cholerae*
186 competence pilus.

187

188 **The ATPase activities of PilT and PilU define the rate of type IV competence pilus**
189 **retraction**

190 Just like PilT, PilU is a PilT-like ATPase with a conserved lysine in its Walker A motif. Because
191 we observed that PilU supports pilus retraction in the *pilT*^{K136A} mutant (**Fig 1B**), we hypothesized
192 that the ATPase activity of PilU may be important for supporting pilus retraction. To test the
193 relative roles of each of these ATPases in pilus retraction, we mutated the conserved lysine in
194 the Walker A motifs of PilT and/or PilU. The *pilU*^{K134A} strain retracts ~1.5-fold slower than the
195 parent strain, similar to the Δ*pilU* mutant (**Fig 2A**). There may be a limited effect of the *pilU*^{K134A}
196 mutation on pilus retraction because this strain still has a functional PilT ATPase. However, we
197 hypothesized that PilU ATPase activity may be critical for retraction in a background where PilT
198 ATPase activity is also inactivated. Consistent with this, we found that a *pilT*^{K136A} *pilU*^{K134A} strain
199 is indistinguishable from a *pilT*^{K136A} Δ*pilU* strain for pilus retraction, piliation, aggregation, and
200 transformation (**Fig 2A-C**). Together, these data suggest that PilU ATPase activity promotes
201 type IV competence pilus retraction.

202 The data above suggest that the ATPase activities of PilT and PilU are critical for pilus
203 retraction. These ATPases are predicted to be motor proteins that facilitate the depolymerization
204 of pilus fibers. Thus, if we alter the ATPase rates of these motors, we hypothesized that this
205 should alter the rates of pilus retraction. To test this hypothesis, we mutated a leucine in the
206 Walker B domain of PilT and PilU to a cysteine, which was previously shown to reduce the rate
207 of ATP hydrolysis of *Neisseria gonorrhoeae* PilT ~2-fold [25]. When these Walker B mutations
208 were tested in isolation, they did not alter the rate of pilus retraction (comparing the parent strain
209 to *pilT*^{L201C} and *pilU*^{L199C}) (**Fig 2A**). This may be due to the fact that these cells still have one fully
210 functional retraction ATPase (i.e. *pilT*^{L201C} still has a fully functional PilU and *pilU*^{L199C} still has a
211 fully functional PilT). We hypothesized that these putatively Walker B "slow" ATPase mutations,
212 however, may have an impact on pilus retraction if they represented the sole functional
213 retraction ATPase in the cell. To that end, we generated both a *pilT*^{L201C} Δ*pilU* strain and a
214 *pilT*^{K136A} *pilU*^{L199C} strain. The *pilT*^{L201C} Δ*pilU* mutant showed a slight (1.3 fold), but significant,

215 reduction in retraction rate compared to the Δ*pilU* strain (**Fig 2A**), which provides genetic
216 evidence to suggest that the ATPase rate of PilT may be linked to the retraction rate of the type
217 IV competence pilus and further supports the idea that PilT promotes pilus retraction through its
218 ATPase activity. The *pilT*^{K136A} *pilU*^{L199C} mutant also showed a slight (1.5-fold) reduction in
219 retraction rate compared to *pilT*^{K136A}, although this difference was not statistically significant (**Fig**
220 **2A**). Because this difference was not statistically significant, it may suggest that the ATPase
221 rate of PilU does not dictate the retraction rate of competence pili even when it is the sole
222 retraction ATPase; however, because this mutant trended towards a decreased retraction rate,
223 this result may still suggest that the ATPase rate of PilU is linked to retraction rates.

224

225 **PilT and PilU directly interact with one another**

226 All of these data presented above indicate that PilT and PilU can both support pilus retraction.
227 Therefore, we hypothesized that PilT and PilU may interact to form a complex that supports
228 pilus retraction. To address this, we utilized a Bacterial Adenylate Cyclase Two-Hybrid (BACTH)
229 assay [32, 33]. As expected for predicted hexameric proteins like PilT and PilU, the BACTH
230 analysis showed PilT-PilT and PilU-PilU self-interactions (**Fig 3** and **S2 Fig**). Additionally, the
231 BACTH assay showed that PilT and PilU interact with one another, which is consistent with prior
232 work in other systems [32, 34], and further demonstrated that Walker A mutations in either
233 protein (PilT^{K136A} and PilU^{K134A}) did not disrupt this interaction (**Fig 3** and **S2 Fig**). Thus, our
234 BACTH results suggest that PilT and PilU may form a complex. These results do not, however,
235 indicate whether PilU and PilT form heteromeric complexes or homomeric complexes to
236 facilitate pilus retraction. We test this further below.

237

238 **PilT and PilU form independent homohexameric rings *in vitro* and *in vivo***

239 PilT in other systems has been shown to form a hexameric complex [35], and by homology we
240 hypothesized that PilU also forms a hexamer. Based on transformation frequency assays, N-
241 terminally tagged ^{6X}His-PilT and ^{6X}His-PilU were fully functional (**S3A Fig**). Therefore, we used
242 our purified ^{6X}His-PilT and ^{6X}His-PilU to characterize these proteins *in vitro*. Negative stain
243 transmission electron microscopy revealed that both ^{6X}His-PilT and ^{6X}His-PilU formed hexameric
244 ring complexes (**Fig 4A**). These results indicate that these proteins are capable of forming
245 independent homohexameric complexes *in vitro*. PilT and PilU have both sequence (~65%
246 similarity) and structural similarity to one another (**Fig 4A**), thus it is also possible that these
247 proteins can be incorporated into one ring and form heterohexameric complexes that facilitate
248 pilus retraction *in vivo*.

249 In order to test if PilT and PilU form heterohexamers or independent homohexamers to facilitate
250 pilus retraction *in vivo*, we hypothesized that overexpression of putative ATPase-inactive
251 mutants (i.e. PilT^{K136A} and PilU^{K134A}) in backgrounds that have native PilT and PilU would allow
252 us to distinguish between these two models. For example, if these proteins form heteromeric
253 complexes, then we would predict that overexpression of either putative ATPase-inactive
254 protein (PilT^{K136A} or PilU^{K134A}) should result in complexes that are mostly composed of ATPase-
255 inactive proteins and result in inhibition of pilus retraction (yielding a hyperpiliated phenotype)
256 and reduce rates of natural transformation (**Fig 4B**). If these proteins solely form homomeric
257 complexes, however, then we would predict that overexpression of only one ATPase-inactive
258 protein (PilT^{K136A} or PilU^{K134A}) should only inhibit the activity of one motor complex (PilT or PilU,
259 respectively) and should not have a dramatic effect on pilus retraction or natural transformation
260 because the other retraction motor would still be intact (**Fig 4B**).

261 In order for us to successfully test this question, we needed to: (1) be able to ectopically
262 overexpress ATPase deficient alleles of PilT or PilU, (2) demonstrate that ATPase deficient
263 alleles can interact with their ATPase sufficient counterparts and form proper hexamers, and (3)

264 show that ectopic expression of ATPase deficient alleles of PilT or PilU can inhibit the activity of
265 their respective natively expressed ATPase. We test each of these in turn below. First, we
266 confirmed that we could ectopically overexpress PilT and PilU. Using functional 3xFLAG-tagged
267 versions of PilT and PilU (**S3A-B Fig**), we show that our chromosomal P_{tac} regulated constructs
268 resulted in dramatic overexpression of these proteins (**S3C Fig**). Importantly, overexpression of
269 WT PilT and PilU did not affect pilus activity or natural transformation (**S1, S3B and S3D Figs**).
270 Next, we purified 6xHis-PilT^{K136A} and 6xHis-PilU^{K134A} and demonstrated that they formed ring
271 structures *in vitro* (**S3E Fig**), indicating that these proteins should form complexes with ATPase
272 sufficient alleles. This is also supported by our BACTH data (**Fig 3**). Finally, we wanted to
273 confirm that overexpressing the ATPase-inactive PilT^{K136A} or PilU^{K134A} could effectively impede
274 the function of the natively expressed ATPase-active PilT or PilU. To test this, we genetically
275 isolated either PilT or PilU as the sole functional retraction ATPase (i.e. PilT activity is isolated in
276 a Δ*pilU* background, while PilU activity is isolated in a *pilT*^{K136A} background) and then
277 overexpressed the cognate ATPase-inactive allele (P_{tac}-*pilT*^{K136A} or P_{tac}-*pilU*^{K134A}, respectively).
278 We assessed piliation, aggregation, and natural transformation as indicators of pilus retraction.
279 We found that, as expected, overexpression of ATPase-inactive alleles was sufficient to disrupt
280 the activity of the natively expressed ATPase (**Fig 4C-D** - compare Δ*pilU* to Δ*pilU* P_{tac}-*pilT*^{K136A}
281 and *pilT*^{K136A} to *pilT*^{K136A} P_{tac}-*pilU*^{K134A}). Also, as expected, overexpression of both ATPase-
282 deficient alleles together (P_{tac}-*pilT*^{K136A} and P_{tac}-*pilU*^{K134A}) in a background that has natively
283 expressed PilT and PilU, results in hyperpiliation, aggregation and reduced natural
284 transformation (**Fig 4C-D**), which further demonstrates that overexpression of these ATPase-
285 deficient proteins inhibits the activity of their natively expressed ATPase–sufficient versions.

286 The experiments above indicated that it would be feasible to test whether PilT and PilU formed
287 homomeric or heteromeric complexes *in vivo* as described in our model (**Fig 4B**). When we
288 overexpressed only one ATPase-deficient protein (P_{tac}-*pilT*^{K136A} or P_{tac}-*pilU*^{K134A}) in a background

289 that has natively expressed PilT and PilU, we found that piliation and transformation were
290 indistinguishable from the parent (**Fig 4C-D**). Thus, these data are consistent with PilT and PilU
291 forming independent homohexamers to facilitate pilus retraction.

292 Using our purified PilT and PilU, we also attempted to directly measure the ATPase activity of
293 these proteins. Unfortunately, the ATPase activity of these purified proteins was
294 indistinguishable from contaminating ATPases and/or below our detection limit (~1 nmol
295 pi/min/mg protein). Poor ATPase activity in purified retraction ATPases is not unique to our
296 system [11, 28, 36]. Alternatively, these results may suggest that the ATPase activities of these
297 proteins are stimulated *in vivo* via interaction with the proteins that compose the pilus machine,
298 as previously suggested [11]. Regardless, our previous *in vivo* data (**Fig 1A-D**) are consistent
299 with the *pilT*^{K136A} mutant being ATPase deficient.

300

301 The presence of PilT is not required for PilU to interact with the pilus platform
302 PilC.

303 Our data thus far indicate that PilU requires the presence of PilT (whether it is a functional
304 ATPase or not) to support optimal pilus retraction. The extension and retraction ATPases are
305 hypothesized to interact with the platform protein PilC to mechanically facilitate polymerization
306 and depolymerization of the pilus fiber [8, 34, 37]. Because PilU is dependent on the presence
307 of PilT to mediate retraction, we hypothesized that PilT can interact with PilC, but that PilU
308 cannot. To test this, we utilized the BACTH assay to test the interactions of PilT and PilU with
309 PilC. This assay showed that PilT and PilU could both interact with PilC, and that the Walker A
310 mutations of these ATPases (PilT^{K136A} and PilU^{K134A}) did not affect these interactions (**Fig 3**). It
311 is necessary to point out, however, that the BACTH assay cannot address relative affinities of
312 protein interactions due to non-native expression levels, but instead indicates the potential

313 presence or absence of an interaction. The biological relevance of these interactions will
314 depend on the relative affinities and concentrations of these proteins in their natural context.
315 The interaction between PilC and PilT supports the canonical model that retraction ATPases
316 interact with PilC to facilitate depolymerization of the pilus fiber. Interestingly, our data suggest
317 that PilC and PilU interact independently of PilT. This result is also supported by prior BACTH
318 analysis of *P. aeruginosa* pilus components [34]. Thus, the simple model of PilU requiring PilT
319 for interaction with the platform PilC appears to be incorrect.

320

321 The function of PilU as a PilT-dependent retraction ATPase is conserved in the 322 *Acinetobacter baylyi* competence pilus

323 As mentioned earlier, many type IVa pilus systems encode PilU in addition to the canonical
324 retraction ATPase PilT. Therefore, we sought to assess whether PilU could facilitate PilT-
325 dependent retraction in other type IV pilus systems. To test this, we studied the type IVa
326 competence pili of a distinct gammaproteobacterium *Acinetobacter baylyi*. *A. baylyi* competence
327 pili also mediate DNA-uptake and the genetic organization of *pilT* and *pilU* is similar to that
328 observed in *V. cholerae*.

329 The competence pili of *A. baylyi* likely facilitate DNA uptake in a retraction-dependent manner,
330 similar to the competence pili of *V. cholerae*. Thus, we employed natural transformation assays
331 to dissect the role that PilT and PilU play in *A. baylyi* competence pilus retraction. These assays
332 showed that the PilT and PilU of *A. baylyi* behave largely like the PilT and PilU of *V. cholerae*.
333 The *pilU* mutant of *A. baylyi* displays a significant (~13-fold) reduction in natural transformation
334 (**Fig 5**), unlike what is observed in *V. cholerae* (**Fig 1A**). This may be because DNA uptake in *A.*
335 *baylyi* requires more forceful retraction or because PilU plays a more important role in pilus
336 retraction in this species. Most importantly, however, we found that PilU facilitates natural

337 transformation (and therefore pilus retraction) in backgrounds where the ATPase activity of PilT
338 is putatively inactivated (by mutation of the invariantly conserved lysine in the Walker A
339 domain), but not in backgrounds where *pilT* is absent (**Fig 5** – compare *pilT*^{K136A} to *pilT*^{K136A}
340 Δ*pilU* and Δ*pilT*). Also, a strain where the ATPase activity of both PilT and PilU were putatively
341 inactivated (*pilT*^{K136A} *pilU*^{K137A}) resulted in the loss of transformation equivalent to a retraction
342 deficient background (e.g. Δ*pilTU*) or a strain lacking competence pili (Δ*comP*). Importantly,
343 strains lacking *pilT* (i.e. Δ*pilT* and Δ*pilTU*) could only be complemented via ectopic expression of
344 *pilT* but not *pilU*, while strains that contained an ATPase defective allele of *pilT* (i.e. *pilT*^{K136A}
345 Δ*pilU* or *pilT*^{K136A} *pilU*^{K137A}) could be complemented by ectopic expression of either *pilT* or *pilU*
346 (**S4 Fig**). These data are consistent with what was observed for *V. cholerae* competence pili
347 (**Fig 1A** and **S1 Fig**). These results demonstrate that PilU ATPase activity facilitates pilus
348 retraction in a PilT-dependent manner in two gammaproteobacteria (*V. cholerae* and *A. baylyi*),
349 and suggest that they may also extend to diverse type IVa pilus systems.

350

351 Discussion

352 This study sheds light on the function of PilU as a retraction ATPase of type IVa competence pili
353 in *V. cholerae*. Specifically, our data indicate that PilU can mediate pilus retraction in a PilT-
354 dependent manner likely through its ATPase activity. Our results also show that PilT and PilU
355 form independent homohexamers and that these proteins likely interact with each other and the
356 platform protein PilC. Furthermore, we demonstrate that the role of PilU in supporting pilus
357 retraction is conserved in at least one other type IVa pilus system.

358 Interestingly, previous work in other species has shown that ATPase mutations in PilT have a
359 greater effect on pilus function compared to the results we present here for both *A. baylyi* and *V.*
360 *cholerae* competence pili [11, 38]. It is possible that PilT ATPase mutations have a greater

361 effect on retraction depending on the pilus activity in question (for example twitching motility vs
362 DNA uptake). It is also possible that previous reports may have overlooked subtle effects of
363 mutations within the *pilT* gene on the expression of *pilU*, which is generally found downstream in
364 the same operon. Finally, it is also possible that PilU may not be able to compensate for the loss
365 of PilT ATPase activity in some pilus systems.

366 Our results indicate that PilU can only facilitate pilus retraction in the presence of PilT,
367 regardless of whether that PilT is a functional ATPase. These results are also supported by a
368 recent preprint from the Blokesch lab [39]. We initially tested the hypothesis that this was due to
369 a requirement for PilT to bridge PilU with the platform protein PilC. Our BACTH results,
370 however, indicated that PilU may directly interact with PilC in the absence of PilT (**Fig 3** and **S2**
371 **Fig**). While they may interact, it is possible that PilU does not bind and engage the PilC platform
372 in a conformation that would facilitate retraction. Alternatively, it is possible that PilU does bind
373 PilC in a conformation that can facilitate retraction but additional interactions with PilT are
374 required to stimulate PilU ATPase activity. Another possibility is that PilT interacts with other
375 components of the pilus machine that are required for stimulating retraction, and that PilU lacks
376 these interactions. Yet another possibility is that PilU enhances the processivity of the PilT
377 ATPase. Future efforts focused on the interaction network of the retraction ATPases with the
378 pilus machine should shed light on these various hypotheses.

379 Previous reports have shown that PilU is necessary for twitching motility in *P. aeruginosa* [12],
380 an activity that likely requires forceful retraction [29]. Consistent with this, our results indicate
381 that PilU is necessary for maximal retraction force for the competence pilus in *V. cholerae* (**Fig**
382 **1G-H**). Interestingly, because the Δ*pilU* mutant transforms similarly to the parent strain (**Figs 1A**
383 and **2B**), the forceful retraction mediated by PilU does not seem to be necessary for the function
384 of the *V. cholerae* competence pilus in DNA uptake under the conditions tested. However,

385 forceful PilU-dependent retraction may be necessary for DNA uptake when tDNA is absorbed
386 onto surfaces and/or in complex environments like biofilms.

387 Beyond altering the force of retraction, many mutants in PilT and PilU also reduced the speed of
388 pilus retraction relative to the parent strain (i.e. Δ*pilU* = ~1.3-fold, *pilT*^{K136A} = ~4.3-fold, *pilT*^{K136A}
389 *pilU*^{L199C} = ~6.5-fold, *pilU*^{K134A} = ~1.5-fold, *pilT*^{L201C} Δ*pilU* = ~1.7-fold) (**Figs 1B** and **2A**). This
390 revealed that altering the rates of these motor ATPases results in a corresponding reduction in
391 the rate of pilus retraction [40]. Additionally, despite this reduction in the speed of pilus
392 retraction, these mutants still transformed at levels that were comparable to the parent strain
393 (**Figs 1A** and **2B**). Thus, these results suggest that the absolute speed of competence pilus
394 retraction is not critical for DNA uptake during natural transformation. On the other hand, all
395 mutants that lack a functional retraction ATPase (Δ*pilT*, Δ*pilT*Δ*pilU*, *pilT*^{K136A} Δ*pilU*, *pilT*^{E204A}
396 Δ*pilU*, *pilT*$^{K136A/E204A}$ Δ*pilU*) showed a ~2-log reduction in the frequency of pilus retraction (**Fig**
397 **1C**). This revealed that functional retraction ATPases are crucial for generating high numbers of
398 retraction events, which may increase the likelihood of retracting a DNA-bound pilus. Further
399 experiments will focus on defining the parameters that are essential for DNA uptake.

400 Mutants that completely inactivated the retraction machinery (e.g. Δ*pilT*, Δ*pilT* Δ*pilU*, *pilT*^{K136A}
401 Δ*pilU*, *pilT*^{K136A} *pilU*^{K134A}) resulted in a hyperpiliated phenotype, lower transformation frequency
402 and a marked reduction in the frequency of pilus retraction (**Figs 1A, 1C-E**, **2A** and **2C**). These
403 strains, however, did display rare pilus retraction, which occurred at rates that were markedly
404 slower than the parent (>40-fold), and which was independent of PilT and PilU (**Figs 1B** and
405 **2A**). Recent work in *Neisseria* indicates that PilTU-independent retraction is not unique to the *V.*
406 *cholerae* type IVa competence pilus [31]. The mechanism underlying PilTU-independent
407 retraction remains unclear. One possibility is that an extension ATPase for another type IV pilus
408 system promotes this retraction. We have tested this in *V. cholerae* by mutating the extension
409 ATPases of the two other type IV pilus systems (MSHA and TCP) and found that PilTU-

410 independent retraction of the competence pilus still occurs in this background (**S5 Fig**). Thus,
411 suggesting that these other ATPases likely do not contribute to PilTU-independent retraction. It
412 remains possible that the competence pilus extension ATPase PilB supports PilTU-independent
413 retraction as suggested for the type IVc tad pili of *Caulobacter crescentus* where the same
414 ATPase bifunctionally promotes both pilus extension and retraction [40]. It is also possible that
415 PilTU-independent pilus retraction is due to an inherent instability of the pilus fiber. Uncovering
416 the mechanism underlying PilTU-independent retraction of the type IVa competence pilus [5] will
417 be the focus of future work.

418

419 # Materials and Methods

420

421 ## Bacterial strains and culture conditions

422 *Vibrio cholerae* and *A. baylyi* strains were routinely grown in LB Miller broth and on LB Miller
423 agar supplemented with erythromycin (10 µg/mL), kanamycin (50 µg/mL), and/or carbenicillin
424 (50 µg/mL) when appropriate.

425

426 ## Construction of mutant strains

427 All *V. cholerae* strains used throughout this study are derivatives of the El Tor isolate E7946. All
428 *A. baylyi* strains used were derivatives of strain ADP1 [41]. All mutant strains were constructed
429 via MuGENT and natural transformation using transforming DNA products made by splicing-by-
430 overlap extension (SOE) PCR exactly as previously described [42-45]. For a detailed list of all
431 mutant strains used throughout this study see **Table S1**. For a detailed list of all primers used to
432 construct mutant strains see **Table S2**.

433

434 **Natural transformation assays**

435 In order to induce competence in *V. cholerae* strains, the master competence regulator TfoX
436 was overexpressed using an IPTG-inducible or constitutive P_{tac} promoter and the cells were
437 genetically locked in a state of high cell density via deletion of *luxO* [43, 46-50]. Chitin-
438 independent transformation assays were performed exactly as previously described [44]. Briefly,
439 strains were grown overnight rolling at 30 ^{o}C with 100 μM IPTG then ~10^8 colony forming units
440 (CFU) were subcultured into 3mL of LB + 100 μM IPTG + 20 mM $MgCl_2$ + 10 mM $CaCl_2$ and
441 grown to late log. Next, ~10^8 CFU of this culture was diluted into instant ocean medium (7 g/L;
442 Aquarium Systems) supplemented with 100 μM IPTG and 500ng of transforming DNA was
443 added to each reaction and incubated statically at 30 ^{o}C overnight. The tDNA targeted VC1807,
444 a frame-shifted transposase, for deletion as previously described [42]. Negative control
445 reactions where no tDNA was added were also performed for each strain. After incubation with
446 tDNA, reactions were outgrown by adding 1mL of LB to each reaction and shaking (250 rpm) at
447 37 ^{o}C for ~2 hours. Reactions were then plated for quantitative culture onto medium selecting for
448 transformants (LB + 10 μg/mL Erythromycin) or onto plain LB for total viable counts. The
449 transformation frequency is defined as the number of transformants divided by the total viable
450 counts. For reactions where no transformants were obtained, a limit of detection was calculated
451 and plotted.

452 In order to sensitize natural transformation assays to differences in the efficiency of DNA
453 uptake, reactions were incubated with transforming DNA for shorter periods of time. These
454 assays were prepared exactly as described above, except that 10 units of DNase I (NEB) was
455 added to reactions 7 minutes after incubation with 500ng of transforming DNA. Reactions were
456 then incubated statically at 30°C overnight, outgrown, and plated exactly as described above.

457 For *A. baylyi*, transformations were performed exactly as previously described [51]. Briefly,
458 strains were grown overnight in LB medium. Then, ~10^8 cells were diluted into fresh LB
459 medium, and tDNA was added (~100 ng). Reactions were incubated at 30°C with agitation for 5
460 h and then plated for quantitative culture as described above to determine the transformation
461 frequency.

462

463 **Pilin labelling, imaging and quantification**

464 In order to label pili for observation with epifluorescence microscopy, strains were grown to the
465 late-log phase exactly as described above for natural transformation assays. Then, ~10^8 CFU
466 were spun down at 18,000 x g for 1 min and resuspended in instant ocean medium. Cells were
467 then incubated with 25 µg/mL AF488-mal for 15 minutes statically at room temperature in the
468 dark. Cells were washed twice using 100µL of instant ocean medium and resuspended to a final
469 concentration of ~10^7 CFU. Next, 2µL of these labeled cells were placed under an 0.2% gelzan
470 pad (made in instant ocean medium) on a coverslip and imaged on an inverted Nikon Ti-2
471 microscope with a Plan Apo ×60 objective, a green fluorescent protein filter cube, a Hamamatsu
472 ORCAFlash 4.0 camera and Nikon NIS Elements imaging software. In order to measure
473 retraction events, labelled cells were imaged by time-lapse microscopy in which a phase-
474 contrast (to image cell bodies) and fluorescent (to image labeled pili) image were taken every
475 second for 1-2 minutes or every 10 seconds for 10-15 minutes. Rates were calculated manually
476 using measurement tools in the NIS Elements analysis software. Only pili that were longer than
477 0.3 µm and completed retracting within the time-lapse window were analyzed.

478 In order to calculate the number of pili per cell, static images of cell bodies and labeled pili were
479 captured using phase-contrast and epifluorescence microscopy, respectively. Images from 3
480 independent biological replicates were sectioned into areas containing ~100-200 cells and the

481 total number of cells and the number of pili displayed on each cell was manually determined.
482 Representative images of the piliation state of strains were gathered and the lookup tables for
483 each phase or fluorescent image were adjusted to the same range.

484 In order to calculate the retraction frequency, time-lapse videos of cell bodies and labeled pili
485 were captured using phase-contrast and epifluorescence microscopy, respectively. Time-lapses
486 from 3 independent biological replicates were sectioned into areas containing ~300-1000 cells.
487 The number of cells that exhibited a pilus retraction event and the total number of cells in the
488 field was manually counted. This analysis was constrained to measuring pili that are greater
489 than 0.1 μM because shorter pili cannot be resolved by our pilus labeling approach.

490 To assess aggregation and pelleting of cultures, strains were grown to late log under the
491 conditions described above. Cultures were then allowed to sit statically at room temperature for
492 30-60 mins. Images of cultures were then taken against a white background.

493

494 **Protein expression and purification**

495 His tagged (6xHis) versions of PilT, PilT^{K136A}, PilU and PilU^{K134A} were cloned into a pHis
496 expression vector and verified by DNA sequencing (Eurofins). Vectors were transformed into *E.*
497 *coli* BL21 DE3 for expression and purification.

498 For purification of His-PilU and His-PilU^{K134A}, cells were grown in a 1L flask at 37°C with aeration
499 to an OD_{600} = 0.6. The culture was then induced by adding IPTG (1 mM) and grown to a final
500 OD_{600} = 4.0 at 30°C with aeration. Cells were harvested by centrifugation at 8,000 x g for 15 min
501 at room temperature and then resuspended in Buffer A [100 mM Tris pH 8.5, 300 mM KCl, 10%
502 glycerol, 20 mM Imidazole] and stored at -80°C. Pellets were thawed on ice and then lysozyme
503 (1 mg/mL) and DNase I (2 mg/L) were added before lysing via sonication with a probe tip
504 sonicator. The soluble fraction was clarified by centrifugation at 12,000 x g for 1 hour at 4°C.

505 The supernatant was loaded onto a nickel-charged HisTrap HP column (1mL; GE) using an
506 ÄKTA FPLC at room temperature. The column was then washed with Buffer A and the protein
507 was eluted with a gradient of Buffer B [100 mM Tris pH 8.5, 300 mM KCl, 10% glycerol, 500 mM
508 imidazole] and fractions were collected on ice. Elution fractions were separated on 15% SDS-
509 PAGE gels and stained with Coomassie Brilliant Blue R-250 (BioRad). Peak fractions were
510 pooled and dialyzed (Fisher, MWCO 12 kDa) into 500 mL Buffer C [100 mM Tris pH 8.5, 300
511 mM KCl, 10% glycerol] overnight, on a stir plate at 4°C. Then a second round of dialysis was
512 performed using 500 mL Buffer C for 4-6 hours, on a stir plate at 4°C. Following dialysis, the
513 protein concentration was determined using a Bradford Assay and aliquots were stored at -80C.

514 For purification of His-PilT and His-PilT^{K136A}, cells were grown in a 1L flask at 37°C with aeration
515 to an OD_{600} = 0.6. The culture was then induced by adding IPTG (1 mM) and grown overnight at
516 22°C with aeration. Cells were harvested by centrifugation at 8,000 x g for 15min at room
517 temperature and then resuspended in Buffer A [25 mM Tris pH 8.5, 300 mM KCl, 10% glycerol,
518 1 mM EDTA, 1 mM $MgCl_2$, 5 mM β-mercaptoethanol, 20 mM Imidazole] and stored at -80°C.
519 Pellets were thawed on ice and lysozyme (1 mg/mL), DNase I (2 mg/L) and PMSF (1 mM) were
520 added before lysing via sonication with a probe tip sonicator. The soluble fraction was clarified
521 by centrifugation at 12,000 x g for 1 hour at 4°C. The supernatant was loaded onto a nickel-
522 charged HisTrap HP column (1 mL; GE) using an ÄKTA FPLC at room temperature. The
523 column was then washed with Buffer A and the protein was eluted with a gradient of Buffer B
524 [25 mM Tris pH 8.5, 300 mM KCl, 10% glycerol, 1 mM EDTA, 1 mM $MgCl_2$, 5 mM β-
525 mercaptoethanol, 500 mM Imidazole] and fractions were collected on ice. Elution fractions were
526 separated on 15% SDS-PAGE gels and stained with Coomassie Brilliant Blue R-250 (BioRad).
527 Peak fractions were pooled and dialyzed (Fisher, MWCO 12 kDa) into 500 mL Buffer C [25 mM
528 Tris pH 8.5, 50 mM KCl, 10% glycerol, 1 mM EDTA, 1 mM $MgCl_2$, 0.5mM TCEP] overnight, on a
529 stir plate at 4°C. The next day, the eluate was concentrated with an Amicon conical filter

530 (MWCO 30 kDa) at 4,000 x g for 15 min at 4°C and resuspended to the original volume in Buffer
531 C twice. The protein concentration was determined using a Bradford Assay and then aliquots of
532 protein were snap-frozen with liquid nitrogen and stored at -80C.

533

534 **Bacterial Adenylate Cyclase Two-hybrid (BACTH) Assays**

535 The Bacterial Adenylate Cyclase Two-Hybrid (BACTH) system was employed to study protein
536 interactions. Gene inserts were amplified by PCR and cloned into pUT18C (Carb^{R}) and pKT25
537 (Kan^{R}) vectors to generate N-terminal fusions to the T18 and T25 fragments of adenylate
538 cyclase, respectively. Miniprepped vectors (Qiagen plasmid miniprep kit) were then
539 cotransformed into *E. coli* BTH101 and outgrown with 500 µL LB for 1 hour at 37°C with
540 shaking. Transformations were isolation streak plated on LB plates containing kanamycin 50
541 µg/mL and carbenicillin 100 µg/mL to select for transformants that had received both plasmids.
542 Strains were then grown statically at 30°C from frozen stocks overnight in LB supplemented with
543 kanamycin 50 µg/mL and carbenicillin 100 µg/mL and 3.5µL of each strain was then spotted
544 onto LB plates containing kanamycin 50 µg/mL, carbenicillin 100µg/mL, 0.5 mM IPTG and 40
545 µg/mL X-gal and incubated at 30°C for 48 hours.

546

547 **BACTH Miller Assays**

548 For BACTH Miller assays strains were prepared by growing the BTH101 strains with the
549 indicated pUT18C and pKT25 vectors statically overnight at 30°C in LB supplemented with
550 kanamycin 50 µg/mL and carbenicillin 100 µg/mL. Then 5 µL of this overnight culture was
551 subcultured into 3mL of LB supplemented with kanamycin 50 µg/mL, carbenicillin 100µg/mL and
552 0.5 mM IPTG and grown rolling at 30°C overnight. Cultures were then pelleted and resuspended

553 in 1 mL of Z buffer [60 mM Na_2HPO_4-$7H_2O$, 40 mM NaH_2PO_4-H_2O, 10 mM KCl, 2 mM $MgSO_4$-
554 $7H_2O$] to an OD_{600} = 0.5. 50µL of 1% SDS was added to each reaction and vortexed. 100µL of
555 chloroform was added to each reaction, vortexed again and then centrifuged for 1 min at 18,000
556 x g. The aqueous fraction was then mixed with ONPG (2.5 mg/mL) in a 96-well plate and the
557 OD_{420} and OD_{550} were measured every 5 minutes for 10 hours. Miller units were then calculated
558 at the time (in mins) when the A_{420} reached 0.3 or at 10 hours using the formula: [1000*(A_{420}-
559 (1.75*A_{550}))/ (mins*0.2 mL*A_{600})].

560

561 **Western Blotting**

562 Strains were grown to mid-log phase in LB with 100 µM IPTG if applicable and then
563 resuspended to an OD_{600} = 100 in TBS containing 1 mM PMSF. Cells were then lysed using a
564 FastPrep-24 (MP Bio). Lysates were centrifuged at 16,000 x g for 10 min at 4°C, and the
565 supernatant was then mixed 1:1 with 2X SDS sample buffer [220 mM Tris pH 6.8, 25% glycerol,
566 1.8% SDS, 0.02% Bromophenol Blue, 5% β-mercaptoethanol] and then 2uL of each sample
567 was separated on a 15% SDS PAGE gel. Proteins were transferred to a PVDF membrane and
568 incubated with one of the following primary antibodies: α-FLAG polyclonal rabbit (Sigma) or α-
569 RpoA monoclonal mouse (Biolegend). Then, blots were washed and incubated with a α-rabbit
570 or α-mouse secondary antibodies conjugated to IRdye 800CW. Blots were then imaged using
571 an Odyssey classic LI-COR system.

572

573 **Negative-stain electron microscopy**

574 Negative stain specimens were prepared by applying 4 µL of protein solution (0.1 mg/mL + 1
575 mM AMP-PnP) onto a glow-discharged 300-mesh copper grid coated with continuous carbon
576 film (EMS). After 30 s the protein solution was blotted with a piece of filter paper. The grid was

577 washed with 4 μL of milli-Q water and stained with 4 μL of stain solution (1% (w/v) uranyl
578 acetate, 0.5% (w/v) trehalose). The excess stain solution was removed by filter paper and the
579 grid was left to air dry. Due to the availability of the instrument, we used two different
580 transmission electron microscopes for data collection. For PilU, the data were collected on a
581 300-kV JEM-3200FS TEM equipped with FEG source and 8k x 8k Direct Electron DE-64
582 camera. A total of 32 micrograph images were taken at a nominal magnification of 60,000x,
583 which is equivalent to 1.56 Å per pixel. For PilT, the data were collected on a 120-kV JEM-
584 1400plus TEM equipped with LaB_6 source and a Gatan Oneview camera. A total of 59 images
585 were taken at a nominal magnification of 60,000x and the pixel size is 1.94 Å. To avoid potential
586 beam induced damage, minimum dose system was employed during data collection. Note that
587 PilU data were collected on a direct electron detector; therefore, each image contains 50 frames
588 and the frame alignment was performed using unblur program with exposure filter applied.
589 Particle picking, defocus estimation and phase flipped particles were all done using EMAN2
590 software package [52]. These particles were then imported into RELION (v2.1) for 2D
591 classification, Initial model building, 3D refinement, and 3D classification [53]. From 2D
592 classification results, we observed clearly 2-fold symmetry [8, 54]; thus, the symmetry operation
593 was applied to subsequent 3D refinement and 3D classification. The final 3D reconstructions
594 were computed from 45204 particles to 15.6 Å for PilU and 17472 particles to 20.8 Å for PilT.
595 The resolution estimation was calculated using gold-standard method at Fourier shell correlation
596 of 0.143 as implemented in RELION. The 3D reconstructions were rendered using UCSF
597 Chimera where the handedness of PilU was chosen to be consistent with PilT [55]. The
598 negative stain 3D reconstruction of PilU and PilT with C2 symmetry have been deposited into
599 EMDB (ID: EMD-20519, EMD-20520 respectively).
600

601 **Micropillar retraction assay**

602 To ensure that all measurements recorded were due to type IV competence pili, all the
603 experiments were performed with *V. cholerae* strains lacking all external appendages other than
604 type IV competence pili as well as exopolysaccharide production (i.e. mutants lacking flagella,
605 MSHA pili, TCP pili and *Vibrio* polysaccharide (VPS) production). Strains were grown overnight
606 in LB either directly from frozen stocks or from a single colony from an LB agar plate. Of the
607 overnight liquid culture, 50 µl was subcultured into 3 ml LB + 100 µM IPTG + 20 mM $MgCl_2$ + 10
608 mM $CaCl_2$ and allowed to grow at 30°C for 4h. Then, 100 µl of this culture was centrifuged for 5
609 min at 20,000 x *g* and the bacteria were resuspended in instant ocean medium. At different
610 times, 23 µl of the resuspension were added to micropillars in an observation chamber as
611 previously reported [14]. Briefly, silica molds were inverted on activated coverslips with
612 polyacrylamide gels in between. The result is an array of flexible micropillars in a hexagonal
613 array of 3 µm × 3 µm.Once the bacteria were in contact with the micropillars, 10-Hz movies of
614 the top of the pillars were recorded. The motion of the tips of the pillars was tracked using a
615 cross-correlation algorithm in ImageJ. The amplitude and speeds of the pillars' motions were
616 then analyzed using MATLAB. Finally, we calibrated the pillars' stiffness constant using optical
617 tweezers as previously described [30]. The pillars used in this study have a stiffness constant of
618 17±4pNµm−1.

619

620 **Statistics**

621 Statistical differences were assessed by one-way ANOVA tests followed by a multiple
622 comparisons post test (either Tukey's or Dunnett's) using GraphPad Prism software. For all
623 transformation frequency experiments and frequency of pilus retraction experiments, statistical
624 analyses were performed on log transformed data. All means and statistical comparisons can
625 be found in **S3** and **S4 Tables**.

Acknowledgements

We would like to thank CK Ellison for helpful discussions. We would like to acknowledge JD Newman and CE Dann III for their advice during protein purification. We thank JC van Kessel for providing strains associated with BACTH assays. We would like to thank Lakshay Khosla and Vijay Deopersaud for technical assistance with micropillar experiments. We also thank JA Lorah for assistance with statistical analyses. This work was supported by grants R35GM128674 and AI118863 from the National Institutes of Health to ABD, and by grant AI116566 from the National Institutes of Health to NB.

References

1. Burrows LL. Pseudomonas aeruginosa twitching motility: type IV pili in action. Annu Rev Microbiol. 2012;66:493-520. Epub 2012/07/04. doi: 10.1146/annurev-micro-092611-150055. PubMed PMID: 22746331.
2. Maier B, Wong GCL. How Bacteria Use Type IV Pili Machinery on Surfaces. Trends Microbiol. 2015;23(12):775-88. doi: 10.1016/j.tim.2015.09.002. PubMed PMID: 26497940.
3. Hospenthal MK, Costa TRD, Waksman G. A comprehensive guide to pilus biogenesis in Gram-negative bacteria. Nat Rev Microbiol. 2017;15(6):365-79. Epub 2017/05/13. doi: 10.1038/nrmicro.2017.40. PubMed PMID: 28496159.
4. Proft T, Baker EN. Pili in Gram-negative and Gram-positive bacteria - structure, assembly and their role in disease. Cell Mol Life Sci. 2009;66(4):613-35. Epub 2008/10/28. doi: 10.1007/s00018-008-8477-4. PubMed PMID: 18953686.
5. Craig L, Forest KT, Maier B. Type IV pili: dynamics, biophysics and functional consequences. Nat Rev Microbiol. 2019. Epub 2019/04/17. doi: 10.1038/s41579-019-0195-4. PubMed PMID: 30988511.
6. Craig L, Pique ME, Tainer JA. Type IV pilus structure and bacterial pathogenicity. Nat Rev Microbiol. 2004;2(5):363-78. doi: 10.1038/nrmicro885. PubMed PMID: 15100690.
7. !!! INVALID CITATION !!! [7-9].
8. McCallum M, Tammam S, Khan A, Burrows LL, Howell PL. The molecular mechanism of the type IVa pilus motors. Nat Commun. 2017;8:15091. doi: 10.1038/ncomms15091. PubMed PMID: 28474682; PubMed Central PMCID: PMCPMC5424180.
9. Chiang P, Habash M, Burrows LL. Disparate subcellular localization patterns of Pseudomonas aeruginosa Type IV pilus ATPases involved in twitching motility. J Bacteriol. 2005;187(3):829-39. doi: 10.1128/JB.187.3.829-839.2005. PubMed PMID: 15659660; PubMed Central PMCID: PMCPMC545728.
10. Craig L, Volkmann N, Arvai AS, Pique ME, Yeager M, Egelman EH, et al. Type IV pilus structure by cryo-electron microscopy and crystallography: implications for pilus assembly and

663 functions. Mol Cell. 2006;23(5):651-62. doi: 10.1016/j.molcel.2006.07.004. PubMed PMID:
664 16949362.
665 11. Jakovljevic V, Leonardy S, Hoppert M, Sogaard-Andersen L. PilB and PilT are ATPases
666 acting antagonistically in type IV pilus function in Myxococcus xanthus. J Bacteriol.
667 2008;190(7):2411-21. doi: 10.1128/JB.01793-07. PubMed PMID: 18223089; PubMed Central
668 PMCID: PMCPMC2293208.
669 12. Whitchurch CB, Mattick JS. Characterization of a gene, pilU, required for twitching
670 motility but not phage sensitivity in Pseudomonas aeruginosa. Mol Microbiol. 1994;13(6):1079-
671 91. Epub 1994/09/01. PubMed PMID: 7854122.
672 13. Blair KM, Turner L, Winkelman JT, Berg HC, Kearns DB. A molecular clutch disables
673 flagella in the Bacillus subtilis biofilm. Science. 2008;320(5883):1636-8. Epub 2008/06/21. doi:
674 10.1126/science.1157877. PubMed PMID: 18566286.
675 14. Ellison CK, Kan J, Dillard RS, Kysela DT, Ducret A, Berne C, et al. Obstruction of pilus
676 retraction stimulates bacterial surface sensing. Science. 2017;358(6362):535-8. Epub
677 2017/10/28. doi: 10.1126/science.aan5706. PubMed PMID: 29074778; PubMed Central PMCID:
678 PMCPMC5805138.
679 15. Ellison CK, Dalia TN, Dalia AB, Brun YV. Real-time microscopy and physical
680 perturbation of bacterial pili using maleimide-conjugated molecules. Nat Protoc. 2019. doi:
681 10.1038/s41596-019-0162-6. PubMed PMID: 31028374.
682 16. Ellison CK, Dalia TN, Vidal Ceballos A, Wang JC, Biais N, Brun YV, et al. Retraction of
683 DNA-bound type IV competence pili initiates DNA uptake during natural transformation in Vibrio
684 cholerae. Nat Microbiol. 2018;3(7):773-80. Epub 2018/06/13. doi: 10.1038/s41564-018-0174-y.
685 PubMed PMID: 29891864.
686 17. Seitz P, Blokesch M. DNA-uptake machinery of naturally competent Vibrio cholerae.
687 Proc Natl Acad Sci U S A. 2013;110(44):17987-92. Epub 2013/10/16. doi:
688 10.1073/pnas.1315647110. PubMed PMID: 24127573; PubMed Central PMCID:
689 PMCPMC3816411.
690 18. Bieber D, Ramer SW, Wu CY, Murray WJ, Tobe T, Fernandez R, et al. Type IV pili,
691 transient bacterial aggregates, and virulence of enteropathogenic Escherichia coli. Science.
692 1998;280(5372):2114-8. PubMed PMID: 9641917.
693 19. Chamot-Rooke J, Mikaty G, Malosse C, Soyer M, Dumont A, Gault J, et al.
694 Posttranslational modification of pili upon cell contact triggers N. meningitidis dissemination.
695 Science. 2011;331(6018):778-82. doi: 10.1126/science.1200729. PubMed PMID: 21311024.
696 20. Helaine S, Carbonnelle E, Prouvensier L, Beretti JL, Nassif X, Pelicic V. PilX, a pilus-
697 associated protein essential for bacterial aggregation, is a key to pilus-facilitated attachment of
698 Neisseria meningitidis to human cells. Mol Microbiol. 2005;55(1):65-77. doi: 10.1111/j.1365-
699 2958.2004.04372.x. PubMed PMID: 15612917.
700 21. Adams DW, Stutzmann S, Stoudmann C, Blokesch M. DNA-uptake pili of Vibrio
701 cholerae are required for chitin colonization and capable of kin recognition via sequence-specific
702 self-interaction. Nat Microbiol. 2019. doi: 10.1038/s41564-019-0479-5. PubMed PMID:
703 31182799.
704 22. Dietrich M, Mollenkopf H, So M, Friedrich A. Pilin regulation in the pilT mutant of
705 Neisseria gonorrhoeae strain MS11. FEMS Microbiol Lett. 2009;296(2):248-56. doi:
706 10.1111/j.1574-6968.2009.01647.x. PubMed PMID: 19486161; PubMed Central PMCID:
707 PMCPMC4428587.
708 23. Merz AJ, So M, Sheetz MP. Pilus retraction powers bacterial twitching motility. Nature.
709 2000;407(6800):98-102. doi: 10.1038/35024105. PubMed PMID: 10993081.
710 24. Pujol C, Eugene E, Marceau M, Nassif X. The meningococcal PilT protein is required for
711 induction of intimate attachment to epithelial cells following pilus-mediated adhesion. Proc Natl
712 Acad Sci U S A. 1999;96(7):4017-22. PubMed PMID: 10097155; PubMed Central PMCID:
713 PMCPMC22412.

714 25. Hockenberry AM, Hutchens DM, Agellon A, So M. Attenuation of the Type IV Pilus
715 Retraction Motor Influences Neisseria gonorrhoeae Social and Infection Behavior. MBio.
716 2016;7(6). doi: 10.1128/mBio.01994-16. PubMed PMID: 27923924; PubMed Central PMCID:
717 PMCPMC5142622.
718 26. Wolfgang M, Lauer P, Park HS, Brossay L, Hebert J, Koomey M. PilT mutations lead to
719 simultaneous defects in competence for natural transformation and twitching motility in piliated
720 Neisseria gonorrhoeae. Mol Microbiol. 1998;29(1):321-30. PubMed PMID: 9701824.
721 27. Leighton TL, Dayalani N, Sampaleanu LM, Howell PL, Burrows LL. Novel Role for PilNO
722 in Type IV Pilus Retraction Revealed by Alignment Subcomplex Mutations. J Bacteriol.
723 2015;197(13):2229-38. doi: 10.1128/JB.00220-15. PubMed PMID: 25917913; PubMed Central
724 PMCID: PMCPMC4455263.
725 28. Aukema KG, Kron EM, Herdendorf TJ, Forest KT. Functional dissection of a conserved
726 motif within the pilus retraction protein PilT. J Bacteriol. 2005;187(2):611-8. doi:
727 10.1128/JB.187.2.611-618.2005. PubMed PMID: 15629932; PubMed Central PMCID:
728 PMCPMC543540.
729 29. Tala L, Fineberg A, Kukura P, Persat A. Pseudomonas aeruginosa orchestrates
730 twitching motility by sequential control of type IV pili movements. Nat Microbiol. 2019. Epub
731 2019/02/26. doi: 10.1038/s41564-019-0378-9. PubMed PMID: 30804544.
732 30. Biais N, Higashi D, So M, Ladoux B. Techniques to measure pilus retraction forces.
733 Methods Mol Biol. 2012;799:197-216. doi: 10.1007/978-1-61779-346-2_13. PubMed PMID:
734 21993648; PubMed Central PMCID: PMCPMC5160128.
735 31. Zollner R, Cronenberg T, Maier B. Motor properties of PilT-independent type 4 pilus
736 retraction in gonococci. J Bacteriol. 2019. doi: 10.1128/JB.00778-18. PubMed PMID: 30692169.
737 32. Georgiadou M, Castagnini M, Karimova G, Ladant D, Pelicic V. Large-scale study of the
738 interactions between proteins involved in type IV pilus biology in Neisseria meningitidis:
739 characterization of a subcomplex involved in pilus assembly. Mol Microbiol. 2012;84(5):857-73.
740 doi: 10.1111/j.1365-2958.2012.08062.x. PubMed PMID: 22486968.
741 33. Karimova G, Pidoux J, Ullmann A, Ladant D. A bacterial two-hybrid system based on a
742 reconstituted signal transduction pathway. Proc Natl Acad Sci U S A. 1998;95(10):5752-6. Epub
743 1998/05/20. PubMed PMID: 9576956; PubMed Central PMCID: PMCPMC20451.
744 34. McCallum M, Tammam S, Little DJ, Robinson H, Koo J, Shah M, et al. PilN Binding
745 Modulates the Structure and Binding Partners of the Pseudomonas aeruginosa Type IVa Pilus
746 Protein PilM. J Biol Chem. 2016;291(21):11003-15. doi: 10.1074/jbc.M116.718353. PubMed
747 PMID: 27022027; PubMed Central PMCID: PMCPMC4900251.
748 35. Forest KT, Satyshur KA, Worzalla GA, Hansen JK, Herdendorf TJ. The pilus-retraction
749 protein PilT: ultrastructure of the biological assembly. Acta Crystallogr D Biol Crystallogr.
750 2004;60(Pt 5):978-82. Epub 2004/04/23. doi: 10.1107/S0907444904006055. PubMed PMID:
751 15103158.
752 36. Jones CJ, Utada A, Davis KR, Thongsomboon W, Zamorano Sanchez D, Banakar V, et
753 al. C-di-GMP Regulates Motile to Sessile Transition by Modulating MshA Pili Biogenesis and
754 Near-Surface Motility Behavior in Vibrio cholerae. PLoS Pathog. 2015;11(10):e1005068. doi:
755 10.1371/journal.ppat.1005068. PubMed PMID: 26505896; PubMed Central PMCID:
756 PMCPMC4624765.
757 37. Takhar HK, Kemp K, Kim M, Howell PL, Burrows LL. The platform protein is essential for
758 type IV pilus biogenesis. J Biol Chem. 2013;288(14):9721-8. doi: 10.1074/jbc.M113.453506.
759 PubMed PMID: 23413032; PubMed Central PMCID: PMCPMC3617274.
760 38. Chiang P, Sampaleanu LM, Ayers M, Pahuta M, Howell PL, Burrows LL. Functional role
761 of conserved residues in the characteristic secretion NTPase motifs of the Pseudomonas
762 aeruginosa type IV pilus motor proteins PilB, PilT and PilU. Microbiology. 2008;154(Pt 1):114-
763 26. doi: 10.1099/mic.0.2007/011320-0. PubMed PMID: 18174131.

764 39. Adams DW, Stutzmann S, Stoudman C, Blokesch M. DNA-uptake pilus of Vibrio
765 cholerae capable of kin-discriminated auto-aggregation. bioRxiv. 2018:doi.org/10.1101/354878.
766 Epub June 26, 2018.
767 40. Ellison CK, Kan J, Chlebek JL, Hummels KR, Panis G, Viollier PH, et al. A bifunctional
768 ATPase drives tad pilus extension and retraction. bioRxiv. 2019:616128. doi: 10.1101/616128.
769 41. Juni E, Janik A. Transformation of Acinetobacter calco-aceticus (Bacterium anitratum). J
770 Bacteriol. 1969;98(1):281-8. PubMed PMID: 5781579; PubMed Central PMCID:
771 PMCPMC249934.
772 42. Dalia AB. Natural Cotransformation and Multiplex Genome Editing by Natural
773 Transformation (MuGENT) of Vibrio cholerae. Methods Mol Biol. 2018;1839:53-64. Epub
774 2018/07/27. doi: 10.1007/978-1-4939-8685-9_6. PubMed PMID: 30047054.
775 43. Dalia AB, McDonough E, Camilli A. Multiplex genome editing by natural transformation.
776 Proc Natl Acad Sci U S A. 2014;111(24):8937-42. Epub 2014/06/04. doi:
777 10.1073/pnas.1406478111. PubMed PMID: 24889608; PubMed Central PMCID:
778 PMCPMC4066482.
779 44. Dalia TN, Yoon SH, Galli E, Barre FX, Waters CM, Dalia AB. Enhancing multiplex
780 genome editing by natural transformation (MuGENT) via inactivation of ssDNA exonucleases.
781 Nucleic Acids Res. 2017;45(12):7527-37. Epub 2017/06/03. doi: 10.1093/nar/gkx496. PubMed
782 PMID: 28575400; PubMed Central PMCID: PMCPMC5499599.
783 45. Dalia AB, Lazinski DW, Camilli A. Characterization of undermethylated sites in Vibrio
784 cholerae. J Bacteriol. 2013;195(10):2389-99. Epub 2013/03/19. doi: 10.1128/JB.02112-12.
785 PubMed PMID: 23504020; PubMed Central PMCID: PMCPMC3650525.
786 46. Zhu J, Miller MB, Vance RE, Dziejman M, Bassler BL, Mekalanos JJ. Quorum-sensing
787 regulators control virulence gene expression in Vibrio cholerae. Proc Natl Acad Sci U S A.
788 2002;99(5):3129-34. doi: 10.1073/pnas.052694299. PubMed PMID: 11854465; PubMed Central
789 PMCID: PMCPMC122484.
790 47. Lo Scrudato M, Blokesch M. The regulatory network of natural competence and
791 transformation of Vibrio cholerae. PLoS Genet. 2012;8(6):e1002778. doi:
792 10.1371/journal.pgen.1002778. PubMed PMID: 22737089; PubMed Central PMCID:
793 PMCPMC3380833.
794 48. Lo Scrudato M, Blokesch M. A transcriptional regulator linking quorum sensing and chitin
795 induction to render Vibrio cholerae naturally transformable. Nucleic Acids Res. 2013;41(6):3644-
796 58. doi: 10.1093/nar/gkt041. PubMed PMID: 23382174; PubMed Central PMCID:
797 PMCPMC3616704.
798 49. Meibom KL, Blokesch M, Dolganov NA, Wu CY, Schoolnik GK. Chitin induces natural
799 competence in Vibrio cholerae. Science. 2005;310(5755):1824-7. doi:
800 10.1126/science.1120096. PubMed PMID: 16357262.
801 50. Dalia AB, Lazinski DW, Camilli A. Identification of a membrane-bound transcriptional
802 regulator that links chitin and natural competence in Vibrio cholerae. MBio. 2014;5(1):e01028-
803 13. Epub 2014/01/30. doi: 10.1128/mBio.01028-13. PubMed PMID: 24473132; PubMed Central
804 PMCID: PMCPMC3903286.
805 51. Nero TM, Dalia TN, Wang JC, Kysela DT, Bochman ML, Dalia AB. ComM is a
806 hexameric helicase that promotes branch migration during natural transformation in diverse
807 Gram-negative species. Nucleic Acids Res. 2018;46(12):6099-111. Epub 2018/05/04. doi:
808 10.1093/nar/gky343. PubMed PMID: 29722872; PubMed Central PMCID: PMCPMC6158740.
809 52. Ludtke SJ. Single-Particle Refinement and Variability Analysis in EMAN2.1. Methods
810 Enzymol. 2016;579:159-89. Epub 2016/08/31. doi: 10.1016/bs.mie.2016.05.001. PubMed
811 PMID: 27572727; PubMed Central PMCID: PMCPMC5101015.
812 53. Scheres SH. Semi-automated selection of cryo-EM particles in RELION-1.3. J Struct
813 Biol. 2015;189(2):114-22. Epub 2014/12/09. doi: 10.1016/j.jsb.2014.11.010. PubMed PMID:
814 25486611; PubMed Central PMCID: PMCPMC4318617.

815 54. Satyshur KA, Worzalla GA, Meyer LS, Heiniger EK, Aukema KG, Misic AM, et al. Crystal
816 structures of the pilus retraction motor PilT suggest large domain movements and subunit
817 cooperation drive motility. Structure. 2007;15(3):363-76. doi: 10.1016/j.str.2007.01.018. PubMed
818 PMID: 17355871; PubMed Central PMCID: PMCPMC1978094.
819 55. Pettersen EF, Goddard TD, Huang CC, Couch GS, Greenblatt DM, Meng EC, et al.
820 UCSF Chimera--a visualization system for exploratory research and analysis. J Comput Chem.
821 2004;25(13):1605-12. Epub 2004/07/21. doi: 10.1002/jcc.20084. PubMed PMID: 15264254.

822

823 # Figure Legends

824

825 **Fig 1. PilU mediates type IVa competence pilus retraction in a PilT-dependent manner in**
826 ***V. cholerae*.**

827 **(A)** Natural transformation assays of the indicated strains. Reactions were incubated with 500
828 ng of transforming DNA overnight. Transformation frequency is reported as the fraction of cells
829 that were transformed in each reaction (i.e. the number of transformants / total viable counts).
830 Parent, *n* = 11, all other strains, *n* = 4. **(B)** Retraction rates of the indicated strains measured by
831 epifluorescence time-lapse microscopy of AF488-mal labeled cells. Data are from three
832 independent biological replicates; Parent, *n* = 68. Δ*pilU*, *n* = 56. Δ*pilT*, *n* = 9. Δ*pilT*Δ*pilU*, *n* = 18.
833 $pilT^{K136A}$, *n* = 66. $pilT^{K136A}$Δ*pilU*, *n* = 9. $pilT^{E204A}$, *n* = 5. $pilT^{E204A/K136A}$, *n* = 50. $pilT^{E204A}$ Δ*pilU*, *n* =
834 17. $pilT^{E204A/K136A}$ Δ*pilU*, *n* = 6. **(C)** Frequency of retraction of the indicated strains measured by
835 counting number of cells that exhibit a retraction event over a given time-lapse. Data are from
836 three independent biological replicates; Parent, *n* = 1141. Δ*pilU*, *n* = 824. Δ*pilT*, *n* = 6681.
837 Δ*pilT*Δ*pilU*, *n* = 3806. $pilT^{K136A}$, *n* = 1048. $pilT^{K136A}$Δ*pilU*, *n* = 997. $pilT^{E204A}$, *n* = 4311.
838 $pilT^{E204A/K136A}$, *n* = 866. $pilT^{E204A}$ Δ*pilU*, *n* = 7243. $pilT^{E204A/K136A}$ Δ*pilU*, *n* = 6216. **(D)**
839 Representative images of surface piliation (top) and aggregation phenotypes (bottom) for the
840 indicated strains. Scale bar, 1 μm. **(E)** The percentage of cells with 0, <3 or ≥3 surface pili was
841 determined from a static image. Data are from three independent biological replicates; Parent, *n*
842 = 453. Δ*pilU*, *n* = 413. Δ*pilT*, *n* = 381. Δ*pilT*Δ*pilU*, *n* = 425. $pilT^{K136A}$, *n* = 417. $pilT^{K136A}$ Δ*pilU*, *n* =
843 413. $pilT^{E204A}$, *n* = 579. $pilT^{E204A/K136A}$, *n* = 713. $pilT^{E204A}$ Δ*pilU*, *n* = 806. $pilT^{E204A/K136A}$ Δ*pilU*, *n* =
844 705. **(F)** Retraction rate (Parent, *n* = 95. Δ*pilU*, *n* = 83. Δ*pilT*, *n* = 324. Δ*pilT* Δ*pilU*, *n* = 125) and
845 the **(G)** Box plot and **(H)** Histogram of the retraction force (Parent, *n* = 101. Δ*pilU*, *n* = 90. Δ*pilT*,
846 *n* = 372. Δ*pilT* Δ*pilU*, *n* = 43) was measured via micropillar assays. All bar graphs are shown as
847 the mean ± SD. All Box plots represent the median and the upper and lower quartile, while the

848 whiskers demarcate the range. Asterisk(s) directly above bars denote comparisons to the parent
849 strain. All comparisons were made by one-way ANOVA with Tukey's post test. LOD, limit of
850 detection; NS, not significant; ** = $P < 0.01$, *** = $P < 0.001$.
851
852 **Fig 2. The ATPase activity of PilT and PilU mediate pilus retraction.**
853 **(A)** Retraction rates of the indicated strains measured by epifluorescence time-lapse
854 microscopy of AF488-mal labeled cells. Box plots represent the median and the upper and
855 lower quartile, while the whiskers demarcate the range. Data are from three independent
856 biological replicates; *pilU*^{K134A}, $n = 70$. *pilT*^{K136A} *pilU*^{K134A}, $n = 8$. *pilT*^{K136A} *pilU*^{L199C}, $n = 46$.
857 *pilU*^{L199C}, $n = 49$. *pilT*^{L201C}, $n = 54$. *pilT*^{L201C} Δ*pilU*, $n = 54$. Δ*pilT pilU*^{L199C}, $n = 11$. Data for the
858 retraction rates of the parent, Δ*pilU,* and *pilT*^{K136A} strains are identical to those shown in **Fig 1B**
859 and plotted again here to facilitate comparisons to the mutant strains indicated. **(B)** Natural
860 transformation assays of the indicated strains incubated with 500 ng of transforming DNA
861 overnight. Data are shown as the mean ± SD. Parent, $n = 6$. All other strains, $n = 4$**. (C)**
862 Representative images of surface piliation (top) and aggregation phenotypes (bottom) for the
863 indicated strains. Scale bar, 1 μm. Asterisk(s) directly above bars denote comparisons to the
864 parent strain. All comparisons were made by one-way ANOVA with Tukey's post test. NS, not
865 significant; * = $P < 0.05$, *** = $P < 0.001$.
866
867 **Fig 3. PilT and PilU interact with each other and the pilus platform protein PilC.**
868 Bacterial Adenylate Cyclase Two-Hybrid (BACTH) assays were performed to test pair-wise
869 interactions between full length PilT, PilU, PilT^{K136A}, PilU^{K134A}, and PilC that were N-terminally
870 fused to the T18- and T25- fragments of adenylate cyclase. Each construct was also tested for
871 interactions with empty T18 and T25 vectors as a negative control. Leucine zipper fusions to
872 T18 and T25 were used as the positive control (+) and empty T18 and T25 vectors served as an

873 additional negative control (-). **(A)** Representative image of the BACTH assay plated on X-gal-
874 containing media. **(B)** BACTH miller assays of the indicated pairwise interactions. The dotted
875 line represents the β-galactosidase activity of the empty vector negative control. Data are shown
876 as the mean ± SD and are from three independent experiments. Statistical analysis of these
877 data can be found in **S2 Fig**.
878
879 **Fig 4. PilT and PilU form independent homomeric complexes *in vitro* and *in vivo* to**
880 **facilitate pilus retraction.**
881 **(A)** Representative negative stain transmission electron micrographs of purified ^{6X}His-PilT and
882 ^{6X}His-PilU (left; scale bar, 50 nm). 2D class averages revealing hexameric rings (middle; scale
883 bar, 10 nm) and 3D reconstructions (right) of the ring complex imposing C2 symmetry. **(B)**
884 Schematic of the experimental approach and expected outcomes for testing whether PilT and
885 PilU form homomeric or heteromeric complexes to facilitate pilus retraction *in vivo*. **(C)** Natural
886 transformation assays of indicated strains incubated with 500 ng of tDNA and after 7 minutes,
887 DNAseI was added to prevent additional DNA uptake. The genotype of native *pilT* and *pilU*
888 alleles are written below each bar graph and the presence or absence of a chromosomally-
889 integrated IPTG-inducible ectopic allele of $pilT^{K136A}$ or $pilU^{K134A}$ is indicated by a + or -. Strains
890 were grown with 100 μM IPTG if they contained an ectopic expression construct. Data are
891 shown as the mean ± SD and are from four independent biological replicates. **(D)**
892 Representative images of surface piliation (top) and aggregation phenotypes (bottom) for the
893 indicated strains. Scale bar, 1 μm. Asterisk(s) directly above bars denote comparisons to the
894 parent strain. All comparisons were made by one-way ANOVA with Tukey's post test. NS, not
895 significant; *** = $P < 0.001$.
896
897 **Fig 5. PilU supports pilus retraction in a PilT-dependent manner in *A. baylyi.***

898 Natural transformation assays of the indicated strains incubated with 500ng of transforming
899 DNA for 5 hours. Data are shown as the mean ± SD. Parent, n = 5. Δ*comP*, n = 6. All other
900 strains, n = 4. Asterisk(s) directly above bars denote comparisons to parent strain. All
901 comparisons were made by one-way ANOVA with Tukey's post test. LOD, limit of detection; NS
902 = not significant; *** = $P < 0.001$.
903

904 ## Supporting Figure Legends

905 **S1 Fig. Complementation analysis of *V. cholerae* mutant strains via ectopic expression of**
906 ***pilT* or *pilU*.**
907 Natural transformation assays of the indicated strains. All strains contain either a
908 chromosomally integrated IPTG-inducible P_{tac}-*pilT* (white bars) or P_{tac}-*pilU* (gray bars) construct
909 as indicated. Data show that ectopic overexpression of PilT and PilU does not affect the
910 transformation frequency of the parent strain. Ectopic overexpression of PilT rescued the
911 transformation of all strains that showed a substantial reduction in natural transformation in **Fig**
912 **1A** and **Fig 2B** (i.e. Δ*pilT*, Δ*pilT* Δ*pilU*, $pilT^{K136A}$ Δ*pilU*, $pilT^{E204A}$ Δ*pilU*, $pilT^{E204A/K136A}$ Δ*pilU*, and
913 $pilT^{K136A}$ $pilU^{K134A}$). Ectopic overexpression of PilU rescued all strains except for strains that
914 lacked a copy of *pilT* (i.e. Δ*pilT*, Δ*pilT* Δ*pilU*). All strains were grown with 100 μM IPTG to
915 ectopically induce PilT or PilU. Data are shown as the mean ± SD. Parent, n = 8. All other
916 strains, n = 4. Asterisk(s) directly above bars denote comparisons to the appropriate parent
917 strain. Comparisons were made by grouping data into the two families indicated by the white
918 and grey bars. A one-way ANOVA was performed for each family with a Dunnet's post to
919 compare each experimental sample to the parent strain. Comparisons were not statistically
920 significantly different unless otherwise noted. *** = $P < 0.001$.
921

922 **S2 Fig. PilT and PilU interact with each other and the pilus platform protein PilC.**
923 BACTH Miller assays showing all data from **Fig 3B** with additional negative controls for every
924 T25- or T18-fusion. Data are shown as the mean ± SD from three independent experiments.
925 The dotted line represents the β-galactosidase activity of the empty vector negative control
926 (T18-empty x T25-empty). Comparisons were made by grouping data into appropriate families
927 indicated by the black lines above the bar graph. A one-way ANOVA was performed on each
928 family with a Dunnet's post test to compare each experimental group to the appropriate negative
929 control (indicated by the longer black line). A single set of asterisks directly above the group line
930 denotes the statistical results for all comparisons in that family unless otherwise noted. NS, not
931 significant; * = $P < 0.05$; *** = $P < 0.001$.
932
933 **S3 Fig. PilT and PilU form homomeric complexes to facilitate pilus retraction**.
934 **(A)** Natural transformation assays showing that 6xHis and 3xFLAG N-terminal fusions to PilT
935 and PilU are functional. The indicated strains were incubated with 500 ng of transforming DNA
936 overnight. Parent, $n = 8$. All others, $n = 4$. **(B)** Natural transformation assays showing that
937 overexpression of 3xFLAG tagged PilT/PilU/PilT^{K136A}/PilU^{K134A} behave the same as non-tagged
938 proteins when ectopically overexpressed in the indicated backgrounds. Strains were incubated
939 with 500 ng of transforming DNA and after 7 minutes, DNAse I was added to prevent additional
940 DNA uptake. Parent, $n = 5$. *pilT*^{K136A}, $n = 5$. All others, $n = 4$. **(C)** Western blot of the indicated
941 strains to detect FLAG tagged-proteins and RpoA as a loading control. Strains containing an
942 IPTG regulated P_{tac} constuct were grown in the presence of 100 μM IPTG. This blot indicates
943 that ectopic induction of 3xFLAG tagged PilT/PilU/PilT^{K136A}/PilU^{K134A} results in robust
944 overexpression of proteins above native levels. Data is representative of three independent
945 experiments. **(D)** Natural transformation assays where the indicated strains were incubated with
946 500 ng of transforming DNA for 7 minutes prior to the addition of DNAse I to prevent additional

947 DNA uptake. These data indicate that ectopic overexpression of PilT or PilU can rescue strains
948 with a substantial reduction in transformation frequency. All strains with P_{tac} constructs were
949 grown with 100 μM IPTG to overexpress PilT or PilU. All bar graphs are shown as the mean ±
950 SD. Asterisk(s) directly above bars denote comparisons to parent strain. All comparisons were
951 made by one-way ANOVA followed with Tukey's post test. LOD, limit of detection; *** = $P <$
952 0.001. **(E)** Representative negative stain transmission electron micrographs showing that
953 purified ^{6X}His-PilT^{K136A} and ^{6X}His-PilU^{K134A} form hexamers *in vitro.* Scale bar, 100 nm.
954
955 **S4 Fig. Complementation analysis of *A. baylyi* mutant strains via ectopic expression of**
956 ***pilT* or *pilU*.**
957 Natural transformation assays of the indicated *A. baylyi* strains. Strains harbored pMMB-*pilT*
958 (white bars), pMMB-*pilU* (gray bars), or no vector (black bar). Data indicate that ectopic
959 overexpression of PilT and PilU do not affect the transformation frequency of the parent strain.
960 Ectopic overexpression of PilT rescued the transformation of all strains that showed a significant
961 reduction in natural transformation in **Fig 5** (i.e. Δ*pilT*, Δ*pilT* Δ*pilU*, *pilT*^{K136A} Δ*pilU*, and *pilT*^{K136A}
962 *pilU*^{K137A}). Ectopic overexpression of PilU rescued all strains except for strains that lacked a
963 copy of pilT (i.e. Δ*pilT* and Δ*pilT* Δ*pilU*). All strains were grown with 100 μM IPTG to induce
964 expression of *pilT* or *pilU*. Data are shown as the mean ± SD and are from three independent
965 experiments. Asterisk(s) directly above bars denote comparisons to the appropriate parent
966 strain. Comparisons were made by grouping data into the two families indicated by the white
967 and grey bars. A one-way ANOVA was performed for each family followed by Dunnet's post test
968 to compare each experimental group to the parent strain. Comparisons were not statistically
969 significantly different from the relevant parent unless otherwise noted. *** = $P < 0.001$.
970

971 **S5 Fig. The components of the *V. cholerae* MSHA or TCP type IV pilus systems do not contribute**
972 **to PilTU-independent retraction of the competence pilus.**
973 Natural transformation assays of the indicated strains. Reactions were incubated with 500 ng of
974 transforming DNA overnight. ΔMSHA and ΔTCP represent deletions of the entire locus for both pilus
975 systems, which includes the extension ATPase associated with each. Data are shown as the mean ± SD
976 and are from four independent biological replicates. All comparisons were made by one-way ANOVA
977 with Tukey's post test. NS, not significant.
978

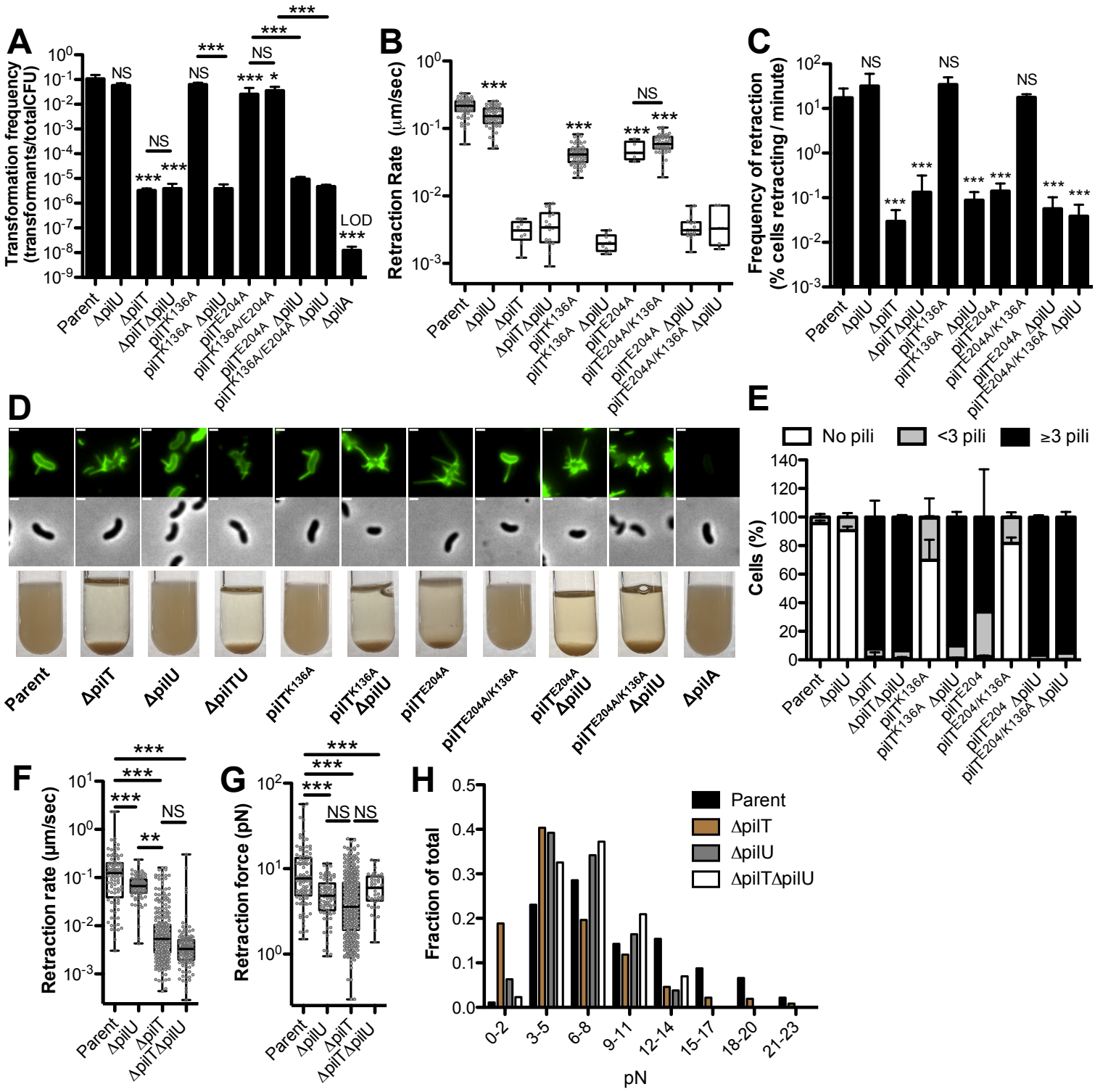

Fig 1. PilU mediates type IVa competence pilus retraction in a PilT-dependent manner in *V. cholerae*. (A) Natural transformation assays of the indicated strains. Reactions were incubated with 500 ng of transforming DNA overnight. Transformation frequency is reported as the fraction of cells that were transformed in each reaction (i.e. the number of transformants / total viable counts). Parent, n = 11, all other strains, n = 4. **(B)** Retraction rates of the indicated strains measured by epifluorescence time-lapse microscopy of AF488-mal labeled cells. Data are from three independent biological replicates; Parent, n = 68. Δ*pilU*, n = 56. Δ*pilT*, n = 9. Δ*pilT*Δ*pilU*, n = 18. *pilT*^{K136A}, n = 66. *pilT*^{K136A}Δ*pilU*, n = 9. *pilT*^{E204A}, n = 5. *pilT*$^{E204A/K136A}$, n = 50. *pilT*^{E204A} Δ*pilU*, n = 17. *pilT*$^{E204A/K136A}$ Δ*pilU*, n = 6. **(C)** Frequency of retraction of the indicated strains measured by counting number of cells that exhibit a retraction event over a given time-lapse. Data are from three independent biological replicates; Parent, n = 1141. Δ*pilU*, n = 824. Δ*pilT*, n = 6681. Δ*pilT*Δ*pilU*, n = 3806. *pilT*^{K136A}, n = 1048. *pilT*^{K136A}Δ*pilU*, n = 997. *pilT*^{E204A}, n = 4311. *pilT*$^{E204A/K136A}$, n = 866. *pilT*^{E204A} Δ*pilU*, n = 7243. *pilT*$^{E204A/K136A}$ Δ*pilU*, n = 6216. **(D)** Representative images of surface piliation (top) and aggregation phenotypes (bottom) for the indicated strains. Scale bar, 1 μm. **(E)** The percentage of cells with 0, <3 or ≥3 surface pili was determined from a static image. Data are from three independent biological replicates; Parent, n = 453. Δ*pilU*, n = 413. Δ*pilT*, n = 381. Δ*pilT*Δ*pilU*, n = 425. *pilT*^{K136A}, n = 417. *pilT*^{K136A} Δ*pilU*, n = 413. *pilT*^{E204A}, n = 579. *pilT*$^{E204A/K136A}$, n = 713. *pilT*^{E204A} Δ*pilU*, n = 806. *pilT*$^{E204A/K136A}$ Δ*pilU*, n = 705. **(F)** Retraction rate (Parent, n = 95. Δ*pilU*, n = 83. Δ*pilT*, n = 324. Δ*pilT* Δ*pilU*, n = 125) and the **(G)** Box plot and **(H)** Histogram of the retraction force (Parent, n = 101. Δ*pilU*, n = 90. Δ*pilT*, n = 372. Δ*pilT* Δ*pilU*, n = 43) was measured via micropillar assays. All bar graphs are shown as the mean ± SD. All Box plots represent the median and the upper and lower quartile, while the whiskers demarcate the range. Asterisk(s) directly above bars denote comparisons to the parent strain. All comparisons were made by one-way ANOVA with Tukey's post test. LOD, limit of detection; NS, not significant; ** = P < 0.01, *** = P < 0.001.

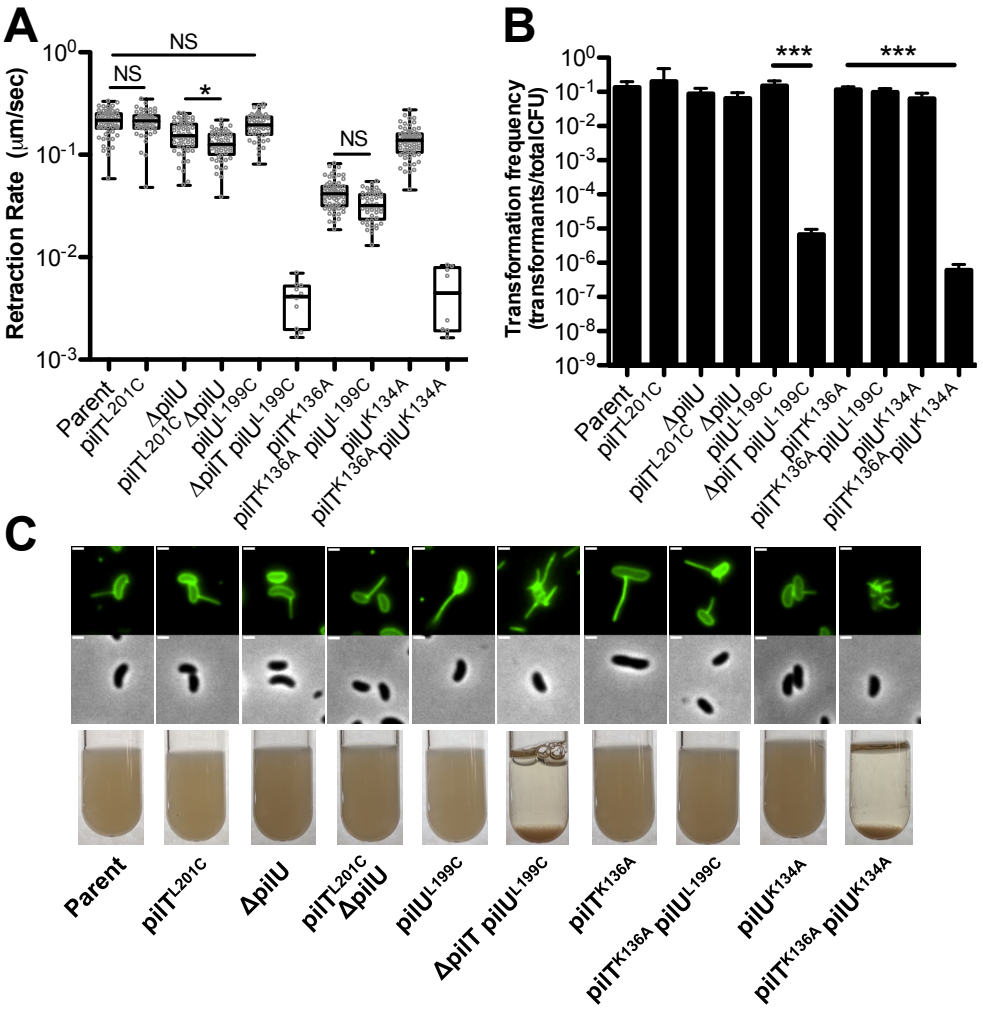

Fig 2. The ATPase activity of PilT and PilU mediate pilus retraction. (A) Retraction rates of the indicated strains measured by epifluorescence time-lapse microscopy of AF488-mal labeled cells. Box plots represent the median and the upper and lower quartile, while the whiskers demarcate the range. Data are from three independent biological replicates; *pilU*^{K134A}, *n* = 70. *pilT*^{K136A} *pilU*^{K134A}, *n* = 8. *pilT*^{K136A} *pilU*^{L199C}, *n* = 46. *pilU*^{L199C}, *n* = 49. *pilT*^{L201C}, *n* = 54. *pilT*^{L201C} Δ*pilU*, *n* = 54. Δ*pilT pilU*^{L199C}, *n* = 11. Data for the retraction rates of the parent, Δ*pilU,* and *pilT*^{K136A} strains are identical to those shown in **Fig 1B** and plotted again here to facilitate comparisons to the mutant strains indicated. **(B)** Natural transformation assays of the indicated strains incubated with 500 ng of transforming DNA overnight. Data are shown as the mean ± SD. Parent, *n* = 6. All other strains, *n* = 4**. (C)** Representative images of surface piliation (top) and aggregation phenotypes (bottom) for the indicated strains. Scale bar, 1 μm. Asterisk(s) directly above bars denote comparisons to the parent strain. All comparisons were made by one-way ANOVA with Tukey's post test. NS, not significant; * = $P < 0.05$, *** = $P < 0.001$.

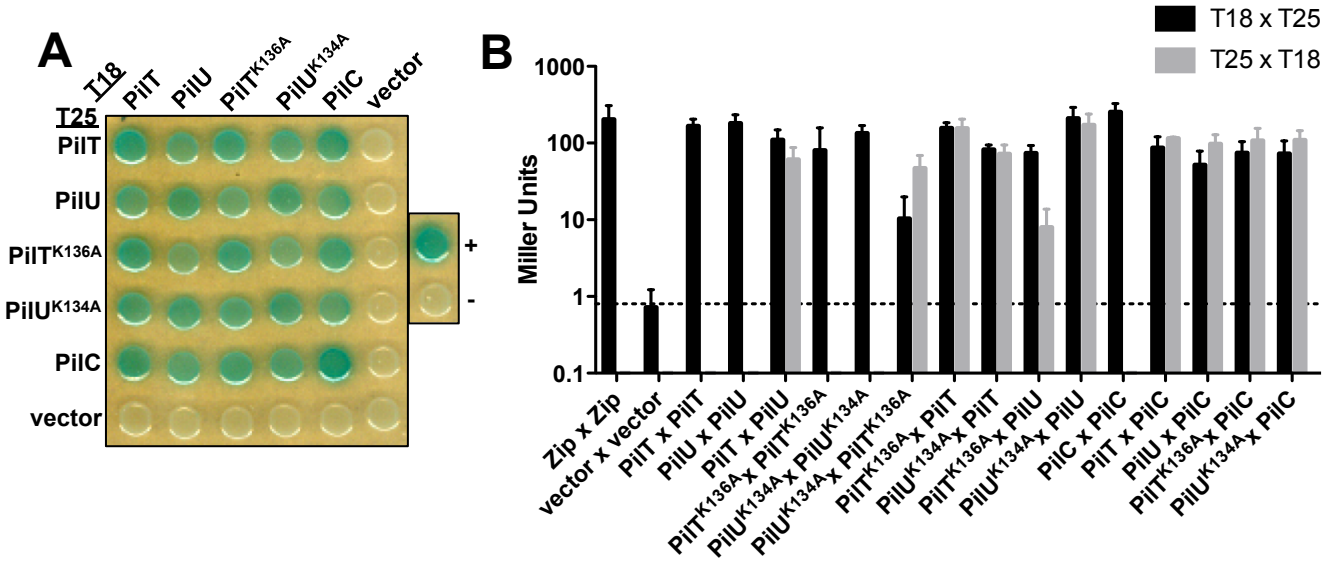

Fig 3. PilT and PilU interact with each other and the pilus platform protein PilC. Bacterial Adenylate Cyclase Two-Hybrid (BACTH) assays were performed to test pair-wise interactions between full length PilT, PilU, PilT^{K136A}, PilU^{K134A}, and PilC that were N-terminally fused to the T18- and T25- fragments of adenylate cyclase. Each construct was also tested for interactions with empty T18 and T25 vectors as a negative control. Leucine zipper fusions to T18 and T25 were used as the positive control (+) and empty T18 and T25 vectors served as an additional negative control (-). **(A)** Representative image of the BACTH assay plated on X-gal-containing media. **(B)** BACTH miller assays of the indicated pairwise interactions. The dotted line represents the β-galactosidase activity of the empty vector negative control. Data are shown as the mean ± SD and are from three independent experiments. Statistical analysis of these data can be found in **S2 Fig**.

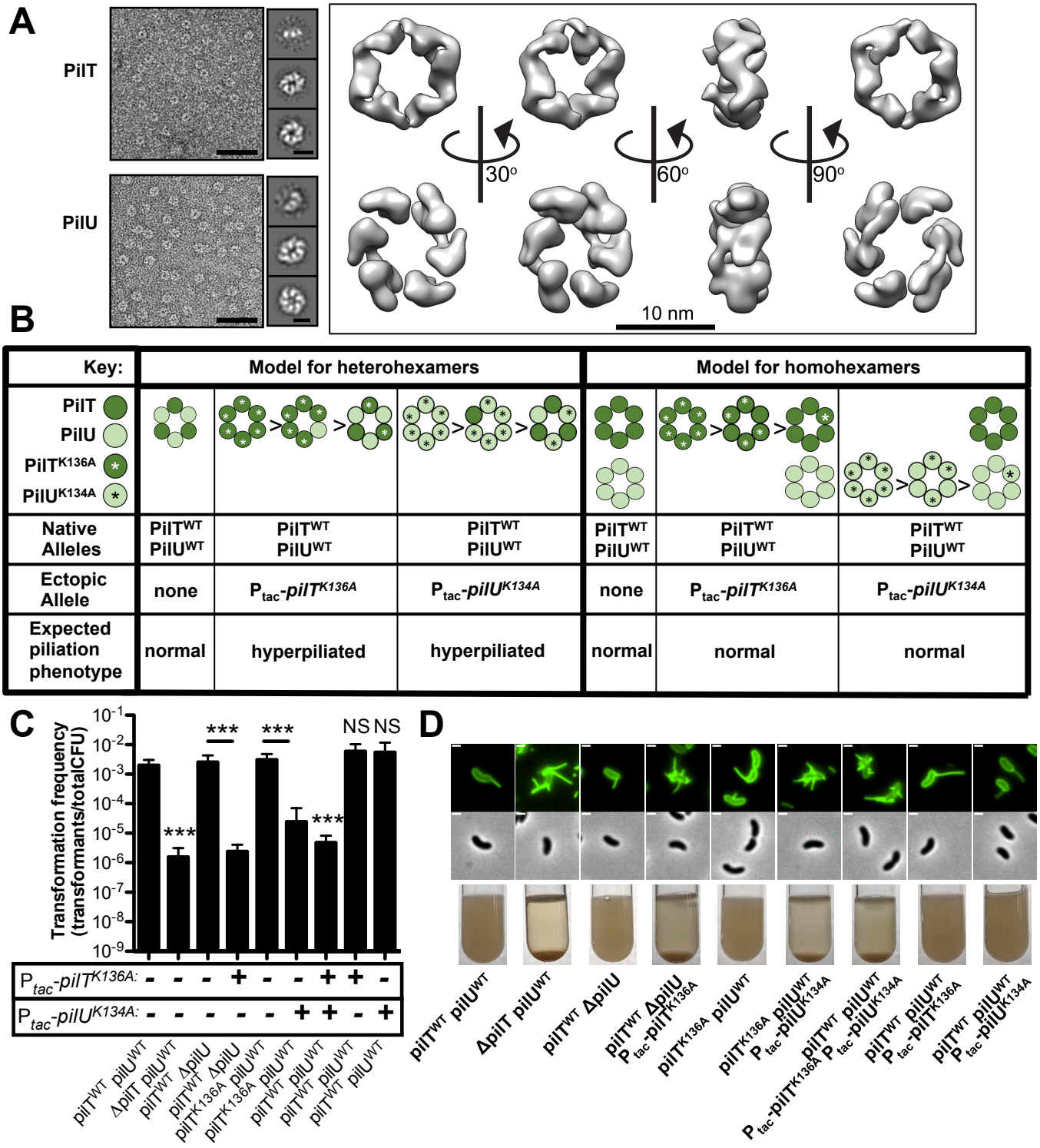

Fig 4. PilT and PilU form independent homomeric complexes *in vitro* and *in vivo* to facilitate pilus retraction. (A) Representative negative stain transmission electron micrographs of purified ^{6X}His-PilT and ^{6X}His-PilU (left; scale bar, 50 nm). 2D class averages revealing hexameric rings (middle; scale bar, 10 nm) and 3D reconstructions (right) of the ring complex imposing C2 symmetry. **(B)** Schematic of the experimental approach and expected outcomes for testing whether PilT and PilU form homomeric or heteromeric complexes to facilitate pilus retraction *in vivo*. **(C)** Natural transformation assays of indicated strains incubated with 500 ng of tDNA and after 7 minutes, DNAseI was added to prevent additional DNA uptake. The genotype of native *pilT* and *pilU* alleles are written below each bar graph and the presence or absence of a chromosomally-integrated IPTG-inducible ectopic allele of *pilT*^{K136A} or *pilU*^{K134A} is indicated by a + or -. Strains were grown with 100 μM IPTG if they contained an ectopic expression construct. Data are shown as the mean ± SD and are from four independent biological replicates. **(D)** Representative images of surface piliation (top) and aggregation phenotypes (bottom) for the indicated strains. Scale bar, 1 μm. Asterisk(s) directly above bars denote comparisons to the parent strain. All comparisons were made by one-way ANOVA with Tukey's post test. NS, not significant; *** = $P < 0.001$.

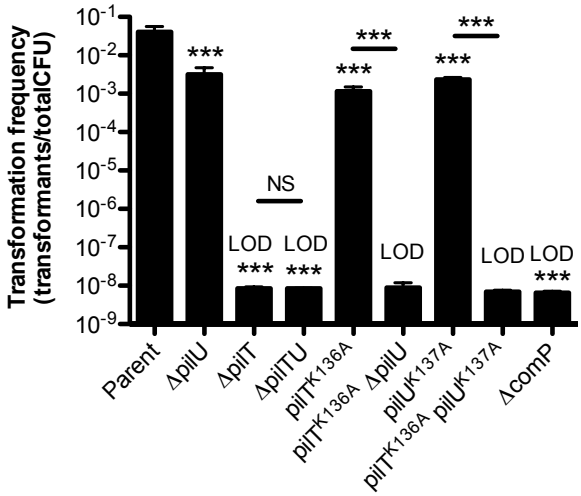

Fig 5. PilU supports pilus retraction in a PilT-dependent manner in *A. baylyi.* Natural transformation assays of the indicated strains incubated with 500ng of transforming DNA for 5 hours. Data are shown as the mean ± SD. Parent, $n = 5$. Δ*comP*, $n = 6$. All other strains, $n = 4$. Asterisk(s) directly above bars denote comparisons to parent strain. All comparisons were made by one-way ANOVA with Tukey's post test. LOD, limit of detection; NS = not significant; *** = $P < 0.001$.

Supporting Information for

PilT and PilU are homohexameric ATPases that coordinate to retract type IVa pili

Jennifer L. Chlebek[1], Hannah Q. Hughes[1], Aleksandra S. Ratkiewicz[2], Rasman Rayyan[2], Joseph Che-Yen Wang[3], Brittany E. Herrin[1], Triana N. Dalia[1], Nicolas Biais[2], and Ankur B. Dalia[1,*]

[1]Department of Biology, Indiana University, 1001 E. 3rd Street, Bloomington, IN 47405.

[2]Biology Department, CUNY Brooklyn College, 2900 Bedford Avenue, Brooklyn, NY 11210 and Graduate Center of CUNY, 365 5th Avenue, NY 10016.

[3]Electron Microscopy Center, Indiana University, Bloomington, IN 47405.

*Correspondence to: ankdalia@indiana.edu.

This PDF file includes:

S1-S5 Figs
S1-S4 Tables

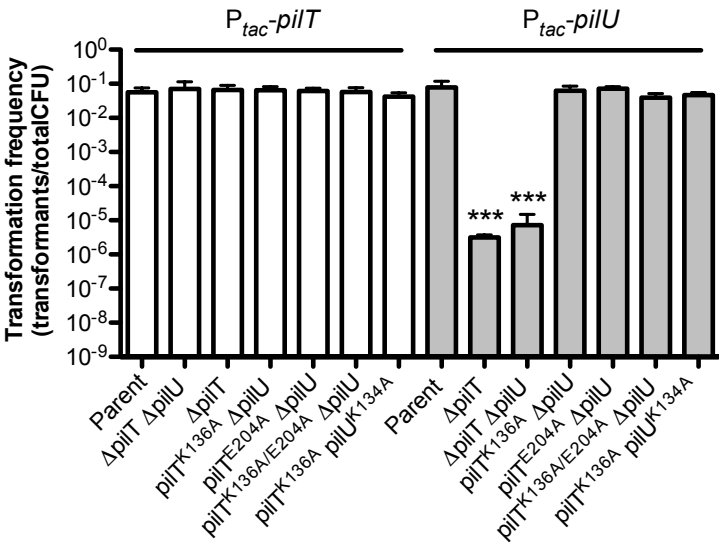

S1 Fig. Complementation analysis of *V. cholerae* mutant strains via ectopic expression of *pilT* or *pilU*. Natural transformation assays of the indicated strains. All strains contain either a chromosomally integrated IPTG-inducible P$_{tac}$-*pilT* (white bars) or P$_{tac}$-*pilU* (gray bars) construct as indicated. Data show that ectopic overexpression of PilT and PilU does not affect the transformation frequency of the parent strain. Ectopic overexpression of PilT rescued the transformation of all strains that showed a substantial reduction in natural transformation in **Fig 1A** and **Fig 2B** (i.e. Δ*pilT*, Δ*pilT* Δ*pilU*, *pilT*^{K136A} Δ*pilU*, *pilT*^{E204A} Δ*pilU*, *pilT*$^{E204A/K136A}$ Δ*pilU*, and *pilT*^{K136A} *pilU*^{K134A}). Ectopic overexpression of PilU rescued all strains except for strains that lacked a copy of *pilT* (i.e. Δ*pilT*, Δ*pilT* Δ*pilU*). All strains were grown with 100 μM IPTG to ectopically induce PilT or PilU. Data are shown as the mean ± SD. Parent, $n = 8$. All other strains, $n = 4$. Asterisk(s) directly above bars denote comparisons to the appropriate parent strain. Comparisons were made by grouping data into the two families indicated by the white and grey bars. A one-way ANOVA was performed for each family with a Dunnet's post to compare each experimental sample to the parent strain. Comparisons were not statistically significantly different unless otherwise noted. *** = $P < 0.001$.

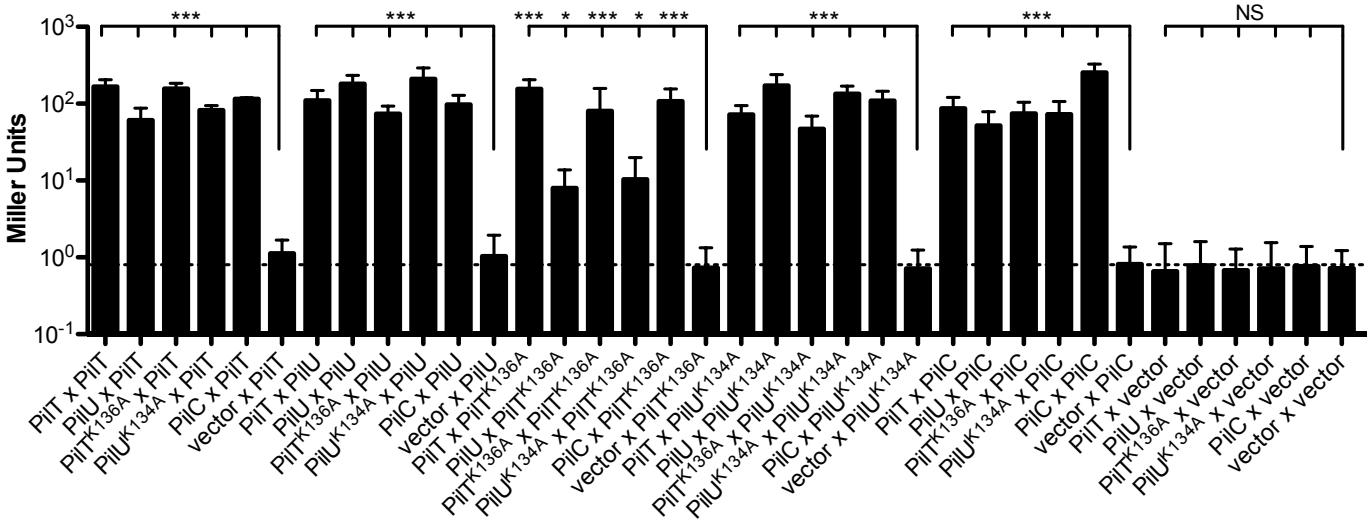

S2 Fig. PilT and PilU interact with each other and the pilus platform protein PilC. BACTH Miller assays showing all data from **Fig 3B** with additional negative controls for every T25- or T18-fusion. Data are shown as the mean ± SD from three independent experiments. The dotted line represents the β-galactosidase activity of the empty vector negative control (T18-empty x T25-empty). Comparisons were made by grouping data into appropriate families indicated by the black lines above the bar graph. A one-way ANOVA was performed on each family with a Dunnet's post test to compare each experimental group to the appropriate negative control (indicated by the longer black line). A single set of asterisks directly above the group line denotes the statistical results for all comparisons in that family unless otherwise noted. NS, not significant; * = $P < 0.05$; *** = $P < 0.001$.

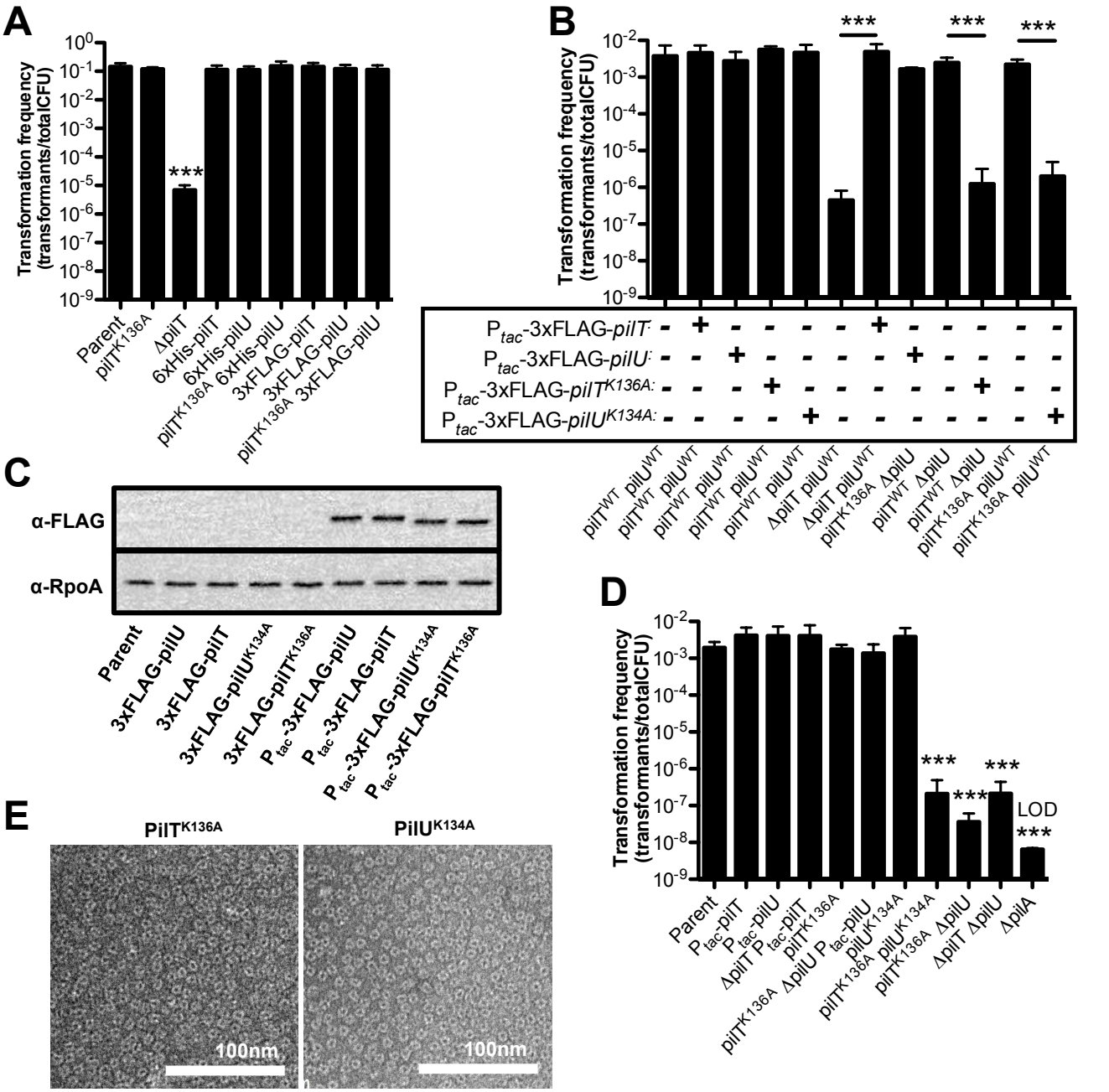

S3 Fig. PilT and PilU form homomeric complexes to facilitate pilus retraction. **(A)** Natural transformation assays showing that 6xHis and 3xFLAG N-terminal fusions to PilT and PilU are functional. The indicated strains were incubated with 500 ng of transforming DNA overnight. Parent, $n = 8$. All others, $n = 4$. **(B)** Natural transformation assays showing that overexpression of 3xFLAG tagged PilT/PilU/PilT^{K136A}/PilU^{K134A} behave the same as non-tagged proteins when ectopically overexpressed in the indicated backgrounds. Strains were incubated with 500 ng of transforming DNA and after 7 minutes, DNAse I was added to prevent additional DNA uptake. Parent, $n = 5$. *pilT^{K136A}*, $n = 5$. All others, $n = 4$. **(C)** Western blot of the indicated strains to detect FLAG tagged-proteins and RpoA as a loading control. Strains containing an IPTG regulated P_{tac} constuct were grown in the presence of 100 μM IPTG. This blot indicates that ectopic induction of 3xFLAG tagged PilT/PilU/PilT^{K136A}/PilU^{K134A} results in robust overexpression of proteins above native levels. Data is representative of three independent experiments. **(D)** Natural transformation assays where the indicated strains were incubated with 500 ng of transforming DNA for 7 minutes prior to the addition of DNAse I to prevent additional DNA uptake. These data indicate that ectopic overexpression of PilT or PilU can rescue strains with a substantial reduction in transformation frequency. All strains with P_{tac} constructs were grown with 100 μM IPTG to overexpress PilT or PilU. All bar graphs are shown as the mean ± SD. Asterisk(s) directly above bars denote comparisons to parent strain. All comparisons were made by one-way ANOVA followed with Tukey's post test. LOD, limit of detection; *** = $P < 0.001$. **(E)** Representative negative stain transmission electron micrographs showing that purified ^{6X}His-PilT^{K136A} and ^{6X}His-PilU^{K134A} form hexamers *in vitro.* Scale bar, 100 nm.

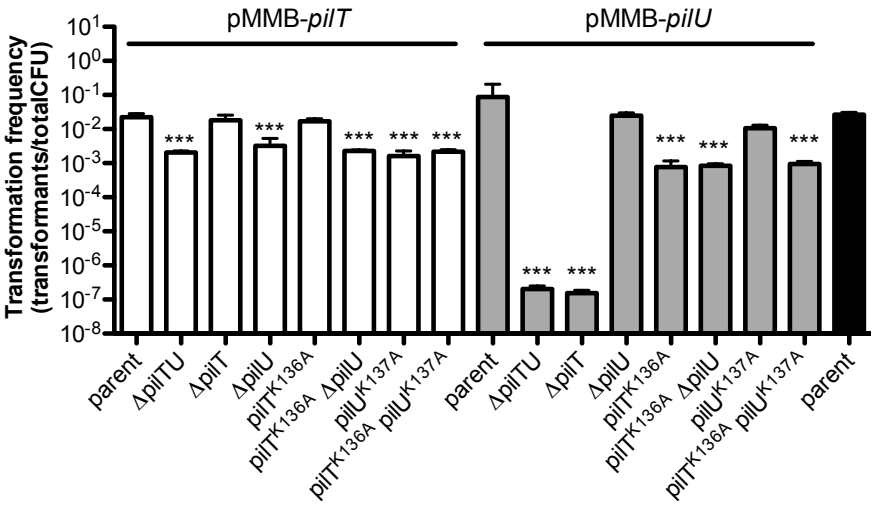

S4 Fig. Complementation analysis of *A. baylyi* mutant strains via ectopic expression of *pilT* or *pilU*. Natural transformation assays of the indicated *A. baylyi* strains. Strains harbored pMMB-*pilT* (white bars), pMMB-*pilU* (gray bars), or no vector (black bar). Data indicate that ectopic overexpression of PilT and PilU do not affect the transformation frequency of the parent strain. Ectopic overexpression of PilT rescued the transformation of all strains that showed a significant reduction in natural transformation in **Fig 5** (i.e. Δ*pilT*, Δ*pilT* Δ*pilU*, *pilT*^{K136A} Δ*pilU*, and *pilT*^{K136A} *pilU*^{K137A}). Ectopic overexpression of PilU rescued all strains except for strains that lacked a copy of pilT (i.e. Δ*pilT* and Δ*pilT* Δ*pilU*). All strains were grown with 100 μM IPTG to induce expression of *pilT* or *pilU*. Data are shown as the mean ± SD and are from three independent experiments. Asterisk(s) directly above bars denote comparisons to the appropriate parent strain. Comparisons were made by grouping data into the two families indicated by the white and grey bars. A one-way ANOVA was performed for each family followed by Dunnet's post test to compare each experimental group to the parent strain. Comparisons were not statistically significantly different from the relevant parent unless otherwise noted. *** = $P < 0.001$.

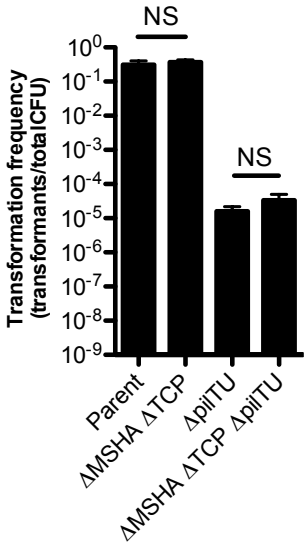

S5 Fig. The components of the *V. cholerae* MSHA or TCP type IV pilus systems do not contribute to PilTU-independent retraction of the competence pilus. Natural transformation assays of the indicated strains. Reactions were incubated with 500 ng of transforming DNA overnight. ΔMSHA and ΔTCP represent deletions of the entire locus for both pilus systems, which includes the extension ATPase associated with each. Data are shown as the mean ± SD and are from four independent biological replicates. All comparisons were made by one-way ANOVA with Tukey's post test. NS, not significant.

S1 Table. Strains used in this study

Strain name in manuscript	Genotype and antibiotic resistances	Figure	Strain #
Parent	E7946 SmR, ΔlacZ::lacIq, P_{tac}-tfoX, ΔluxO::miniFRT, ΔVC1807::ZeoR, pilA S67C	Fig 1, Fig 2	TND0905 (SAD2468)
ΔpilU	E7946 SmR, ΔlacZ::lacIq, P_{tac}-tfoX, ΔluxO::SpecR, ΔVC1807::CmR, pilA S67C, comEA-mCherry, ΔpilU::TmR *	Fig 1, Fig 2	SAD2135
ΔpilT	E7946 SmR, ΔlacZ::lacIq, P_{tac}-tfoX, ΔluxO::miniFRT, ΔVC1807::ZeoR, pilA S67C, ΔpilT::TmR	Fig 1, Supp Fig 3	TND1035 (SAD2469)
ΔpilTU	E7946 SmR, ΔlacZ::lacIq, P_{tac}-tfoX, ΔluxO::miniFRT, ΔVC1807::ZeoR, pilA S67C, ΔpilTU::TmR	Fig 1	JLC227 (SAD2470)
$pilT^{K136A}$	E7946 SmR, ΔlacZ::lacIq, P_{tac}-tfoX, ΔluxO::miniFRT, ΔVC1807::KanR, pilA S67C, $pilT^{K136A}$	Fig 1, Fig 2	TND1077 (SAD2471)
$pilT^{K136A}$ ΔpilU	E7946 SmR, ΔlacZ::lacIq, P_{tac}-tfoX, ΔluxO::miniFRT, ΔVC1807::ZeoR, pilA S67C, $pilT^{K136A}$, ΔpilU::TmR	Fig 1	JLC444 (SAD2472)
$pilT^{E204A}$	E7946 SmR, ΔlacZ::lacIq, P_{tac}-tfoX, ΔluxO::miniFRT, ΔVC1807::CmR, pilA S67C, $pilT^{E204A}$	Fig 1	TND1203 (SAD2473)
$pilT^{E204A/K136A}$	E7946 SmR, ΔlacZ::lacIq, P_{tac}-tfoX, ΔluxO::miniFRT, ΔVC1807::CmR, pilA S67C, $pilT^{E204A/K136A}$	Fig 1	JLC324 (SAD2474)
$pilT^{E204A/K136A}$ ΔpilU	E7946 SmR, ΔlacZ::lacIq, P_{tac}-tfoX, ΔluxO::miniFRT, ΔVC1807::CmR, pilA S67C, $pilT^{E204A/K136A}$, ΔpilU::TmR	Fig 1	JLC530 (SAD2475)
$pilT^{E204A}$ ΔpilU	E7946 SmR, ΔlacZ::lacIq, P_{tac}-tfoX, ΔluxO::miniFRT, ΔVC1807::CmR, pilA S67C, $pilT^{E204A}$, ΔpilU::TmR	Fig 1	JLC531 (SAD2476)
ΔpilA	E7946 SmR, ΔlacZ::lacIq, P_{tac}-tfoX, ΔluxO::SpecR, ΔVC1807::KanR, ΔpilA::miniFRT	Fig 1	TND0855 (SAD2477)
Parent (micropillar assays)	E7946 SmR, ΔlacZ::lacIq, P_{tac}-tfoX, ΔluxO::SpecR, ΔVC1807::CmR, pilA S67C, ΔflaA::CarbR, ΔmshA::miniFRT, Δvps-rbmA::ZeoR, ΔtcpA::KanR	Fig 1	TND0752 (SAD2478)
ΔpilT (micropillar assays)	E7946 SmR, ΔlacZ::lacIq, P_{tac}-tfoX, ΔluxO::SpecR, ΔVC1807::CmR, pilA S67C, ΔflaA::CarbR, ΔmshA::miniFRT, Δvps-rbmA::ZeoR, ΔtcpA::KanR, ΔpilT::TmR	Fig 1	TND0767 (SAD2479)
ΔpilU (micropillar assays)	E7946 SmR, ΔlacZ::lacIq, P_{tac}-tfoX, ΔluxO::SpecR, ΔVC1807::CmR, pilA S67C, ΔflaA::CarbR, ΔmshA::miniFRT, Δvps-rbmA::ZeoR, ΔtcpA::KanR, ΔpilU::TmR	Fig 1	TND1168 (SAD2480)
ΔpilT ΔpilU (micropillar assays)	E7946 SmR, ΔlacZ::lacIq, P_{tac}-tfoX, ΔluxO::SpecR, ΔVC1807::CmR, pilA S67C,	Fig 1	TND1174 (SAD2635)

	ΔflaA::CarbR, ΔmshA::miniFRT, Δvps-rbmA::ZeoR, ΔtcpA::KanR, ΔpilTU::TmR		
P_{tac}-PilT	E7946 SmR, P_{tac}-tfoX, ΔluxO::miniFRT, ΔVC1807::ZeoR, pilA S67C, ΔlacZ::P_{tac}-PilT SpecR	Supp Fig 1	JLC426 (SAD2481)
P_{tac}-PilU	E7946 SmR, P_{tac}-tfoX, ΔluxO::miniFRT, ΔVC1807::ZeoR, pilA S67C, ΔlacZ::P_{tac}-PilU SpecR	Supp Fig 1	JLC427 (SAD2482)
P_{tac}-PilT ΔpilTU	E7946 SmR, P_{tac}-tfoX, ΔluxO::miniFRT, ΔVC1807::ZeoR, pilA S67C, ΔlacZ::P_{tac}-PilT SpecR, ΔpilTU::TmR	Supp Fig 1	JLC420 (SAD2483)
P_{tac}-PilU ΔpilTU	E7946 SmR, P_{tac}-tfoX, ΔluxO::miniFRT, ΔVC1807::ZeoR, pilA S67C, ΔlacZ::P_{tac}-PilU SpecR, ΔpilTU::TmR	Supp Fig 1	JLC421 (SAD2484)
P_{tac}-PilT pilT^{K136A} ΔpilU	E7946 SmR, P_{tac}-tfoX, ΔluxO::miniFRT, ΔVC1807::KanR, pilA S67C, ΔlacZ::P_{tac}-PilT SpecR, pilT ^{K136A}, ΔpilU::TmR	Supp Fig 1	JLC450 (SAD2485)
P_{tac} -PilU pilT^{K136A} ΔpilU	E7946 SmR, P_{tac}-tfoX, ΔluxO::miniFRT, ΔVC1807::KanR, pilA S67C, ΔlacZ::P_{tac}-PilU SpecR, pilT ^{K136A}, ΔpilU::TmR	Supp Fig 1	JLC451 (SAD2486)
P_{tac} -PilT pilT^{K136A} pilU^{K134A}	E7946 SmR, P_{tac}-tfoX, ΔluxO::miniFRT, ΔVC1807::KanR, pilA S67C, ΔlacZ::P_{tac}-PilT SpecR, pilT ^{K136A} pilU ^{K134A}	Supp Fig 1	JLC424 (SAD2487)
P_{tac}-PilU pilT^{K136A} pilU^{K134A}	E7946 SmR, P_{tac}-tfoX, ΔluxO::miniFRT, ΔVC1807::KanR, pilA S67C, ΔlacZ::P_{tac}-PilU SpecR, pilT ^{K136A} pilU ^{K134A}	Supp Fig 1	JLC425 (SAD2488)
P_{tac}-PilT ΔpilTU	E7946 SmR, P_{tac}-tfoX, ΔluxO::miniFRT, ΔVC1807::ZeoR, pilA S67C, ΔlacZ::P_{tac}-PilT SpecR, ΔpilTU::TmR	Supp Fig 1	JLC438 (SAD2489)
P_{tac}-PilU ΔpilTU	E7946 SmR, P_{tac}-tfoX, ΔluxO::miniFRT, ΔVC1807::ZeoR, pilA S67C, ΔlacZ::P_{tac}-PilU SpecR, ΔpilTU::TmR	Supp Fig 1	JLC439 (SAD2490)
P_{tac}-PilT pilT$^{E204A/K136A}$ ΔpilU	E7946 SmR, P_{tac}-tfoX, ΔluxO::miniFRT, ΔVC1807::CmR, pilA S67C, pilT ^{E204A}/^{K136A}, ΔpilU::TmR, ΔlacZ::P_{tac}-PilT SpecR	Supp Fig 1	JLC540 (SAD2491)
P_{tac}-PilU pilT$^{E204A/K136A}$ ΔpilU	E7946 SmR, P_{tac}-tfoX, ΔluxO::miniFRT, ΔVC1807::CmR, pilA S67C, pilT ^{E204A}/^{K136A}, ΔpilU::TmR, ΔlacZ::P_{tac}-PilU SpecR	Supp Fig 1	JLC541 (SAD2492)
P_{tac}-PilT pilT^{E204A} ΔpilU	E7946 SmR, P_{tac}-tfoX, ΔluxO::miniFRT, ΔVC1807::CmR, pilA S67C, pilT ^{E204A}, ΔpilU::TmR, ΔlacZ::P_{tac}-PilT SpecR	Supp Fig 1	JLC542 (SAD2493)
P_{tac}-PilU pilT^{E204A} ΔpilU	E7946 SmR, P_{tac}-tfoX, ΔluxO::miniFRT, ΔVC1807::CmR, pilA S67C, pilT ^{E204A}, ΔpilU::TmR, , ΔlacZ::P_{tac}-PilU SpecR	Supp Fig 1	JLC543 (SAD2494)
PilU^{L199C}	E7946 SmR, ΔlacZ::lacIq, P_{tac}-tfoX, ΔluxO::miniFRT, ΔVC1807::CmR, pilA S67C, pilU ^{L199C}	Fig 2	JLC409 (SAD2495)
ΔpilT PilU^{L199C}	E7946 SmR, ΔlacZ::lacIq, P_{tac}-tfoX, ΔluxO::miniFRT, ΔVC1807::ZeoR, pilA S67C, ΔpilT::TmR, pilU ^{L199C}	Fig 2	JLC411 (SAD2496)

pilT^{K136A} pilU^{L199C}	E7946 SmR, ΔlacZ::lacIq, P_{tac}-tfoX, ΔluxO::miniFRT, ΔVC1807::CmR, pilA S67C, pilU ^{L199C}, pilT ^{K136A}	Fig 2	JLC414 (SAD2497)
pilT^{L201C}	E7946 SmR, ΔlacZ::lacIq, P_{tac}-tfoX, ΔluxO::SpecR, ΔVC1807::CmR, pilA S67C, comEA-mCherry, pilT ^{L201C} *	Fig 2	TND0989 (SAD2498)
pilT^{L201C} ΔpilU	E7946 SmR, ΔlacZ::lacIq, P_{tac}-tfoX, ΔluxO::SpecR, ΔVC1807::CmR, pilA S67C, comEA-mCherry, pilT ^{L201C}, ΔpilU::TmR *	Fig 2	TND1140 (SAD2499)
pilU^{K134A}	E7946 SmR, ΔlacZ::lacIq, P_{tac}-tfoX, ΔluxO::miniFRT, ΔVC1807::KanR, pilA S67C, pilU ^{K134A}	Fig 2	TND1092 (SAD2500)
pilT^{K136A} pilU^{K134A}	E7946 SmR, ΔlacZ::lacIq, P_{tac}-tfoX, ΔluxO::miniFRT, ΔVC1807::KanR, pilA S67C, pilT ^{K136A}, pilU ^{K134A}	Fig 2	TND1094 (SAD2501)
^{6X}His-pilU, pilT^{K136A}	E7946 SmR, ΔlacZ::lacIq, P_{tac}-tfoX, ΔluxO::miniFRT, ΔVC1807::CmR, pilA S67C, ^{6X}His-pilU, pilT ^{K136A}	Supp Fig 3	JLC298 (SAD2502)
^{6X}His-pilT	E7946 SmR, ΔlacZ::lacIq, P_{tac}-tfoX, ΔluxO::miniFRT, ΔVC1807::CmR, pilA S67C, ^{6X}His-pilT	Supp Fig 3	HKQ046 (SAD2503)
^{6X}His-pilU	E7946 SmR, ΔlacZ::lacIq, P_{tac}-tfoX, ΔluxO::miniFRT, ΔVC1807::CmR, pilA S67C, ^{6X}His-pilU	Supp Fig 3	JLC398 (SAD2504)
pilT^{K136A} 3xFLAG-pilU	E7946 SmR, ΔlacZ::lacIq, P_{tac}-tfoX, ΔluxO::miniFRT, ΔVC1807::CmR, pilA S67C, pilT ^{K136A}, 3xFLAG-pilU	Supp Fig 3	JLC396 (SAD2505)
3xFLAG-pilU	E7946 SmR, ΔlacZ::lacIq, P_{tac}-tfoX, ΔluxO::miniFRT, ΔVC1807::CmR, pilA S67C, 3xFLAG-pilU	Supp Fig 3	JLC326 (SAD2506)
3xFLAG-pilU^{K134A}	E7946 SmR, ΔlacZ::lacIq, P_{tac}-tfoX, ΔluxO::miniFRT, ΔVC1807::CmR, pilA S67C, 3xFLAG-pilU^{K134A}	Supp Fig 3	JLC316 (SAD2507)
3xFLAG-pilT	E7946 SmR, ΔlacZ::lacIq, P_{tac}-tfoX, ΔluxO::miniFRT, ΔVC1807::CmR, pilA S67C, 3xFLAG-pilT	Supp Fig 3	JLC310 (SAD2508)
3xFLAG-pilT^{K136A}	E7946 SmR, ΔlacZ::lacIq, P_{tac}-tfoX, ΔluxO::miniFRT, ΔVC1807::CmR, pilA S67C, 3xFLAG-pilT ^{K136A}	Supp Fig 3	JLC349 (SAD2509)
^{6X}His-pilU (purification)	BL21 DE3 pHisTev-6xHis-pilU	Fig 4	HKQ051 (SAD2510)
^{6X}His-pilU^{K134A} (purification)	BL21 DE3 pHisTev-6xHis-pilU ^{K134A}	Supp Fig 3	SAD2316
^{6X}His-pilT (purification)	BL21 DE3 pHisTev-6xHis-pilT	Fig 4	TND1277 (SAD2511)
^{6X}His-pilT^{K136A} (purification)	BL21 DE3 pHisTev-6xHis-pilT ^{K136A}	Supp Fig 3	TND1281 (SAD2512)
PilT x PilT	BTH101 pUT18C-PilT (CarbR), pKT25-PilT (KanR)	Fig 3, Supp Fig 2	JLC465

PilU x PilT	BTH101 pUT18C-PilU (CarbR), pKT25-PilT (KanR)	Fig 3, Supp Fig 2	JLC466
PilT^{K136A} x PilT	BTH101 pUT18C-PilT ^{K136A} (CarbR), pKT25-PilT (KanR)	Fig 3, Supp Fig 2	JLC467
PilU^{K134A} x PilT	BTH101 pUT18C-PilU ^{K134A} (CarbR), pKT25-PilT (KanR)	Fig 3, Supp Fig 2	JLC468
PilC x PilT	BTH101 pUT18C-PilC (CarbR), pKT25-PilT (KanR)	Fig 3, Supp Fig 2	JLC469
vector x PilT	BTH101 pUT18C-vector (CarbR), pKT25-PilT (KanR)	Fig 3, Supp Fig 2	JLC470
PilT x PilU	BTH101 pUT18C-PilT (CarbR), pKT25-PilU (KanR)	Fig 3, Supp Fig 2	JLC471
PilU x PilU	BTH101 pUT18C-PilU (CarbR), pKT25-PilU (KanR)	Fig 3, Supp Fig 2	JLC472
PilT^{K136A} x PilU	BTH101 pUT18C-PilT ^{K136A} (CarbR), pKT25-PilU (KanR)	Fig 3, Supp Fig 2	JLC473
PilU^{K134A} x PilU	BTH101 pUT18C-PilU ^{K134A} (CarbR), pKT25-PilU (KanR)	Fig 3, Supp Fig 2	JLC474
PilC x PilU	BTH101 pUT18C-PilC (CarbR), pKT25-PilU (KanR)	Fig 3, Supp Fig 2	JLC475
vector x PilU	BTH101 pUT18C-vector (CarbR), pKT25-PilU (KanR)	Fig 3, Supp Fig 2	JLC476
PilT x PilT^{K136A}	BTH101 pUT18C-PilT (CarbR), pKT25-PilT ^{K136A} (KanR)	Fig 3, Supp Fig 2	JLC477
PilU x PilT^{K136A}	BTH101 pUT18C-PilU (CarbR), pKT25-PilT ^{K136A} (KanR)	Fig 3, Supp Fig 2	JLC478
PilT^{K136A} x PilT^{K136A}	BTH101 pUT18C-PilT ^{K136A} (CarbR), pKT25-PilT ^{K136A} (KanR)	Fig 3, Supp Fig 2	JLC479
PilU^{K134A} x PilT^{K136A}	BTH101 pUT18C-PilU ^{K134A} (CarbR), pKT25-PilT ^{K136A} (KanR)	Fig 3, Supp Fig 2	JLC480
PilC x PilT^{K136A}	BTH101 pUT18C-PilC (CarbR), pKT25-PilT ^{K136A} (KanR)	Fig 3, Supp Fig 2	JLC481

vector x PilT^{K136A}	BTH101 pUT18C-vector (CarbR), pKT25-PilT ^{K136A} (KanR)	Fig 3, Supp Fig 2	JLC482
PilT x PilU^{K134A}	BTH101 pUT18C-PilT (CarbR), pKT25-PilU ^{K134A} (KanR)	Fig 3, Supp Fig 2	JLC483
PilU x PilU^{K134A}	BTH101 pUT18C-PilU (CarbR), pKT25-PilU ^{K134A} (KanR)	Fig 3, Supp Fig 2	JLC484
PilT^{K136A} x PilU^{K134A}	BTH101 pUT18C-PilT ^{K136A} (CarbR), pKT25-PilU ^{K134A} (KanR)	Fig 3, Supp Fig 2	JLC485
PilU^{K134A} x PilU^{K134A}	BTH101 pUT18C-PilU ^{K134A} (CarbR), pKT25-PilU ^{K134A} (KanR)	Fig 3, Supp Fig 2	JLC486
PilC x PilU^{K134A}	BTH101 pUT18C-PilC (CarbR), pKT25-PilU ^{K134A} (KanR)	Fig 3, Supp Fig 2	JLC487
vector x PilU^{K134A}	BTH101 pUT18C-vector (CarbR), pKT25-PilU ^{K134A} (KanR)	Fig 3, Supp Fig 2	JLC488
PilT x PilC	BTH101 pUT18C-PilT (CarbR), pKT25-PilC (KanR)	Fig 3, Supp Fig 2	JLC489
PilU x PilC	BTH101 pUT18C-PilU (CarbR), pKT25-PilC (KanR)	Fig 3, Supp Fig 2	JLC490
PilT^{K136A} x PilC	BTH101 pUT18C-PilT ^{K136A} (CarbR), pKT25-PilC (KanR)	Fig 3, Supp Fig 2	JLC491
PilU^{K134A} x PilC	BTH101 pUT18C-PilU ^{K134A} (CarbR), pKT25-PilC (KanR)	Fig 3, Supp Fig 2	JLC492
PilC x PilC	BTH101 pUT18C-PilC (CarbR), pKT25-PilC (KanR)	Fig 3, Supp Fig 2	JLC493
vector x PilC	BTH101 pUT18C-vector (CarbR), pKT25-PilC (KanR)	Fig 3, Supp Fig 2	JLC494
PilT x vector	BTH101 pUT18C-PilT (CarbR), pKT25-vector (KanR)	Fig 3, Supp Fig 2	JLC495
PilU x vector	BTH101 pUT18C-PilU (CarbR), pKT25-vector (KanR)	Fig 3, Supp Fig 2	JLC496
PilT^{K136A} x vector	BTH101 pUT18C-PilT ^{K136A} (CarbR), pKT25-vector (KanR)	Fig 3, Supp Fig 2	JLC497

PilU^{K134A} x vector	BTH101 pUT18C-PilU ^{K134A} (CarbR), pKT25-vector (KanR)	Fig 3, Supp Fig 2	JLC498
PilC x vector	BTH101 pUT18C-PilC (CarbR), pKT25-vector (KanR)	Fig 3, Supp Fig 2	JLC499
vector x vector	BTH101 pUT18C-vector (CarbR), pKT25-vector (KanR)	Fig 3, Supp Fig 2	JLC500
Zip x Zip	BTH101 pUT18C-Leucine Zipper (CarbR), pKT25-Leucine Zipper (KanR)	Fig 3, Supp Fig 2	JLC501
Parent (P_{const}-tfoX)	E7946 SmR, ΔlacZ::lacIq, P_{const}-tfoX, ΔluxO::miniFRT, ΔVC1807::KanR, pilA S67C	Fig 4, Supp Fig 3	TND1076 (SAD2513)
ΔpilU	E7946 SmR, ΔlacZ::lacIq, P_{const}-tfoX, ΔluxO::miniFRT, ΔVC1807::KanR, pilA S67C, ΔpilU::TmR	Fig 4, Supp Fig 3	JLC251 (SAD2514)
ΔpilT	E7946 SmR, ΔlacZ::lacIq, P_{const}-tfoX, ΔluxO::miniFRT, ΔVC1807::KanR, pilA S67C, ΔpilT::TmR	Fig 4, Supp Fig 3	JLC250 (SAD2515)
pilT^{K136A}	E7946 SmR, ΔlacZ::lacIq, P_{const}-tfoX, ΔluxO::miniFRT, ΔVC1807::CmR, pilA S67C, pilT ^{K136A}	Fig 4	JLC299 (SAD2516)
P_{tac}-pilT^{K136A}	E7946 SmR, P_{const}-tfoX, ΔluxO::miniFRT, ΔVC1807::KanR, pilA S67C, ΔlacZ::P_{tac} -pilT ^{K136A} SpecR	Fig 4	JLC277 (SAD2517)
ΔpilU P_{tac}-pilT^{K136A}	E7946 SmR, P_{const}-tfoX, ΔluxO::miniFRT, ΔVC1807::KanR, pilA S67C, ΔpilU::TmR, ΔlacZ::Ptac-pilT ^{K136A} SpecR	Fig 4	SAD2243
P_{tac}-pilU^{K134A}	E7946 SmR, P_{const}-tfoX, ΔluxO::miniFRT, ΔVC1807::KanR, pilA S67C, ΔlacZ::P_{tac}-pilU ^{K134A} SpecR	Fig 4	JLC282 (SAD2518)
pilT^{K136A} P_{tac}-pilU^{K134A}	E7946 SmR, P_{const}-tfoX, ΔluxO::miniFRT, ΔVC1807::CmR, pilA S67C, ΔlacZ::P_{tac}-pilU ^{K134A} SpecR, pilT ^{K136A}	Fig 4	JLC300 (SAD2519)
P_{tac}-pilT^{K136A} P_{tac}-pilU^{K134A}	E7946 SmR, P_{const}-tfoX, ΔluxO::miniFRT, pilA S67C, ΔlacZ::P_{tac}-pilU ^{K134A} SpecR, ΔVC1807::Ptac-pilT ^{K136A} CmR	Fig 4	SAD2242
P_{tac}-3xFLAG-PilU	E7946 SmR, P_{const}-tfoX, ΔluxO::miniFRT, ΔVC1807::KanR, pilA S67C, ΔlacZ::P_{tac}-3xFLAG-pilU SpecR	Supp Fig 3	JLC333 (SAD2520)
P_{tac}-3x FLAG-PilU ^{K134A}	E7946 SmR, P_{const}-tfoX, ΔluxO::miniFRT, ΔVC1807::KanR, pilA S67C, ΔlacZ::P_{tac}-3xFLAG-pilU ^{K134A} SpecR	Supp Fig 3	JLC336 (SAD2521)
P_{tac}-3x FLAG-PilT	E7946 SmR, ΔlacZ::lacIq, P_{const}-tfoX, ΔluxO::miniFRT, ΔVC1807::KanR, pilA S67C, ΔlacZ::P_{tac}-3xFLAG-pilT SpecR	Supp Fig 3	JLC337 (SAD2522)

P_{tac}-3x FLAG-PilT^{K136A}	E7946 SmR, P_{const}-tfoX, ΔluxO::miniFRT, ΔVC1807::KanR, pilA S67C, ΔlacZ::P_{tac}-3xFLAG-pilT ^{K136A} SpecR	Supp Fig 3	JLC353 (SAD2523)
ΔpilA	E7946 SmR, ΔlacZ::lacIq, P_{const}-tfoX, ΔluxO::miniFRT, ΔVC1807::TmR, ΔpilA::miniFRT	Supp Fig 3	TND1357 (SAD2524)
ΔpilTU	E7946 SmR, ΔlacZ::lacIq, P_{const}-tfoX, ΔluxO::miniFRT, ΔVC1807::KanR, pilA S67C, ΔpilTU::TmR	Supp Fig 3	JLC252 (SAD2525)
pilU^{K134A}	E7946 SmR, ΔlacZ::lacIq, P_{const}-tfoX, ΔluxO::miniFRT, ΔVC1807::CmR, pilA S67C, pilU ^{K134A}	Supp Fig 3	JLC308 (SAD2526)
pilT^{K136A} ΔpilU	E7946 SmR, ΔlacZ::lacIq, P_{const}-tfoX, ΔluxO::miniFRT, ΔVC1807::KanR, pilA S67C, pilT ^{K136A}, ΔpilU::TmR	Supp Fig 3	JLC447 (SAD2527)
pilT^{K136A} pilU^{K134A}	E7946 SmR, ΔlacZ::lacIq, P_{const}-tfoX, ΔluxO::miniFRT, ΔVC1807::KanR, pilA S67C, pilT ^{K136A}, pilU ^{K134A}	Supp Fig 3	JLC307 (SAD2528)
P_{tac}-pilT	E7946 SmR, P_{const}-tfoX, ΔluxO::miniFRT, ΔVC1807::KanR, pilA S67C, ΔlacZ::P_{tac}-pilT SpecR	Supp Fig 3	JLC279 (SAD2529)
ΔpilT P_{tac}-pilT	E7946 SmR, P_{const}-tfoX, ΔluxO::miniFRT, ΔVC1807::KanR, pilA S67C, ΔlacZ::P_{tac}-pilT SpecR, ΔpilT::TmR	Supp Fig 3	JLC280 (SAD2530)
P_{tac}-pilU	E7946 SmR, P_{const}-tfoX, ΔluxO::miniFRT, ΔVC1807::KanR, pilA S67C, ΔlacZ::P_{tac}-pilU SpecR	Supp Fig 3	JLC283 (SAD2531)
pilT^{K136A} ΔpilU P_{tac}-pilU	E7946 SmR, P_{const}-tfoX, ΔluxO::miniFRT, ΔVC1807::KanR, pilA S67C, ΔlacZ::P_{tac}-pilU SpecR, pilT ^{K136A}, ΔpilU::TmR	Supp Fig 3	JLC449 (SAD2532)
ΔpilT P_{tac}-3xFLAG-pilT	E7946 SmR, P_{const}-tfoX, ΔluxO::miniFRT, ΔVC1807::KanR, pilA S67C, ΔlacZ::P_{tac}-3x-FLAG-pilT SpecR, ΔpilT::TmR	Supp Fig 3	JLC373 (SAD2533)
pilT^{K136A} ΔpilU P_{tac}-3x FLAG-pilU	E7946 SmR, P_{const}-tfoX, ΔluxO::miniFRT, ΔVC1807::KanR, pilA S67C, ΔlacZ::P_{tac}-3x-FLAG-pilU SpecR, pilT ^{K136A}, ΔpilU::TmR	Supp Fig 3	JLC448 (SAD2534)
ΔpilU P_{tac}-3x FLAG-PilT^{K136A}	E7946 SmR, P_{const}-tfoX, ΔluxO::miniFRT, ΔVC1807::KanR, pilA S67C, ΔlacZ::P_{tac}-3xFLAG-pilT ^{K136A} SpecR, ΔpilU::TmR	Supp Fig 3	JLC379 (SAD2535)
pilT^{K136A} P_{tac}-3x FLAG-pilU^{K134A}	E7946 SmR, P_{const}-tfoX, ΔluxO::miniFRT, ΔVC1807::KanR, pilA S67C, ΔlacZ::P_{tac}-3x-FLAG-pilU ^{K134A} SpecR, pilT ^{K136A}	Supp Fig 3	JLC380 (SAD2536)
Parent (*A. baylyi*)	ADP1, comP T129C	Fig 5	TND0428 (SAD2537)
PilT^{K136A} ΔpilU	ADP1, comP T129C, PilT ^{K136A} ΔpilU::ZeoR	Fig 5	TND1135 (SAD2538)
PilT^{K136A} PilU^{K137A}	ADP1, , comP T129C, PilT ^{K136A} PilU ^{K137A}	Fig 5	TND1142 (SAD2539)
PilT^{K136A}	ADP1, comP T129C, PilT ^{K136A}	Fig 5	TND1122 (SAD2540)

PilU^{K137A}	ADP1, comP T129C, PilU ^{K137A}	Fig 5	TND1111 (SAD2541)
ΔpilT	ADP1, comP T129C, ΔpilT::SpecR	Fig 5	TND0779 (SAD2542)
ΔpilU	ADP1, comP T129C, ΔpilU::ZeoR	Fig 5	TND0798 (SAD2543)
ΔpilTU	ADP1, comP T129C, ΔpilTU::ZeoR	Fig 5	TND0799 (SAD2544)
ΔcomP	ADP1, ΔcomP::SpecR	Fig 5	TND0115 (SAD2545)
P_{tac}-pilT	ADP1, comP T129C, pMMB67EH- P_{tac}-pilT	Supp Fig 4	TND1703 (SAD2546)
P_{tac}-pilT ΔpilTU	ADP1, comP T129C, pMMB67EH- P_{tac}-pilT, ΔpilTU::ZeoR	Supp Fig 4	TND1704 (SAD2547)
P_{tac}-pilT ΔpilT	ADP1, comP T129C, pMMB67EH- P_{tac}-pilT, ΔpilT::SpecR	Supp Fig 4	TND1705 (SAD2548)
P_{tac}-pilT ΔpilU	ADP1, comP T129C, pMMB67EH- P_{tac}-pilT, ΔpilU::ZeoR	Supp Fig 4	TND1706 (SAD2549)
P_{tac}-pilT pilT^{K136A}	ADP1, comP T129C, pMMB67EH- P_{tac}-pilT, pilT ^{K136A}	Supp Fig 4	TND1707 (SAD2550)
P_{tac}-pilT pilT^{K136A} ΔpilU	ADP1, comP T129C, pMMB67EH- P_{tac}-pilT, pilT ^{K136A}, ΔpilU::ZeoR	Supp Fig 4	TND1708 (SAD2551)
P_{tac}-pilT pilU^{K137A}	ADP1, comP T129C, pMMB67EH- P_{tac}-pilT, pilU ^{K137A}	Supp Fig 4	TND1709 (SAD2552)
P_{tac}-pilT pilT^{K136A} pilU^{K137A}	ADP1, comP T129C, pMMB67EH- P_{tac}-pilT, pilT ^{K136A}, pilU ^{K137A}	Supp Fig 4	TND1710 (SAD2553)
P_{tac}-pilU	ADP1, comP T129C, pMMB67EH- P_{tac}-pilU	Supp Fig 4	TND1711 (SAD2554)
P_{tac}-pilU ΔpilTU	ADP1, comP T129C, pMMB67EH- P_{tac}-pilU, ΔpilTU::ZeoR	Supp Fig 4	TND1712 (SAD2555)
P_{tac}-pilU ΔpilT	ADP1, comP T129C, pMMB67EH- P_{tac}-pilU, ΔpilT::SpecR	Supp Fig 4	TND1713 (SAD2556)
P_{tac}-pilU ΔpilU	ADP1, comP T129C, pMMB67EH- P_{tac}-pilU, ΔpilU::ZeoR	Supp Fig 4	TND1714 (SAD2557)
P_{tac}-pilU pilT^{K136A}	ADP1, comP T129C, pMMB67EH- P_{tac}-pilU, pilT ^{K136A}	Supp Fig 4	TND1715 (SAD2558)
P_{tac}-pilU pilT^{K136A} ΔpilU	ADP1, comP T129C, pMMB67EH- P_{tac}-pilU, pilT ^{K136A}, ΔpilU::ZeoR	Supp Fig 4	TND1716 (SAD2559)
P_{tac}-pilU pilU^{K137A}	ADP1, comP T129C, pMMB67EH- P_{tac}-pilU, pilU ^{K137A}	Supp Fig 4	TND1717 (SAD2560)
P_{tac}-pilU pilT^{K136A} pilU^{K137A}	ADP1, comP T129C, pMMB67EH- P_{tac}-pilU, pilT ^{K136A}, pilU ^{K137A}	Supp Fig 4	TND1718 (SAD2561)
Parent	E7946 SmR, ΔlacZ::lacIq, P_{tac}-tfoX, ΔluxO::miniFRT, ΔVC1807::CmR, pilA S67C, comEA-mCherry	Supp Fig 5	TND0904 (SAD2636)
ΔMSHA ΔTCP	E7946 SmR, ΔlacZ::lacIq, P_{tac}-tfoX, ΔluxO::miniFRT, ΔVC1807::CmR, pilA S67C, comEA-mCherry, ΔMSHA::CarbR, ΔTCP::ZeoR	Supp Fig 5	SAD2087 (SAD2637)

ΔpilTU	E7946 SmR, ΔlacZ::lacIq, P_{tac}-tfoX, ΔluxO::miniFRT, ΔVC1807::CmR, pilA S67C, comEA-mCherry, ΔpilTU::TmR	Supp Fig 5	JLC765 (SAD2638)
ΔpilTU ΔMSHA ΔTCP	E7946 SmR, ΔlacZ::lacIq, P_{tac}-tfoX, ΔluxO::miniFRT, ΔVC1807::CmR, pilA S67C, comEA-mCherry, ΔpilTU::TmR, ΔMSHA::CarbR, ΔTCP::ZeoR	Supp Fig 5	JLC832 (SAD2639)

* comEA-mCherry does not affect natural transformation or retraction rates [17].

S2 Table. Primers used in this study

Primer name	Sequence (5' –> 3')	Description
BBC374	TGGCAAAAAGCGAGAGAAGAAG	ΔluxO F1
BBC375	gtcgacggatccccggaatCATGAGGACATATTTTGTTTTCTGC	ΔluxO R1
BBC376	gaagcagctccagcctacaTAAGCGATGAGAGAATGGATCAAC	ΔluxO F2
BBC377	TCACACCCGAATTTCCATCATGC	ΔluxO R2
ABD344	GATTAGCAACGATTCTAGCGCAGGAG	ΔVC1807 F1
ABD340	gtcgacggatccccggaatACGTTTCATTAGTCACCTCTATTGT TAACTTGTTC	ΔVC1807 R1
ABD341	gaagcagctccagcctacaTAGTCGAAAATAAAAAAAAGAGG CTCGCCTC	ΔVC1807 F2
ABD345	CTTGCTAACCGTTGGTGTTACCAGC	ΔVC1807 R2
pilA S81C F	AAAACTAATATTGAAGATTATATTGCGACAGAAGGC TgTTTTCCTGCAACAACTGCAGG	pilA S67C F
pilA R2	CATTAATCGCGGTTTCAAAGTGCA	pilA S67C R2
DOG0400	ACTTCTGGCTGAAGGTCAATTTTC	ΔpilT/U F1
DOG0401	gtcgacggatccccggaatCATTTAAATTCCTTAATAAAGTCTG GC	ΔpilT R1
DOG0402	gaagcagctccagcctacaTAGGTAGGTAAAGACAGATGGAG	ΔpilT F2
DOG0403	TCACGTGTTCGGCCAAAATC	ΔpilT/U R2
HQP0001	GGGCTCGGGTgctTCGACGACCTTGGCG	PilT ^{K136A} R1
HQP0002	CGCCAAGGTCGTCGAagcACCCGAGCCC	PilT ^{K136A} F2
BBC2508	GTTTCTTGGTCACGCAGagCACCGACGAGGATCAC	PilT ^{E204A} R1
BBC2509	GTGATCCTCGTCGGTGctCTGCGTGACCAAGAAAC	PilT ^{E204A} F2
BBC401	ACCAGCAAAGCTAATAAAATCGAG	ΔpilA F1
BBC402	gtcgacggatccccggaatGAGCATATGCCTTGCTACACAAG	ΔpilA R1
BBC403	gaagcagctccagcctacaACTGCAGGTGCAACAATTAACTAA	ΔpilA F2
BBC404	CGCCATACTAACCCAATACACTC	ΔpilA R2
BBC1752	CTGAATGATTTCCATGAGACG	ΔflaA F1
BBC1753	gtcgacggatccccggaatCATAGTTTGCTCTCCTATCGAG	ΔflaA R1
BBC1754	gaagcagctccagcctacaTTGCAGTAGTTCACGGTACCTTC	ΔflaA F2
BBC1755	TTATACGCTCTTTTGCGTGATGG	ΔflaA R2
BBC1450	CACTCAACGAGCTCAATACG	ΔmshA F1
ABD653	gtcgacggatccccggaatCATCTCTCTTTCATGTGAATACGCA GC	ΔmshA R1
ABD654	gaagcagctccagcctacaGCGCAATAATTTAAATATGGCTCG TGC	ΔmshA F2

BBC1453	ATAGCCTTGCTGTTCATTTTGG	ΔmshA R2
BBC2022	TGCCGATCTCGTTTATGGACG	Δvps-rbmA locus F1
BBC2023	gtcgacggatccccggaatTGCCATTTTGATTGCCTCTGG	Δvps-rbmA locus R1
BBC2024	gaagcagctccagcctacaCAAAGAGAGCCTTATTAGGCTCTC	Δvps-rbmA locus F2
BBC2025	TGAAAGAGGTTGCTCTAGAACTCG	Δvps-rbmA locus R2
BBC1457	TTTCAAGACTTTGGGCAATAG	ΔtcpA F1
BBC1968	gtcgacggatccccggaatCTGTTTTAATAATTGCATATTTATA TAACTCCACC	ΔtcpA R1
BBC1969	gaagcagctccagcctacaTTTGGTAACAGTTAATCTACACCAT TATCTTG	ΔtcpA F2
BBC1463	TTGAATTCGTCCATCATCTAAG	ΔtcpA R2
BBC1833	GATATCCATGTCCATGTCCCAG	comEA-mCherry F1
BBC1834	cttgctcactccaccacttccacctgcTAACAAGATCCTTGCGGCATTG	comEA-mCherry R1
BBC1837	acgagctgtacaagtaaGCTGCAATCATGTGTCTCG	comEA-mCherry F2
BBC1838	GTCTTTCTATCAGTTCGGACTTAGTC	comEA-mCherry R2
BBC1835	gcaggtggaagtggtggaGTGAGCAAGGGCGAGGAGG	mCherry (for comEAmCherry) F
BBC1836	gattgcagcTTACTTGTACAGCTCGTCC	mCherry (for comEAmCherry) R
DOG0405	gtcgacggatccccggaatCATCTGTCTTTACCTACCTAAAATGC	ΔpilU R1
DOG0406	gaagcagctccagcctacaTAGCGATGGTTACTTTGTGCG	ΔpilU F2
JCP048	CAAGCCCCCGATATGATTTgcATTGGTGAAATCCGCAGC	PilU ^{L199C} F
JCP049	GCTGCGGATTTCACCAATgcAAATCATATCGGGGGCTTG	PilU ^{L199C} R
BBC2287	CATTGCGCTCGGCATTGCGTGAAGACCCAGATGTGATCtgtGTCGGTGAGCTGCGTGAC	PilT ^{L201C} F2
BBC2288	CGCAATGCCGAGCGCAATG	PilT ^{L201C} R1
BBC2369	GGCTGCCATAGTGGTCGAggcACCCGAACCGGTTGCGC	PilU ^{K134A} R1
BBC2347	GCGCAACCGGTTCGGGTgccTCGACCACTATGGCAGCC	PilU ^{K134A} F2
BBC2313	gcaggtggaagtggtggaCATCATCATCATCATCACgcaggtggagcaggtgga	6xHis (for 6xHis-PilU/T) F
BBC2314	tccacctgctccacctgcGTGATGATGATGATGATGtccaccacttccacctgc	6xHis (for 6xHis-PilU/T) R
BBC2272	gcaggtggaagtggtggagattataaagaccatgatggtgactacaaggatcacgacattgattataaggatgacgatgacaaagcaggtggagcaggtgga	3xFLAG (for 3xFLAG-PilU/T) F
BBC2273	tccacctgctccacctgctttgtcatcgtcatccttataatcaatgtcgtgatccttgtagtcaccatcatggtctttataatctccaccacttccacctgc	3xFLAG (for 3xFLAG-PilU/T) R
JCP028	tccaccacttccacctgcCATCTGTCTTTACCTACCTAAAATGC	X-PilU (N-term tags) R1

JCP029	gcaggtggagcaggtggaGAGTTGAATCAATATCTGGATGGC	X-PilU (N-term tags OR BACTH TXX-pilU) F2
JCP026	tccaccacttccacctgcCATTTAAATTCCTTAATAAAGTCTGGCTATG	X-PilT (N-term tags) R1
JCP027	gcaggtggagcaggtggaGATATCGCTGAGTTACTGGAATTTAG	X-PilT (N-term tags or BACTH TXX-pilT) F2
ABD332	GGCTGAACGTGGTTGTCGAAAATGAC	P_{tac}-PilT/U @lacZ F1
BBC244	CCCGGGATCCTGTGTGAAATTGTTATCCGC	P_{tac}-PilT/U @lacZ or @VC1807 R1
ABD255	TTAAGCTACTAAAGCGTAGTTTTCG	P_{tac}-PilT/U @lacZ F2
ABD256	CAATTTCACACAGGATCCCGGGAGGAGGTAACGTAATGGTGAGCAAAGGCGAAG	P_{tac}-PilT/U @lacZ R2
BBC1723	caatttcacacaggatcccgggAGGAGGTATTTAAATGGATATCGCTGAGTTAC	Amplify pilT (for P_{tac}-pilT) F
BBC1724	tgtaggctggagctgcttcCTAAAATGCTTTTAAATCCAACTCG	Amplify pilT (for P_{tac}-pilT OR BACTH TXX-pilT) R
BBC1725	caatttcacacaggatcccgggAGGAGGTAGACAGATGGAGTTGAATCAATATC	Amplify pilU (for P_{tac}-pilU) F
BBC1726	tgtaggctggagctgcttcCTACTCCATATCAATCTTCACATTC	Amplify pilU (for P_{tac}-pilU OR BACTH TXX-pilU) R
ABD342	ATTTTTCAGTTGGCCTACAATGCTTTCC	P_{tac}-PilT/U @VC1807 F1
BBC719	CACCATACCCACGCCGAAACAAGGATTTTGAATTAAACGTTTCATTAGTC	P_{tac}-PilT/U @VC1807 R1
BBC243	TTGTTTCGGCGTGGGTATGGTG	P_{tac}-PilT/U @VC1807 F2
BBC2667	tccaccacttccacctgcCATTACGTTACCTCCTCCCG	P_{tac}-X-PilT/U (X is 3xFLAG or 6xHis) R
BBC2513	gaagcagctccagcctacaGATCCCCGGGTACCTAAGTAAC	BACTH pKT25-X F
BBC2512	tccacctgctccacctgcCTCTAGAGTCGACCCTGCAG	BACTH pKT25-X R
BBC2515	gaagcagctccagcctacaCCGAGCTCGAATTCATCGATATAAC	BACTH pUT18C-X F
BBC2514	tccacctgctccacctgcCTCTAGAGTCGACCTGCAG	BACTH pUT18C-X R
BBC2518	gcaggtggagcaggtggaAAAGCGACCCAAACCTTACC	BACTH TXX-PilC F
BBC2524	tgtaggctggagctgcttcTTAACCCAATACACTCATTAAGTTAAAG	BACTH TXX-PilC R
BBC2358	GGTATATCTCCTTCTTAAAGTTAAACAAAATTATTTCTAGAGGGGAATTGTTATCC	pHisTev-X F
BBC2360	cggatccGGCTGCTAACAAAGCCCGAAAGGAAGCTGAGTTGGCTGCTGC	pHisTev-X R
BBC2478	TTTTGTTTAACTTTAAGAAGGAGATATACCATGgcaggtggaagtggtgga	Amplify 6xHis-pilT or 6xHis-PilU to clone into pHistev F
BBC2479	CCTTTCGGGCTTTGTTAGCAGCCggatccgCTAAAATGCTTTTAAATCCAACTCG	Amplify 6xHis-pilT to clone into pHistev R
BBC2480	CCTTTCGGGCTTTGTTAGCAGCCggatccgCTACTCCATATCAATCTTCACATTCTG	Amplify 6xHis-pilU to clone into pHistev R
BBC706	CCACACATTATACGAGCCGATG	P_{const}-tfoX R1
BBC2226	catcggctcgtataatgtgtggaGGGGAACGTGATTAAAGGA	P_{const}-tfoX F2

ABD332	GGCTGAACGTGGTTGTCGAAAATGAC	ΔlacZ::lacIq F1
ABD331	GAACATGGGGTGTACGGCAGTGCtATTTAACGATGTGCGGGTTTTGCCAATCTTG	ΔlacZ::lacIq R1
ABD255	gaagcagctccagcctacaCCACAATAAGCCAGAGAGCCTTAAG	ΔlacZ::lacIq F2
ABD256	CCCAAATACGGCAACTTGGCG	ΔlacZ::lacIq R2
ABD841	GGCACTGCCGTACACCCCATGTTCCGGTACCCGACACCATCGAATG	Amplify lacIq F
ABD842	GGCTCTCTGGCTTATTGTGGGGGGAAACCTGTCGTGCCAGCTGC	Amplify lacIq R
DOG0175	AAACTATCCAGATAAGGGAAAGC	comP (*A. baylyi*) F1
CE87	GAAGTTGTCGTACATTTCCAacaTACAGCGCCACTAGCATATG	comP T129C (*A. baylyi*) R1
CE88	CATATGCTAGTGGCGCTGTATGTTGGAAATGTACGACAACTTC	comP T129C (*A. baylyi*) F2
DOG0178	AGGATCTGTAATGACGGGTTGAG	comP (*A. baylyi*) R2
DOG0176	gtcgacggatccccggaatCATAAAATTTCTCCACCAATGTTG	ΔcomP (*A. baylyi*) R1
DOG0177	gaagcagctccagcctacaTGATAGTAGTACTATATGGCTTTAAAAG	ΔcomP (*A. baylyi*) F2
BBC1934	GTTACAAAGTCAGGGACGTAAAG	pilT or pilU (*A. baylyi*) F1
BBC1935	gtcgacggatccccggaatATCCATATTTTCCCCGAAGATCG	ΔpilT (*A. baylyi*) R1
BBC1936	gaagcagctccagcctacaTAAGAATAACGCTACTCGATCTG	ΔpilT (*A. baylyi*) F2
BBC1939	GGTATTCAGATTGATCGTCAGTTAG	pilT or pilU (*A. baylyi*) R2
BBC1937	gtcgacggatccccggaatCATCGTATTGTTTTCCTCTCAGATC	ΔpilU (*A. baylyi*) R1
BBC1938	gaagcagctccagcctacaCGCCGTAATCTCAAATAAAAGAG	ΔpilU (*A. baylyi*) F2
BBC2403	GCTGCAAGGGTGGTTGAagcACCGGAACCAGTGG	pilT^{K136A} (*A. baylyi*) R1
BBC2404	CCACTGGTTCCGGTgctTCAACCACCCTTGCAGC	pilT^{K136A} (*A. baylyi*) F2
BBC2408	GGATGCCAAAGACGTGGAagcTCCTGTACCAGTTGC	pilU^{K137A} (*A. baylyi*) R1
BBC2409	GCAACTGGTACAGGAgctTCCACGTCTTTGGCATCC	pilU^{K137A} (*A. baylyi*) F2
BBC2807	caatttcacacaggatcccgggAGGAGGTGAAAATATGGATATAACAGAATTACTCG	pilT amplify for insertion into P_{tac} construct (*A. baylyi*) F
BBC2808	tgtaggctggagctgcttcTTAGAACGACTCTGGAGATTTTG	pilT amplify for insertion into P_{tac} construct or pMMB67EH (*A. baylyi*) R
BBC2809	caatttcacacaggatcccgggAGGAGGTAATACGATGGACTTTAATGATTTACTC	pilU amplify for insertion into P_{tac} construct (*A. baylyi*) F
BBC2810	tgtaggctggagctgcttcTTATTTGAGATTACGGCGTTGAC	pilU amplify for insertion into P_{tac} construct or pMMB67EH (*A. baylyi*) R

BBC2822	aatttcacacaggaaacagaattcgagctcTTGTTTCGGCGTGGGTATGGTG	Clone P_{tac}-pilT or P_{tac}-PilU into pMMB67EH (*A. baylyi*) F
BBC2824	gagctcgaattctgtttcctgtgtgaaattTTTGCCAGAACCGTTATGATGTC	Amplify pMMB67EH to clone P_{tac}-pilT or P_{tac}-pilU (*A. baylyi*) F
BBC2357	GGTACCCGGGGATCCTCTAGAGTCGACCTGCAGGCATGCAAGCTTGGC	Amplify pMMB67EH to clone P_{tac}-pilT or P_{tac}-pilU (*A. baylyi*) R
DOG0436	AAGCGTTCTGGTTCAATCACC	ΔMSHA locus (VC0399-VC0414) F1
DOG0434	gtcgacggatccccggaatCATTCTCTACCACTGCTATTTGGTTC	ΔMSHA locus (VC0399-VC0414) R1
BBC2129	gaagcagctccagcctacaTAATGATTAAGCACTCAATGGATCCAG	ΔMSHA locus (VC0399-VC0414) F2
BBC2130	TTTTGCATCAGCAAAATCACGC	ΔMSHA locus (VC0399-VC0414) R2
BBC2123	TGATGGTAACTACTATAGGGTCG	ΔTCP locus (VC0825-VC0838) F1
BBC2124	gtcgacggatccccggaatTAAATTAGGCTAGTGCCAGTCAG	ΔTCP locus (VC0825-VC0838) R1
BBC2125	gaagcagctccagcctacaACAGGAGTTGCAGAAAAATAATGG	ΔTCP locus (VC0825-VC0838) F2
BBC2126	ACTAAGATAATTGCTTCACGCATG	ΔTCP locus (VC0825-VC0838) R2

S3 Table. Mean values for each data set

Figure	Strain Name	Mean		Figure	Strain Name	Mean
Fig 1A	Parent	1.08E-01		S2 Fig	PilT x PilT	1.67E+02
Fig 1A	ΔpilA	1.22E-08		S2 Fig	PilU x PilT	6.10E+01
Fig 1A	ΔpilU	5.78E-02		S2 Fig	$PilT^{K136A}$ x PilT	1.57E+02
Fig 1A	ΔpilT	3.29E-06		S2 Fig	$PilU^{K134A}$ x PilT	8.23E+01
Fig 1A	ΔpilTΔpilU	3.91E-06		S2 Fig	PilC x PilT	1.15E+02
Fig 1A	$pilT^{K136A}$	6.22E-02		S2 Fig	vector x PilT	1.13E+00
Fig 1A	$pilT^{K136A}$ ΔpilU	3.89E-06		S2 Fig	PilT x PilU	1.10E+02
Fig 1A	$pilT^{E204A}$	2.55E-02		S2 Fig	PilU x PilU	1.81E+02
Fig 1A	$pilT^{K136A/E204A}$	3.53E-02		S2 Fig	$PilT^{K136A}$ x PilU	7.37E+01
Fig 1A	$pilT^{E204A}$ ΔpilU	9.36E-06		S2 Fig	$PilU^{K134A}$ x PilU	2.11E+02
Fig 1A	$pilT^{K136A/E204A}$ ΔpilU	4.66E-06		S2 Fig	PilC x PilU	9.71E+01
Fig 1B	Parent	2.12E-01		S2 Fig	vector x PilU	1.04E+00
Fig 1B	ΔpilU	1.57E-01		S2 Fig	PilT x $PilT^{K136A}$	1.56E+02
Fig 1B	ΔpilT	3.07E-03		S2 Fig	PilU x $PilT^{K136A}$	7.99E+00
Fig 1B	ΔpilTΔpilU	3.85E-03		S2 Fig	$PilT^{K136A}$ x $PilT^{K136A}$	8.06E+01
Fig 1B	$pilT^{K136A}$	4.26E-02		S2 Fig	$PilU^{K134A}$ x $PilT^{K136A}$	1.04E+01

Fig 1B	pilT^{K136A} ΔpilU	2.06E-03
Fig 1B	pilT^{E204A}	4.82E-02
Fig 1B	pilT$^{E204A/K136A}$	6.12E-02
Fig 1B	pilT^{E204A} ΔpilU	3.58E-03
Fig 1B	pilT$^{E204A/K136A}$ ΔpilU	4.09E-03
Fig 1C	Parent	1.73E+01
Fig 1C	ΔpilU	3.16E+01
Fig 1C	ΔpilT	2.93E-02
Fig 1C	ΔpilTΔpilU	1.33E-01
Fig 1C	pilT^{K136A}	3.43E+01
Fig 1C	pilT^{K136A} ΔpilU	8.75E-02
Fig 1C	pilT^{E204A}	1.41E-01
Fig 1C	pilT$^{E204A/K136A}$	1.77E+01
Fig 1C	pilT^{E204A}ΔpilU	5.65E-02
Fig 1C	pilT$^{E204A/K136A}$ΔpilU	3.86E-02
Fig 1F	Parent	1.05E+01
Fig 1F	ΔpilT	4.93E+00
Fig 1F	ΔpilU	5.08E+00
Fig 1F	ΔpilTΔpilU	6.08E+00
Fig 1H	Parent	1.93E-01
Fig 1H	ΔpilT	1.37E-02
Fig 1H	ΔpilU	7.23E-02
Fig 1H	ΔpilTΔpilU	8.19E-03
Fig 2A	Parent	1.37E-01
Fig 2A	pilU^{L199C}	1.51E-01
Fig 2A	pilT^{K136A}pilU^{L199C}	9.81E-02
Fig 2A	ΔpilT pilU^{L199C}	6.79E-06
Fig 2A	pilT^{L201C}	2.04E-01
Fig 2A	pilT^{L201C} ΔpilU	6.47E-02
Fig 2A	pilT^{K136A}	1.17E-01
Fig 2A	pilU^{K134A}	6.33E-02
Fig 2A	pilT^{K136A}pilU^{K134A}	6.07E-07
Fig 2A	ΔpilU	8.80E-02

S2 Fig	PilC x PilT^{K136A}	1.08E+02
S2 Fig	vector x PilT^{K136A}	7.32E-01
S2 Fig	PilT x PilU^{K134A}	7.20E+01
S2 Fig	PilU x PilU^{K134A}	1.72E+02
S2 Fig	PilT^{K136A} x PilU^{K134A}	4.69E+01
S2 Fig	PilU^{K134A} x PilU^{K134A}	1.34E+02
S2 Fig	PilC x PilU^{K134A}	1.10E+02
S2 Fig	vector x PilU^{K134A}	7.14E-01
S2 Fig	PilT x PilC	8.69E+01
S2 Fig	PilU x PilC	5.20E+01
S2 Fig	PilT^{K136A} x PilC	7.43E+01
S2 Fig	PilU^{K134A} x PilC	7.25E+01
S2 Fig	PilC x PilC	2.55E+02
S2 Fig	vector x PilC	8.15E-01
S2 Fig	PilT x vector	6.59E-01
S2 Fig	PilU x vector	7.85E-01
S2 Fig	PilT^{K136A} x vector	6.81E-01
S2 Fig	PilU^{K134A} x vector	7.14E-01
S2 Fig	PilC x vector	7.68E-01
S2 Fig	vector x vector	7.22E-01
S3-A Fig	Parent	1.46E-01
S3-A Fig	ΔpilT	6.94E-06
S3-A Fig	pilT^{K136A}, 6xHis-pilU	1.53E-01
S3-A Fig	6xHis-pilT	1.14E-01
S3-A Fig	6xHis-pilU	1.11E-01
S3-A Fig	pilT^{K136A}, 3xFLAG-pilU	1.14E-01
S3-A Fig	3xFLAG-pilT	1.45E-01
S3-A Fig	3xFLAG-pilU	1.23E-01
S3-A Fig	pilT^{K136A}	1.20E-01
S3-B Fig	Parent	3.75E-03
S3-B Fig	ΔpilT	4.46E-07
S3-B Fig	Ptac-3xFLAG-pilT	4.60E-03
S3-B Fig	Ptac-3xFLAG-pilT ΔpilT	4.94E-03

Fig 2B	Parent	2.12E-01
Fig 2B	ΔpilU	1.57E-01
Fig 2B	pilT^{K136A}	4.26E-02
Fig 2B	pilU^{K134A}	1.37E-01
Fig 2B	pilT^{K136A}pilU^{K134A}	4.77E-03
Fig 2B	pilT^{K136A} pilU^{L199C}	3.26E-02
Fig 2B	pilU^{L199C}	1.96E-01
Fig 2B	pilT^{L201C}	2.11E-01
Fig 2B	pilT^{L201C}ΔpilU	1.28E-01
Fig 2B	ΔpilT pilU^{L199C}	3.91E-03
Fig 4C	Parent	2.02E-03
Fig 4C	ΔpilU	2.57E-03
Fig 4C	ΔpilT	1.57E-06
Fig 4C	pilT^{K136A}	3.08E-03
Fig 4C	Ptac-pilT^{K136A}	5.94E-03
Fig 4C	Ptac-pilT^{K136A} ΔpilU	2.41E-06
Fig 4C	Ptac-pilU^{K134A}	5.55E-03
Fig 4C	Ptac-pilU^{K134A} pilT^{K136A}	2.46E-05
Fig 4C	Ptac-pilT^{K136A} Ptac-pilU^{K134A}	4.82E-06
Fig 5	pilT^{K136A} ΔpilU	8.95E-09
Fig 5	pilT^{K136A} pilU^{K137A}	7.00E-09
Fig 5	pilT^{K136A}	1.17E-03
Fig 5	pilU^{K137A}	2.34E-03
Fig 5	Parent	4.10E-02
Fig 5	ΔpilT	8.52E-09
Fig 5	ΔpilU	3.17E-03
Fig 5	ΔpilTU	8.48E-09
Fig 5	ΔcomP	6.53E-09
S1 Fig	ΔpilT ΔpilU Ptac-PilT	7.05E-02
S1 Fig	ΔpilT ΔpilU Ptac-PilU	7.26E-06

S3-B Fig	Ptac-3xFLAG-pilU	2.78E-03
S3-B Fig	Ptac-3xFLAG-pilU, pilT^{K136A} ΔpilU	1.66E-03
S3-B Fig	Ptac-3xFLAG-pilT^{K136A}	5.66E-03
S3-B Fig	Ptac-3xFLAG-pilU^{K134A}	4.71E-03
S3-B Fig	Ptac-3xFLAG-pilT^{K136A}, ΔpilU	1.25E-06
S3-B Fig	P_{tac}-3xFLAG-pilU^{K134A}, pilT^{K136A}	2.00E-06
S3-B Fig	ΔpilU	2.48E-03
S3-B Fig	pilT^{K136A}	2.24E-03
S3-D Fig	Parent	1.97E-03
S3-D Fig	ΔpilT ΔpilU	2.15E-07
S3-D Fig	pilU^{K134A}	3.90E-03
S3-D Fig	pilT^{K136A} ΔpilU	3.62E-08
S3-D Fig	pilT^{K136A} pilU^{K134A}	2.12E-07
S3-D Fig	P_{tac}-pilT	4.18E-03
S3-D Fig	ΔpilT Ptac-pilT	4.08E-03
S3-D Fig	P_{tac}-pilU	4.07E-03
S3-D Fig	pilT^{K136A} ΔpilU Ptac-pilU	1.39E-03
S3-D Fig	ΔpilA	6.49E-09
S3-D Fig	pilT^{K136A}	1.75E-03
S4 Fig	Parent pmmB-pilT	2.23E-02
S4 Fig	ΔpilTU pmmB-pilT	2.05E-03
S4 Fig	ΔpilT pmmB-pilT	1.80E-02
S4 Fig	ΔpilU pmmB-pilT	3.24E-03
S4 Fig	pilT^{K136A} pmmB-pilT	1.68E-02
S4 Fig	pilT^{K136A} ΔpilU pmmB-pilT	2.30E-03
S4 Fig	pilU^{K137A} pmmB-pilT	1.63E-03
S4 Fig	pilT^{K136A} pilU^{K137A} pmmB-pilT	2.19E-03
S4 Fig	Parent pmmB-pilU	8.67E-02
S4 Fig	ΔpilTU pmmB-pilU	2.04E-07
S4 Fig	ΔpilT pmmB-pilU	1.55E-07

S1 Fig	pilT^{K136A} ΔpilU Ptac-PilT	6.53E-02		S4 Fig	ΔpilU pmmB-pilU	2.48E-02
S1 Fig	pilT^{K136A} ΔpilU Ptac-PilU	6.27E-02		S4 Fig	pilT^{K136A} pmmB-pilU	7.66E-04
S1 Fig	pilT^{K136A} pilU^{K134A} Ptac-PilT	4.21E-02		S4 Fig	pilT^{K136A} ΔpilU pmmB-pilU	8.35E-04
S1 Fig	pilT^{K136A} pilU^{K134A} Ptac-PilU	4.65E-02		S4 Fig	pilU^{K137A} pmmB-pilU	1.07E-02
S1 Fig	Parent Ptac-PilT	6.74E-02		S4 Fig	pilT^{K136A} pilU^{K137A} pmmB-pilU	9.52E-04
S1 Fig	Parent Ptac-PilU	8.85E-02		S4 Fig	Parent pmmB-pilU	2.66E-02
S1 Fig	ΔpilT Ptac-PilT	6.55E-02		S5 Fig	Parent	3.12E-01
S1 Fig	ΔpilT Ptac-PilU	3.13E-06		S5 Fig	ΔMSHA ΔTCP	3.73E-01
S1 Fig	pilT$^{K136A/E204A}$ ΔpilU Ptac-PilT	6.32E-02		S5 Fig	ΔpilTU	1.59E-05
S1 Fig	pilT$^{K136A/E204A}$ ΔpilU Ptac-PilU	4.05E-02		S5 Fig	ΔpilTU ΔMSHA ΔTCP	3.34E-05
S1 Fig	pilT^{E204A} ΔpilU Ptac-PilT	6.02E-02				
S1 Fig	pilT^{E204A} ΔpilU Ptac-PilU	7.81E-02				

S4 Table. Statistical Comparisons.

Comparison	P value#		Information
Figure 1A - Tukey's multiple comparison test			
Parent vs. ΔpilA	****	<0.0001	# of families = 1
Parent vs. ΔpilU	ns	0.6432	# of comparisons per family = 55
Parent vs. ΔpilT	****	<0.0001	Alpha = 0.05
Parent vs. ΔpilTΔpilU	****	<0.0001	
Parent vs. pilT^{K136A}	ns	0.804	
Parent vs. pilT^{K136A} ΔpilU	****	<0.0001	
Parent vs. pilT^{E204A}	****	<0.0001	
Parent vs. pilT$^{K136A/E204A}$	*	0.0135	
Parent vs. pilT^{E204A} ΔpilU	****	<0.0001	
Parent vs. pilT$^{K136A/E204A}$ ΔpilU	****	<0.0001	
ΔpilA vs. ΔpilU	****	<0.0001	
ΔpilA vs. ΔpilT	****	<0.0001	
ΔpilA vs. ΔpilTΔpilU	****	<0.0001	
ΔpilA vs. pilT^{K136A}	****	<0.0001	
ΔpilA vs. pilT^{K136A} ΔpilU	****	<0.0001	
ΔpilA vs. pilT^{E204A}	****	<0.0001	
ΔpilA vs. pilT$^{K136A/E204A}$	****	<0.0001	
ΔpilA vs. pilT^{E204A} ΔpilU	****	<0.0001	
ΔpilA vs. pilT$^{K136A/E204A}$ ΔpilU	****	<0.0001	
ΔpilU vs. ΔpilT	****	<0.0001	
ΔpilU vs. ΔpilTΔpilU	****	<0.0001	
ΔpilU vs. pilT^{K136A}	ns	>0.9999	

ΔpilU vs. pilT^{K136A} ΔpilU	****	<0.0001	
ΔpilU vs. pilT^{E204A}	ns	0.0523	
ΔpilU vs. pilT$^{K136A/E204A}$	ns	0.8854	
ΔpilU vs. pilT^{E204A} ΔpilU	****	<0.0001	
ΔpilU vs. pilT$^{K136A/E204A}$ ΔpilU	****	<0.0001	
ΔpilT vs. ΔpilTΔpilU	ns	>0.9999	
ΔpilT vs. pilT^{K136A}	****	<0.0001	
ΔpilT vs. pilT^{K136A} ΔpilU	ns	>0.9999	
ΔpilT vs. pilT^{E204A}	****	<0.0001	
ΔpilT vs. pilT$^{K136A/E204A}$	****	<0.0001	
ΔpilT vs. pilT^{E204A} ΔpilU	ns	0.1222	
ΔpilT vs. pilT$^{K136A/E204A}$ ΔpilU	ns	0.994	
ΔpilTΔpilU vs. pilT^{K136A}	****	<0.0001	
ΔpilTΔpilU vs. pilT^{K136A} ΔpilU	ns	>0.9999	
ΔpilTΔpilU vs. pilT^{E204A}	****	<0.0001	
ΔpilTΔpilU vs. pilT$^{K136A/E204A}$	****	<0.0001	
ΔpilTΔpilU vs. pilT^{E204A} ΔpilU	ns	0.1655	
ΔpilTΔpilU vs. pilT$^{K136A/E204A}$ ΔpilU	ns	0.9983	
pilT^{K136A} vs. pilT^{K136A} ΔpilU	****	<0.0001	
pilT^{K136A} vs. pilT^{E204A}	*	0.03	
pilT^{K136A} vs. pilT$^{K136A/E204A}$	ns	0.7787	
pilT^{K136A} vs. pilT^{E204A} ΔpilU	****	<0.0001	
pilT^{K136A} vs. pilT$^{K136A/E204A}$ ΔpilU	****	<0.0001	
pilT^{K136A} ΔpilU vs. pilT^{E204A}	****	<0.0001	
pilT^{K136A} ΔpilU vs. pilT$^{K136A/E204A}$	****	<0.0001	
pilT^{K136A} ΔpilU vs. pilT^{E204A} ΔpilU	ns	0.1909	
pilT^{K136A} ΔpilU vs. pilT$^{K136A/E204A}$ ΔpilU	ns	0.9992	
pilT^{E204A} vs. pilT$^{K136A/E204A}$	ns	0.7599	
pilT^{E204A} vs. pilT^{E204A} ΔpilU	****	<0.0001	
pilT^{E204A} vs. pilT$^{K136A/E204A}$ ΔpilU	****	<0.0001	
pilT$^{K136A/E204A}$ vs. pilT^{E204A} ΔpilU	****	<0.0001	
pilT$^{K136A/E204A}$ vs. pilT$^{K136A/E204A}$ ΔpilU	****	<0.0001	
pilT^{E204A} ΔpilU vs. pilT$^{K136A/E204A}$ ΔpilU	ns	0.6405	
Figure 1B - Tukey's multiple comparison test			
Parent vs. ΔpilU	****	<0.0001	# of families = 1
Parent vs. ΔpilT	****	<0.0001	# of comparisons per family = 45
Parent vs. ΔpilTΔpilU	****	<0.0001	Alpha = 0.05
Parent vs. pilT^{K136A}	****	<0.0001	
Parent vs. pilT^{K136A} ΔpilU	****	<0.0001	
Parent vs. pilT^{E204A}	****	<0.0001	
Parent vs. pilT$^{E204A/K136A}$	****	<0.0001	
Parent vs. pilT^{E204A} ΔpilU	****	<0.0001	

Parent vs. pilT$^{E204A/K136A}$ ΔpilU	****	<0.0001	
ΔpilU vs. ΔpilT	****	<0.0001	
ΔpilU vs. ΔpilTΔpilU	****	<0.0001	
ΔpilU vs. pilT^{K136A}	****	<0.0001	
ΔpilU vs. pilT^{K136A} ΔpilU	****	<0.0001	
ΔpilU vs. pilT^{E204A}	****	<0.0001	
ΔpilU vs. pilT$^{E204A/K136A}$	****	<0.0001	
ΔpilU vs. pilT^{E204A} ΔpilU	****	<0.0001	
ΔpilU vs. pilT$^{E204A/K136A}$ ΔpilU	****	<0.0001	
ΔpilT vs. ΔpilTΔpilU	ns	>0.9999	
ΔpilT vs. pilT^{K136A}	ns	0.0674	
ΔpilT vs. pilT^{K136A} ΔpilU	ns	>0.9999	
ΔpilT vs. pilT^{E204A}	ns	0.4312	
ΔpilT vs. pilT$^{E204A/K136A}$	***	0.0005	
ΔpilT vs. pilT^{E204A} ΔpilU	ns	>0.9999	
ΔpilT vs. pilT$^{E204A/K136A}$ ΔpilU	ns	>0.9999	
ΔpilTΔpilU vs. pilT^{K136A}	**	0.0027	
ΔpilTΔpilU vs. pilT^{K136A} ΔpilU	ns	>0.9999	
ΔpilTΔpilU vs. pilT^{E204A}	ns	0.3118	
ΔpilTΔpilU vs. pilT$^{E204A/K136A}$	****	<0.0001	
ΔpilTΔpilU vs. pilT^{E204A} ΔpilU	ns	>0.9999	
ΔpilTΔpilU vs. pilT$^{E204A/K136A}$ ΔpilU	ns	>0.9999	
pilT^{K136A} vs. pilT^{K136A} ΔpilU	ns	0.0538	
pilT^{K136A} vs. pilT^{E204A}	ns	>0.9999	
pilT^{K136A} vs. pilT$^{E204A/K136A}$	ns	0.1608	
pilT^{K136A} vs. pilT^{E204A} ΔpilU	**	0.0034	
pilT^{K136A} vs. pilT$^{E204A/K136A}$ ΔpilU	ns	0.2706	
pilT^{K136A} ΔpilU vs. pilT^{E204A}	ns	0.3977	
pilT^{K136A} ΔpilU vs. pilT$^{E204A/K136A}$	***	0.0004	
pilT^{K136A} ΔpilU vs. pilT^{E204A} ΔpilU	ns	>0.9999	
pilT^{K136A} ΔpilU vs. pilT$^{E204A/K136A}$ ΔpilU	ns	>0.9999	
pilT^{E204A} vs. pilT$^{E204A/K136A}$	ns	0.9989	
pilT^{E204A} vs. pilT^{E204A} ΔpilU	ns	0.3122	
pilT^{E204A} vs. pilT$^{E204A/K136A}$ ΔpilU	ns	0.5871	
pilT$^{E204A/K136A}$ vs. pilT^{E204A} ΔpilU	****	<0.0001	
pilT$^{E204A/K136A}$ vs. pilT$^{E204A/K136A}$ ΔpilU	*	0.0109	
pilT^{E204A} ΔpilU vs. pilT$^{E204A/K136A}$ ΔpilU	ns	>0.9999	
Figure 1C - Tukey's multiple comparison test			
Parent vs. ΔpilU	ns	>0.9999	# of families = 1
Parent vs. ΔpilT	****	<0.0001	# of comparisons per family = 45
Parent vs. ΔpilTΔpilU	****	<0.0001	Alpha = 0.05
Parent vs. pilT^{K136A}	ns	0.9963	
Parent vs. pilT^{K136A} ΔpilU	***	0.0002	

Parent vs. pilT^{E204A}	***	0.0006	
Parent vs. pilT$^{E204A/K136A}$	ns	>0.9999	
Parent vs. pilT^{E204A} ΔpilU	****	<0.0001	
Parent vs. pilT$^{E204A/K136A}$ ΔpilU	****	<0.0001	
ΔpilU vs. ΔpilT	****	<0.0001	
ΔpilU vs. ΔpilTΔpilU	****	<0.0001	
ΔpilU vs. pilT^{K136A}	ns	>0.9999	
ΔpilU vs. pilT^{K136A} ΔpilU	****	<0.0001	
ΔpilU vs. pilT^{E204A}	***	0.0002	
ΔpilU vs. pilT$^{E204A/K136A}$	ns	>0.9999	
ΔpilU vs. pilT^{E204A} ΔpilU	****	<0.0001	
ΔpilU vs. pilT$^{E204A/K136A}$ ΔpilU	****	<0.0001	
ΔpilT vs. ΔpilTΔpilU	ns	0.9878	
ΔpilT vs. pilT^{K136A}	****	<0.0001	
ΔpilT vs. pilT^{K136A} ΔpilU	ns	0.9085	
ΔpilT vs. pilT^{E204A}	ns	0.6143	
ΔpilT vs. pilT$^{E204A/K136A}$	****	<0.0001	
ΔpilT vs. pilT^{E204A} ΔpilU	ns	>0.9999	
ΔpilT vs. pilT$^{E204A/K136A}$ ΔpilU	ns	>0.9999	
ΔpilTΔpilU vs. pilT^{K136A}	****	<0.0001	
ΔpilTΔpilU vs. pilT^{K136A} ΔpilU	ns	>0.9999	
ΔpilTΔpilU vs. pilT^{E204A}	ns	0.9904	
ΔpilTΔpilU vs. pilT$^{E204A/K136A}$	****	<0.0001	
ΔpilTΔpilU vs. pilT^{E204A} ΔpilU	ns	>0.9999	
ΔpilTΔpilU vs. pilT$^{E204A/K136A}$ ΔpilU	ns	0.9718	
pilT^{K136A} vs. pilT^{K136A} ΔpilU	****	<0.0001	
pilT^{K136A} vs. pilT^{E204A}	****	<0.0001	
pilT^{K136A} vs. pilT$^{E204A/K136A}$	ns	0.9992	
pilT^{K136A} vs. pilT^{E204A} ΔpilU	****	<0.0001	
pilT^{K136A} vs. pilT$^{E204A/K136A}$ ΔpilU	****	<0.0001	
pilT^{K136A} ΔpilU vs. pilT^{E204A}	ns	0.9998	
pilT^{K136A} ΔpilU vs. pilT$^{E204A/K136A}$	***	0.0001	
pilT^{K136A} ΔpilU vs. pilT^{E204A} ΔpilU	ns	0.9936	
pilT^{K136A} ΔpilU vs. pilT$^{E204A/K136A}$ ΔpilU	ns	0.8538	
pilT^{E204A} vs. pilT$^{E204A/K136A}$	***	0.0004	
pilT^{E204A} vs. pilT^{E204A} ΔpilU	ns	0.8779	
pilT^{E204A} vs. pilT$^{E204A/K136A}$ ΔpilU	ns	0.5286	
pilT$^{E204A/K136A}$ vs. pilT^{E204A} ΔpilU	****	<0.0001	
pilT$^{E204A/K136A}$ vs. pilT$^{E204A/K136A}$ ΔpilU	****	<0.0001	
pilT^{E204A} ΔpilU vs. pilT$^{E204A/K136A}$ ΔpilU	ns	0.9996	
Figure 1F - Tukey's multiple comparison test			
Parent vs. ΔpilT	****	<0.0001	# of families = 1

Parent vs. ΔpilU	****	<0.0001	# of comparisons per family = 6
Parent vs. ΔpilTΔpilU	****	<0.0001	Alpha = 0.05
ΔpilT vs. ΔpilU	ns	0.9956	
ΔpilT vs. ΔpilTΔpilU	ns	0.5137	
ΔpilU vs. ΔpilTΔpilU	ns	0.738	
Figure 1H - Tukey's multiple comparison test			
Parent vs. ΔpilT	****	<0.0001	# of families = 1
Parent vs. ΔpilU	****	<0.0001	# of comparisons per family = 6
Parent vs. ΔpilTΔpilU	****	<0.0001	Alpha = 0.05
ΔpilT vs. ΔpilU	**	0.0028	
ΔpilT vs. ΔpilTΔpilU	ns	0.9806	
ΔpilU vs. ΔpilTΔpilU	**	0.0051	
Figure 2A - Tukey's multiple comparison test			
Parent vs. pilU^{L199C}	ns	>0.9999	# of families = 1
Parent vs. pilT^{K136A} pilU^{L199C}	ns	0.9978	# of comparisons per family = 45
Parent vs. ΔpilT pilU^{L199C}	****	<0.0001	Alpha = 0.05
Parent vs. pilT^{L201C}	ns	>0.9999	
Parent vs. pilT^{L201C} ΔpilU	ns	0.4971	
Parent vs. pilT^{K136A}	ns	>0.9999	
Parent vs. pilU^{K134A}	ns	0.4696	
Parent vs. pilT^{K136A} pilU^{K134A}	****	<0.0001	
Parent vs. ΔpilU	ns	0.9608	
pilU^{L199C} vs. pilT^{K136A} pilU^{L199C}	ns	0.9864	
pilU^{L199C} vs. ΔpilT pilU^{L199C}	****	<0.0001	
pilU^{L199C} vs. pilT^{L201C}	ns	0.9999	
pilU^{L199C} vs. pilT^{L201C} ΔpilU	ns	0.4266	
pilU^{L199C} vs. pilT^{K136A}	ns	>0.9999	
pilU^{L199C} vs. pilU^{K134A}	ns	0.403	
pilU^{L199C} vs. pilT^{K136A} pilU^{K134A}	****	<0.0001	
pilU^{L199C} vs. ΔpilU	ns	0.9085	
pilT^{K136A} pilU^{L199C} vs. ΔpilT pilU^{L199C}	****	<0.0001	
pilT^{K136A} pilU^{L199C} vs. pilT^{L201C}	ns	>0.9999	
pilT^{K136A} pilU^{L199C} vs. pilT^{L201C} ΔpilU	ns	0.9608	
pilT^{K136A} pilU^{L199C} vs. pilT^{K136A}	ns	>0.9999	
pilT^{K136A} pilU^{L199C} vs. pilU^{K134A}	ns	0.9525	
pilT^{K136A} pilU^{L199C} vs. pilT^{K136A} pilU^{K134A}	****	<0.0001	
pilT^{K136A} pilU^{L199C} vs. ΔpilU	ns	>0.9999	
ΔpilT pilU^{L199C} vs. pilT^{L201C}	****	<0.0001	
ΔpilT pilU^{L199C} vs. pilT^{L201C} ΔpilU	****	<0.0001	
ΔpilT pilU^{L199C} vs. pilT^{K136A}	****	<0.0001	
ΔpilT pilU^{L199C} vs. pilU^{K134A}	****	<0.0001	
ΔpilT pilU^{L199C} vs. pilT^{K136A} pilU^{K134A}	****	<0.0001	

ΔpilT pilU^{L199C} vs. ΔpilU	****	<0.0001	
pilT^{L201C} vs. pilT^{L201C} ΔpilU	ns	0.7827	
pilT^{L201C} vs. pilT^{K136A}	ns	>0.9999	
pilT^{L201C} vs. pilU^{K134A}	ns	0.7604	
pilT^{L201C} vs. pilT^{K136A} pilU^{K134A}	****	<0.0001	
pilT^{L201C} vs. ΔpilU	ns	0.9968	
pilT^{L201C} ΔpilU vs. pilT^{K136A}	ns	0.7609	
pilT^{L201C} ΔpilU vs. pilU^{K134A}	ns	>0.9999	
pilT^{L201C} ΔpilU vs. pilT^{K136A} pilU^{K134A}	****	<0.0001	
pilT^{L201C} ΔpilU vs. ΔpilU	ns	0.9969	
pilT^{K136A} vs. pilU^{K134A}	ns	0.7378	
pilT^{K136A} vs. pilT^{K136A} pilU^{K134A}	****	<0.0001	
pilT^{K136A} vs. ΔpilU	ns	0.9956	
pilU^{K134A} vs. pilT^{K136A} pilU^{K134A}	****	<0.0001	
pilU^{K134A} vs. ΔpilU	ns	0.9957	
pilT^{K136A} pilU^{K134A} vs. ΔpilU	****	<0.0001	
Figure 2B - Tukey's multiple comparison test			
Parent vs. ΔpilU	****	<0.0001	# of families = 1
Parent vs. pilT^{K136A}	****	<0.0001	# of comparisons per family = 45
Parent vs. pilU^{K134A}	****	<0.0001	Alpha = 0.05
Parent vs. pilT^{K136A} pilU^{K134A}	****	<0.0001	
Parent vs. pilT^{K136A} pilU^{L199C}	****	<0.0001	
Parent vs. pilU^{L199C}	ns	0.6117	
Parent vs. pilT^{L201C}	ns	>0.9999	
Parent vs. pilT^{L201C} ΔpilU	****	<0.0001	
Parent vs. ΔpilT pilU^{L199C}	****	<0.0001	
ΔpilU vs. pilT^{K136A}	****	<0.0001	
ΔpilU vs. pilU^{K134A}	ns	0.1821	
ΔpilU vs. pilT^{K136A} pilU^{K134A}	****	<0.0001	
ΔpilU vs. pilT^{K136A} pilU^{L199C}	****	<0.0001	
ΔpilU vs. pilU^{L199C}	***	0.0003	
ΔpilU vs. pilT^{L201C}	****	<0.0001	
ΔpilU vs. pilT^{L201C} ΔpilU	*	0.014	
ΔpilU vs. ΔpilT pilU^{L199C}	****	<0.0001	
pilT^{K136A} vs. pilU^{K134A}	****	<0.0001	
pilT^{K136A} vs. pilT^{K136A} pilU^{K134A}	ns	0.3556	
pilT^{K136A} vs. pilT^{K136A} pilU^{L199C}	ns	0.9694	
pilT^{K136A} vs. pilU^{L199C}	****	<0.0001	
pilT^{K136A} vs. pilT^{L201C}	****	<0.0001	
pilT^{K136A} vs. pilT^{L201C} ΔpilU	****	<0.0001	
pilT^{K136A} vs. ΔpilT pilU^{L199C}	ns	0.1504	
pilU^{K134A} vs. pilT^{K136A} pilU^{K134A}	****	<0.0001	

pilU^{K134A} vs. pilT^{K136A} pilU^{L199C}	****	<0.0001	
pilU^{K134A} vs. pilU^{L199C}	****	<0.0001	
pilU^{K134A} vs. pilT^{L201C}	****	<0.0001	
pilU^{K134A} vs. pilT^{L201C} ΔpilU	ns	0.9841	
pilU^{K134A} vs. ΔpilT pilU^{L199C}	****	<0.0001	
pilT^{K136A} pilU^{K134A} vs. pilT^{K136A} pilU^{L199C}	ns	0.8001	
pilT^{K136A} pilU^{K134A} vs. pilU^{L199C}	****	<0.0001	
pilT^{K136A} pilU^{K134A} vs. pilT^{L201C}	****	<0.0001	
pilT^{K136A} pilU^{K134A} vs. pilT^{L201C} ΔpilU	****	<0.0001	
pilT^{K136A} pilU^{K134A} vs. ΔpilT pilU^{L199C}	ns	>0.9999	
pilT^{K136A} pilU^{L199C} vs. pilU^{L199C}	****	<0.0001	
pilT^{K136A} pilU^{L199C} vs. pilT^{L201C}	****	<0.0001	
pilT^{K136A} pilU^{L199C} vs. pilT^{L201C} ΔpilU	****	<0.0001	
pilT^{K136A} pilU^{L199C} vs. ΔpilT pilU^{L199C}	ns	0.6067	
pilU^{L199C} vs. pilT^{L201C}	ns	0.7303	
pilU^{L199C} vs. pilT^{L201C} ΔpilU	****	<0.0001	
pilU^{L199C} vs. ΔpilT pilU^{L199C}	****	<0.0001	
pilT^{L201C} vs. pilT^{L201C} ΔpilU	****	<0.0001	
pilT^{L201C} vs. ΔpilT pilU^{L199C}	****	<0.0001	
pilT^{L201C} ΔpilU vs. ΔpilT pilU^{L199C}	****	<0.0001	
Figure 4C - Tukey's multiple comparison test			
Parent vs. ΔpilU	ns	>0.9999	# of families = 1
Parent vs. ΔpilT	****	<0.0001	# of comparisons per family = 36
Parent vs. pilT^{K136A}	ns	0.9998	Alpha = 0.05
Parent vs. Ptac-pilT^{K136A}	ns	0.9537	
Parent vs. Ptac-pilT^{K136A} ΔpilU	****	<0.0001	
Parent vs. Ptac-pilU^{K134A}	ns	0.9996	
Parent vs. Ptac-pilU^{K134A} pilT^{K136A}	****	<0.0001	
Parent vs. Ptac-pilT^{K136A} Ptac-pilU^{K134A}	****	<0.0001	
ΔpilU vs. ΔpilT	****	<0.0001	
ΔpilU vs. pilT^{K136A}	ns	>0.9999	
ΔpilU vs. Ptac-pilT^{K136A}	ns	0.9844	
ΔpilU vs. Ptac-pilT^{K136A} ΔpilU	****	<0.0001	
ΔpilU vs. Ptac-pilU^{K134A}	ns	>0.9999	
ΔpilU vs. Ptac-pilU^{K134A} pilT^{K136A}	****	<0.0001	
ΔpilU vs. Ptac-pilT^{K136A} Ptac-pilU^{K134A}	****	<0.0001	
ΔpilT vs. pilT^{K136A}	****	<0.0001	
ΔpilT vs. Ptac-pilT^{K136A}	****	<0.0001	
ΔpilT vs. Ptac-pilT^{K136A} ΔpilU	ns	0.9408	
ΔpilT vs. Ptac-pilU^{K134A}	****	<0.0001	
ΔpilT vs. Ptac-pilU^{K134A} pilT^{K136A}	ns	0.3939	
ΔpilT vs. Ptac-pilT^{K136A} Ptac-pilU^{K134A}	ns	0.542	

pilT^{K136A} vs. Ptac-pilT^{K136A}	ns	0.9988	
pilT^{K136A} vs. Ptac-pilT^{K136A} ΔpilU	****	<0.0001	
pilT^{K136A} vs. Ptac-pilU^{K134A}	ns	>0.9999	
pilT^{K136A} vs. Ptac-pilU^{K134A} pilT^{K136A}	****	<0.0001	
pilT^{K136A} vs. Ptac-pilT^{K136A} Ptac-pilU^{K134A}	****	<0.0001	
Ptac-pilT^{K136A} vs. Ptac-pilT^{K136A} ΔpilU	****	<0.0001	
Ptac-pilT^{K136A} vs. Ptac-pilU^{K134A}	ns	0.9994	
Ptac-pilT^{K136A} vs. Ptac-pilU^{K134A} pilT^{K136A}	****	<0.0001	
Ptac-pilT^{K136A} vs. Ptac-pilT^{K136A} Ptac-pilU^{K134A}	****	<0.0001	
Ptac-pilT^{K136A} ΔpilU vs. Ptac-pilU^{K134A}	****	<0.0001	
Ptac-pilT^{K136A} ΔpilU vs. Ptac-pilU^{K134A} pilT^{K136A}	ns	0.9789	
Ptac-pilT^{K136A} ΔpilU vs. Ptac-pilT^{K136A} Ptac-pilU^{K134A}	ns	0.9964	
Ptac-pilU^{K134A} vs. Ptac-pilU^{K134A} pilT^{K136A}	****	<0.0001	
Ptac-pilU^{K134A} vs. Ptac-pilT^{K136A} Ptac-pilU^{K134A}	****	<0.0001	
Ptac-pilU^{K134A} pilT^{K136A} vs. Ptac-pilT^{K136A} Ptac-pilU^{K134A}	ns	>0.9999	
Figure 5 - Tukey's multiple comparison test			
pilT^{K136A} ΔpilU vs. pilT^{K136A} pilU^{K137A}	ns	0.9546	# of families = 1
pilT^{K136A} ΔpilU vs. pilT^{K136A}	****	<0.0001	# of comparisons per family = 36
pilT^{K136A} ΔpilU vs. pilU^{K137A}	****	<0.0001	Alpha = 0.05
pilT^{K136A} ΔpilU vs. Parent	****	<0.0001	
pilT^{K136A} ΔpilU vs. ΔpilT	ns	>0.9999	
pilT^{K136A} ΔpilU vs. ΔpilU	****	<0.0001	
pilT^{K136A} ΔpilU vs. ΔpilTU	ns	>0.9999	
pilT^{K136A} ΔpilU vs. ΔcomP	ns	0.7185	
pilT^{K136A} pilU^{K137A} vs. pilT^{K136A}	****	<0.0001	
pilT^{K136A} pilU^{K137A} vs. pilU^{K137A}	****	<0.0001	
pilT^{K136A} pilU^{K137A} vs. Parent	****	<0.0001	
pilT^{K136A} pilU^{K137A} vs. ΔpilT	ns	0.9681	
pilT^{K136A} pilU^{K137A} vs. ΔpilU	****	<0.0001	
pilT^{K136A} pilU^{K137A} vs. ΔpilTU	ns	0.9694	
pilT^{K136A} pilU^{K137A} vs. ΔcomP	ns	>0.9999	
pilT^{K136A} vs. pilU^{K137A}	**	0.0082	
pilT^{K136A} vs. Parent	****	<0.0001	
pilT^{K136A} vs. ΔpilT	****	<0.0001	
pilT^{K136A} vs. ΔpilU	***	0.0003	
pilT^{K136A} vs. ΔpilTU	****	<0.0001	
pilT^{K136A} vs. ΔcomP	****	<0.0001	
pilU^{K137A} vs. Parent	****	<0.0001	
pilU^{K137A} vs. ΔpilT	****	<0.0001	
pilU^{K137A} vs. ΔpilU	ns	0.9315	
pilU^{K137A} vs. ΔpilTU	****	<0.0001	

pilU^{K137A} vs. ΔcomP	****	<0.0001	
Parent vs. ΔpilT	****	<0.0001	
Parent vs. ΔpilU	****	<0.0001	
Parent vs. ΔpilTU	****	<0.0001	
Parent vs. ΔcomP	****	<0.0001	
ΔpilT vs. ΔpilU	****	<0.0001	
ΔpilT vs. ΔpilTU	ns	>0.9999	
ΔpilT vs. ΔcomP	ns	0.7633	
ΔpilU vs. ΔpilTU	****	<0.0001	
ΔpilU vs. ΔcomP	****	<0.0001	
ΔpilTU vs. ΔcomP	ns	0.7681	
Supplemental Figure 1 - Dunnett's multiple comparison test			
Parent Ptac-PilT vs. ΔpilT ΔpilU Ptac-PilT	ns	0.9999	# of families = 2
Parent Ptac-PilT vs. pilT^{K136A} ΔpilU Ptac-PilT	ns	0.9999	# of comparisons per family = 6
Parent Ptac-PilT vs. pilT^{K136A} pilU^{K134A} Ptac-PilT	ns	0.37	Alpha = 0.05
Parent Ptac-PilT vs. ΔpilT Ptac-PilT	ns	0.9999	
Parent Ptac-PilT vs. pilT$^{K136A/E204A}$ ΔpilU Ptac-PilT	ns	0.9996	
Parent Ptac-PilT vs. pilT^{E204A} ΔpilU Ptac-PilT	ns	0.9779	
Parent Ptac-PilU vs. ΔpilT ΔpilU Ptac-PilU	****	0.0001	
Parent Ptac-PilU vs. pilT^{K136A} ΔpilU Ptac-PilU	ns	0.8282	
Parent Ptac-PilU vs. pilT^{K136A} pilU^{K134A} Ptac-PilU	ns	0.3199	
Parent Ptac-PilU vs. ΔpilT Ptac-PilU	****	0.0001	
Parent Ptac-PilU vs. pilT$^{K136A/E204A}$ ΔpilU Ptac-PilU	ns	0.0732	
Parent Ptac-PilU vs. pilT^{E204A} ΔpilU Ptac-PilU	ns	0.9999	
Supplemental Figure 2 (T18 x T25) - Dunnett's multiple comparison test			
vector x PilT vs. PilT x PilT	****	<0.0001	# of families = 6
vector x PilT vs. PilU x PilT	*	0.0343	# of comparisons per family = 6
vector x PilT vs. PilT^{K136A} x PilT	****	<0.0001	Alpha = 0.05
vector x PilT vs. PilU^{K134A} x PilT	**	0.0043	
vector x PilT vs. PilC x PilT	***	0.0002	
vector x PilU vs. PilT x PilU	*	0.0464	
vector x PilU vs. PilU x PilU	**	0.0016	
vector x PilU vs. PilT^{K136A} x PilU	ns	0.2389	
vector x PilU vs. PilU^{K134A} x PilU	***	0.0005	
vector x PilU vs. PilC x PilU	ns	0.0849	
vector x PilT^{K136A} vs. PilT x PilT^{K136A}	**	0.0031	
vector x PilT^{K136A} vs. PilU x PilT^{K136A}	ns	0.9997	
vector x PilT^{K136A} vs. PilT^{K136A} x PilT^{K136A}	ns	0.1368	
vector x PilT^{K136A} vs. PilU^{K134A} x PilT^{K136A}	ns	0.9984	
vector x PilT^{K136A} vs. PilC x PilT^{K136A}	*	0.0349	
vector x PilU^{K134A} vs. PilT x PilU^{K134A}	ns	0.1185	

vector x PilU^{K134A} vs. PilU x PilU^{K134A}	***	0.0004	
vector x PilU^{K134A} vs. PilT^{K136A} x PilU^{K134A}	ns	0.4273	
vector x PilU^{K134A} vs. PilU^{K134A} x PilU^{K134A}	**	0.003	
vector x PilU^{K134A} vs. PilC x PilU^{K134A}	*	0.013	
vector x PilC vs. PilT x PilC	ns	0.0724	
vector x PilC vs. PilU x PilC	ns	0.4038	
vector x PilC vs. PilT^{K136A} x PilC	ns	0.1408	
vector x PilC vs. PilU^{K134A} x PilC	ns	0.1544	
vector x PilC vs. PilC x PilC	****	0.0001	
vector x vector vs. PilT x vector	ns	0.9999	
vector x vector vs. PilU x vector	ns	0.9999	
vector x vector vs. PilT^{K136A} x vector	ns	0.9999	
vector x vector vs. PilU^{K134A} x vector	ns	0.9999	
vector x vector vs. PilC x vector	ns	0.9999	
Supplemental Figure 3A - Tukey's multiple comparison test			
Parent vs. ΔpilT	***	0.0002	# of families = 1
Parent vs. pilT^{K136A}, 6xHis-pilU	ns	>0.9999	# of comparisons per family = 36
Parent vs. 6xHis-pilT	ns	0.9508	Alpha = 0.05
Parent vs. 6xHis-pilU	ns	0.9235	
Parent vs. pilT^{K136A}, 3xFLAG-pilU	ns	0.9553	
Parent vs. 3xFLAG-pilT	ns	>0.9999	
Parent vs. 3xFLAG-pilU	ns	0.9949	
Parent vs. pilT^{K136A}	ns	0.9865	
ΔpilT vs. pilT^{K136A}, 6xHis-pilU	***	0.0007	
ΔpilT vs. 6xHis-pilT	*	0.0209	
ΔpilT vs. 6xHis-pilU	*	0.0261	
ΔpilT vs. pilT^{K136A}, 3xFLAG-pilU	*	0.0201	
ΔpilT vs. 3xFLAG-pilT	**	0.0014	
ΔpilT vs. 3xFLAG-pilU	**	0.0093	
ΔpilT vs. pilT^{K136A}	*	0.0126	
pilT^{K136A}, 6xHis-pilU vs. 6xHis-pilT	ns	0.9279	
pilT^{K136A}, 6xHis-pilU vs. 6xHis-pilU	ns	0.8986	
pilT^{K136A}, 6xHis-pilU vs. pilT^{K136A}, 3xFLAG-pilU	ns	0.9329	
pilT^{K136A}, 6xHis-pilU vs. 3xFLAG-pilT	ns	>0.9999	
pilT^{K136A}, 6xHis-pilU vs. 3xFLAG-pilU	ns	0.9862	
pilT^{K136A}, 6xHis-pilU vs. pilT^{K136A}	ns	0.9724	
6xHis-pilT vs. 6xHis-pilU	ns	>0.9999	
6xHis-pilT vs. pilT^{K136A}, 3xFLAG-pilU	ns	>0.9999	
6xHis-pilT vs. 3xFLAG-pilT	ns	0.98	
6xHis-pilT vs. 3xFLAG-pilU	ns	>0.9999	
6xHis-pilT vs. pilT^{K136A}	ns	>0.9999	
6xHis-pilU vs. pilT^{K136A}, 3xFLAG-pilU	ns	>0.9999	

6xHis-pilU vs. 3xFLAG-pilT	ns	0.9671	
6xHis-pilU vs. 3xFLAG-pilU	ns	>0.9999	
6xHis-pilU vs. pilT^{K136A}	ns	>0.9999	
pilT^{K136A}, 3xFLAG-pilU vs. 3xFLAG-pilT	ns	0.982	
pilT^{K136A}, 3xFLAG-pilU vs. 3xFLAG-pilU	ns	>0.9999	
pilT^{K136A}, 3xFLAG-pilU vs. pilT^{K136A}	ns	>0.9999	
3xFLAG-pilT vs. 3xFLAG-pilU	ns	0.9983	
3xFLAG-pilT vs. pilT^{K136A}	ns	0.9951	
3xFLAG-pilU vs. pilT^{K136A}	ns	>0.9999	
Supplemental Figure 3B - Tukey's multiple comparison test			
Parent vs. ΔpilT	ns	0.2194	# of families = 1
Parent vs. Ptac-3xFLAG-pilT	ns	>0.9999	# of comparisons per family = 66
Parent vs. Ptac-3xFLAG-pilT ΔpilT	ns	0.9989	Alpha = 0.05
Parent vs. Ptac-3xFLAG-pilU	ns	0.9995	
Parent vs. Ptac-3xFLAG-pilU, pilT^{K136A} ΔpilU	ns	0.9127	
Parent vs. Ptac-3xFLAG-pilT^{K136A}	ns	0.9505	
Parent vs. Ptac-3xFLAG-pilU^{K134A}	ns	0.9999	
Parent vs. Ptac-3xFLAG-pilT^{K136A}, ΔpilU	ns	0.2197	
Parent vs. Ptac-3xFLAG-pilU^{K134A}, pilT^{K136A}	ns	0.2199	
Parent vs. ΔpilU	ns	0.998	
Parent vs. pilT^{K136A}	ns	0.9912	
ΔpilT vs. Ptac-3xFLAG-pilT	ns	0.0832	
ΔpilT vs. Ptac-3xFLAG-pilT ΔpilT	*	0.0472	
ΔpilT vs. Ptac-3xFLAG-pilU	ns	0.5898	
ΔpilT vs. Ptac-3xFLAG-pilU, pilT^{K136A} ΔpilU	ns	0.9879	
ΔpilT vs. Ptac-3xFLAG-pilT^{K136A}	*	0.0123	
ΔpilT vs. Ptac-3xFLAG-pilU^{K134A}	ns	0.0697	
ΔpilT vs. Ptac-3xFLAG-pilT^{K136A}, ΔpilU	ns	>0.9999	
ΔpilT vs. Ptac-3xFLAG-pilU^{K134A}, pilT^{K136A}	ns	>0.9999	
ΔpilT vs. ΔpilU	ns	0.8312	
ΔpilT vs. pilT^{K136A}	ns	0.9042	
Ptac-3xFLAG-pilT vs. Ptac-3xFLAG-pilT ΔpilT	ns	>0.9999	
Ptac-3xFLAG-pilT vs. Ptac-3xFLAG-pilU	ns	0.9531	
Ptac-3xFLAG-pilT vs. Ptac-3xFLAG-pilU, pilT^{K136A} ΔpilU	ns	0.6364	
Ptac-3xFLAG-pilT vs. Ptac-3xFLAG-pilT^{K136A}	ns	0.9998	
Ptac-3xFLAG-pilT vs. Ptac-3xFLAG-pilU^{K134A}	ns	>0.9999	
Ptac-3xFLAG-pilT vs. Ptac-3xFLAG-pilT^{K136A}, ΔpilU	ns	0.0833	
Ptac-3xFLAG-pilT vs. Ptac-3xFLAG-pilU^{K134A}, pilT^{K136A}	ns	0.0834	
Ptac-3xFLAG-pilT vs. ΔpilU	ns	0.9305	
Ptac-3xFLAG-pilT vs. pilT^{K136A}	ns	0.8688	
Ptac-3xFLAG-pilT ΔpilT vs. Ptac-3xFLAG-pilU	ns	0.8682	

Ptac-3xFLAG-pilT ΔpilT vs. Ptac-3xFLAG-pilU, pilT^{K136A} ΔpilU	ns	0.4801	
Ptac-3xFLAG-pilT ΔpilT vs. Ptac-3xFLAG-pilT^{K136A}	ns	>0.9999	
Ptac-3xFLAG-pilT ΔpilT vs. Ptac-3xFLAG-pilU^{K134A}	ns	>0.9999	
Ptac-3xFLAG-pilT ΔpilT vs. Ptac-3xFLAG-pilT^{K136A}, ΔpilU	*	0.0473	
Ptac-3xFLAG-pilT ΔpilT vs. Ptac-3xFLAG-pilU^{K134A}, pilT^{K136A}	*	0.0473	
Ptac-3xFLAG-pilT ΔpilT vs. ΔpilU	ns	0.8381	
Ptac-3xFLAG-pilT ΔpilT vs. pilT^{K136A}	ns	0.7454	
Ptac-3xFLAG-pilU vs. Ptac-3xFLAG-pilU, pilT^{K136A} ΔpilU	ns	0.9991	
Ptac-3xFLAG-pilU vs. Ptac-3xFLAG-pilT^{K136A}	ns	0.5332	
Ptac-3xFLAG-pilU vs. Ptac-3xFLAG-pilU^{K134A}	ns	0.9319	
Ptac-3xFLAG-pilU vs. Ptac-3xFLAG-pilT^{K136A}, ΔpilU	ns	0.5902	
Ptac-3xFLAG-pilU vs. Ptac-3xFLAG-pilU^{K134A}, pilT^{K136A}	ns	0.5906	
Ptac-3xFLAG-pilU vs. ΔpilU	ns	>0.9999	
Ptac-3xFLAG-pilU vs. pilT^{K136A}	ns	>0.9999	
Ptac-3xFLAG-pilU, pilT^{K136A} ΔpilU vs. Ptac-3xFLAG-pilT^{K136A}	ns	0.2052	
Ptac-3xFLAG-pilU, pilT^{K136A} ΔpilU vs. Ptac-3xFLAG-pilU^{K134A}	ns	0.5864	
Ptac-3xFLAG-pilU, pilT^{K136A} ΔpilU vs. Ptac-3xFLAG-pilT^{K136A}, ΔpilU	ns	0.988	
Ptac-3xFLAG-pilU, pilT^{K136A} ΔpilU vs. Ptac-3xFLAG-pilU^{K134A}, pilT^{K136A}	ns	0.988	
Ptac-3xFLAG-pilU, pilT^{K136A} ΔpilU vs. ΔpilU	ns	>0.9999	
Ptac-3xFLAG-pilU, pilT^{K136A} ΔpilU vs. pilT^{K136A}	ns	>0.9999	
Ptac-3xFLAG-pilT^{K136A} vs. Ptac-3xFLAG-pilU^{K134A}	ns	>0.9999	
Ptac-3xFLAG-pilT^{K136A} vs. Ptac-3xFLAG-pilT^{K136A}, ΔpilU	*	0.0123	
Ptac-3xFLAG-pilT^{K136A} vs. Ptac-3xFLAG-pilU^{K134A}, pilT^{K136A}	*	0.0123	
Ptac-3xFLAG-pilT^{K136A} vs. ΔpilU	ns	0.5225	
Ptac-3xFLAG-pilT^{K136A} vs. pilT^{K136A}	ns	0.4139	
Ptac-3xFLAG-pilU^{K134A} vs. Ptac-3xFLAG-pilT^{K136A}, ΔpilU	ns	0.0698	
Ptac-3xFLAG-pilU^{K134A} vs. Ptac-3xFLAG-pilU^{K134A}, pilT^{K136A}	ns	0.0699	
Ptac-3xFLAG-pilU^{K134A} vs. ΔpilU	ns	0.906	
Ptac-3xFLAG-pilU^{K134A} vs. pilT^{K136A}	ns	0.8338	
Ptac-3xFLAG-pilT^{K136A}, ΔpilU vs. Ptac-3xFLAG-pilU^{K134A}, pilT^{K136A}	ns	>0.9999	

Ptac-3xFLAG-pilT^{K136A}, ΔpilU vs. ΔpilU	ns	0.8315	
Ptac-3xFLAG-pilT^{K136A}, ΔpilU vs. pilT^{K136A}	ns	0.9044	
Ptac-3xFLAG-pilU^{K134A}, pilT^{K136A} vs. ΔpilU	ns	0.8318	
Ptac-3xFLAG-pilU^{K134A}, pilT^{K136A} vs. pilT^{K136A}	ns	0.9046	
ΔpilU vs. pilT^{K136A}	ns	>0.9999	
Supplemental Figure 3D - Tukey's multiple comparison test			
Parent vs. ΔpilT ΔpilU	****	<0.0001	# of families = 1
Parent vs. pilU^{K134A}	ns	0.9994	# of comparisons per family = 55
Parent vs. pilT^{K136A} ΔpilU	****	<0.0001	Alpha = 0.05
Parent vs. pilT^{K136A} pilU^{K134A}	****	<0.0001	
Parent vs. P_{tac}-pilT	ns	0.999	
Parent vs. ΔpilT Ptac-pilT	ns	>0.9999	
Parent vs. P_{tac}-pilU	ns	0.999	
Parent vs. pilT^{K136A} ΔpilU Ptac-pilU	ns	0.9481	
Parent vs. ΔpilA	****	<0.0001	
Parent vs. pilT^{K136A}	ns	>0.9999	
ΔpilT ΔpilU vs. pilU^{K134A}	****	<0.0001	
ΔpilT ΔpilU vs. pilT^{K136A} ΔpilU	ns	0.4878	
ΔpilT ΔpilU vs. pilT^{K136A} pilU^{K134A}	ns	>0.9999	
ΔpilT ΔpilU vs. Ptac-pilT	****	<0.0001	
ΔpilT ΔpilU vs. ΔpilT Ptac-pilT	****	<0.0001	
ΔpilT ΔpilU vs. Ptac-pilU	****	<0.0001	
ΔpilT ΔpilU vs. pilT^{K136A} ΔpilU Ptac-pilU	****	<0.0001	
ΔpilT ΔpilU vs. ΔpilA	**	0.0028	
ΔpilT ΔpilU vs. pilT^{K136A}	****	<0.0001	
pilU^{K134A} vs. pilT^{K136A} ΔpilU	****	<0.0001	
pilU^{K134A} vs. pilT^{K136A} pilU^{K134A}	****	<0.0001	
pilU^{K134A} vs. P_{tac}-pilT	ns	>0.9999	
pilU^{K134A} vs. ΔpilT Ptac-pilT	ns	>0.9999	
pilU^{K134A} vs. P_{tac}-pilU	ns	>0.9999	
pilU^{K134A} vs. pilT^{K136A} ΔpilU Ptac-pilU	ns	0.6391	
pilU^{K134A} vs. ΔpilA	****	<0.0001	
pilU^{K134A} vs. pilT^{K136A}	ns	0.9972	
pilT^{K136A} ΔpilU vs. pilT^{K136A} pilU^{K134A}	ns	0.6518	
pilT^{K136A} ΔpilU vs. Ptac-pilT	****	<0.0001	
pilT^{K136A} ΔpilU vs. ΔpilT Ptac-pilT	****	<0.0001	
pilT^{K136A} ΔpilU vs. Ptac-pilU	****	<0.0001	
pilT^{K136A} ΔpilU vs. pilT^{K136A} ΔpilU Ptac-pilU	****	<0.0001	
pilT^{K136A} ΔpilU vs. ΔpilA	ns	0.4692	
pilT^{K136A} ΔpilU vs. pilT^{K136A}	****	<0.0001	
pilT^{K136A} pilU^{K134A} vs. P_{tac}-pilT	****	<0.0001	
pilT^{K136A} pilU^{K134A} vs. ΔpilT Ptac-pilT	****	<0.0001	

pilT^{K136A} pilU^{K134A} vs. P_{tac}-pilU	****	<0.0001	
pilT^{K136A} pilU^{K134A} vs. pilT^{K136A} ΔpilU Ptac-pilU	****	<0.0001	
pilT^{K136A} pilU^{K134A} vs. ΔpilA	**	0.0057	
pilT^{K136A} pilU^{K134A} vs. pilT^{K136A}	****	<0.0001	
Ptac-pilT vs. ΔpilT Ptac-pilT	ns	>0.9999	
P_{tac}-pilT vs. P_{tac}-pilU	ns	>0.9999	
Ptac-pilT vs. pilT^{K136A} ΔpilU Ptac-pilU	ns	0.6089	
Ptac-pilT vs. ΔpilA	****	<0.0001	
P_{tac}-pilT vs. pilT^{K136A}	ns	0.9957	
ΔpilT Ptac-pilT vs. Ptac-pilU	ns	>0.9999	
ΔpilT Ptac-pilT vs. pilT^{K136A} ΔpilU Ptac-pilU	ns	0.7364	
ΔpilT Ptac-pilT vs. ΔpilA	****	<0.0001	
ΔpilT Ptac-pilT vs. pilT^{K136A}	ns	0.9995	
Ptac-pilU vs. pilT^{K136A} ΔpilU Ptac-pilU	ns	0.6068	
Ptac-pilU vs. ΔpilA	****	<0.0001	
P_{tac}-pilU vs. pilT^{K136A}	ns	0.9956	
pilT^{K136A} ΔpilU Ptac-pilU vs. ΔpilA	****	<0.0001	
pilT^{K136A} ΔpilU Ptac-pilU vs. pilT^{K136A}	ns	0.9772	
ΔpilA vs. pilT^{K136A}	****	<0.0001	
Supplemental Figure 4 - Dunnett's multiple comparison test			
Parent pmmB-pilT vs. ΔpilTU pmmB-pilT	****	0.0001	# of families = 2
Parent pmmB-pilT vs. ΔpilT pmmB-pilT	ns	0.8827	# of comparisons per family = 8
Parent pmmB-pilT vs. ΔpilU pmmB-pilT	****	0.0001	Alpha = 0.05
Parent pmmB-pilT vs. pilT^{K136A} pmmB-pilT	ns	0.8666	
Parent pmmB-pilT vs. pilT^{K136A} ΔpilU pmmB-pilT	****	0.0001	
Parent pmmB-pilT vs. pilU^{K137A} pmmB-pilT	****	0.0001	
Parent pmmB-pilT vs. pilT^{K136A} pilU^{K137A} pmmB-pilT	****	0.0001	
Parent pmmB-pilU vs. ΔpilTU pmmB-pilU	Yes	****	
Parent pmmB-pilU vs. ΔpilT pmmB-pilU	Yes	****	
Parent pmmB-pilU vs. ΔpilU pmmB-pilU	No	ns	
Parent pmmB-pilU vs. pilT^{K136A} pmmB-pilU	Yes	****	
Parent pmmB-pilU vs. pilT^{K136A} ΔpilU pmmB-pilU	Yes	****	
Parent pmmB-pilU vs. pilU^{K137A} pmmB-pilU	Yes	*	
Parent pmmB-pilU vs. pilT^{K136A} pilU^{K137A} pmmB-pilU	Yes	****	
Parent pmmB-pilU vs. Parent pmmB-pilU	No	ns	
Supplemental Figure 5 - Tukey's multiple comparison test			
Parent vs. ΔMSHA ΔTCP	ns	0.8726	# of families = 1
Parent vs. ΔpilTU	****	<0.0001	# of comparisons per family = 6
Parent vs. ΔpilTU ΔMSHA ΔTCP	****	<0.0001	Alpha = 0.05
ΔMSHA ΔTCP vs. ΔpilTU	****	<0.0001	
ΔMSHA ΔTCP vs. ΔpilTU ΔMSHA ΔTCP	****	<0.0001	
ΔpilTU vs. ΔpilTU ΔMSHA ΔTCP	ns	0.0927	

[#]Statistical differences were assessed by one-way ANOVA tests followed by a multiple comparisons post test (either Tukey's or Dunnett's) using GraphPad Prism software. For all transformation frequency experiments and frequency of pilus retraction experiments, statistical analyses were performed on the log transformed data (i.e. **Figs 1A, 1C, 2B, 4C** and **S1, S3A, S3B, S3D, S4, S5 Figs**).